Neurochemical Investigation of Locally Induced Epilepsy and Subsequent Oxidative Damage Using Microdialysis Sampling

By

Amanda Marie Furness

B.S., B.A., Briar Cliff University

Sioux City, IA, 51104

Submitted to the graduate degree program in Chemistry and the Graduate Faculty of the University of Kansas in partial fulfillment of the requirements for the degree of Doctor of Philosophy.

_____

Chair: Susan M. Lunte

_____

Elias K. Michaelis

_____

Michael Johnson

_____

Bob Dunn

_____

Mario Rivera

Date Defended: January, 31, 2017

The dissertation committee for Amanda Marie Furness certifies that this is the approved version of the following dissertation:

Neurochemical Investigation of Locally Induced Epilepsy and Subsequent Oxidative Damage Using Microdialysis Sampling

_____

Chairperson: Susan M. Lunte

Date Approved: February, 24, 2017

Abstract

Amanda Marie Furness, Ph.D.

R.N. Adams Institute for Bioanalytical Chemistry

Department of Chemistry, January 2017

The University of Kansas

The goal of this research was to develop and understand an anesthetized, multiple-seizure rat model for local epilepsy. Local seizures are not as well understood as global seizures due to their specificity and unpredictability. Furthermore, patients are diagnosed with epilepsy after experiencing two or more unprovoked seizures. In this model, two separate seizure episodes were induced by locally administering the epileptic agent 3-mercaptopropionic acid through a microdialysis probe to the CA1 region of the hippocampus. Upon development of the model, attenuation in glutamate release was observed in the second seizure stimulation. To investigate neurochemical and biochemical pathways which may be responsible for the glutamate diminution, the perfusion fluid was spiked with either glucose, lactate, or dihydrokainic acid. Additionally, as it is well known that high levels of extracellular glutamate can result in excitotoxicity, neuronal staining was performed to determine the neuronal viability after the induction of the first seizure. It was determined that the attenuation in glutamate release in the second seizure episode was primarily due to a combination of mitochondrial starvation and cell damage.

The local seizure model was then used to correlate local seizure induction to oxidative damage. Glutathione (GSH) and malondialdehyde (MDA) were selected as biomarkers of oxidative stress. Intracellular levels GSH were up regulated and down regulated in hopes of modifying the amount of seizure induced oxidative damage. There was no statistically significant change in MDA formation with changing GSH levels; however, GSH did appear to serve as a release modifier of the redox cycle. Extracellular GSH increased significantly during the seizure induction and returned to basal after the seizure ended. This increase in extracellular GSH concentration can be accounted for by astrocytes and glial cells releasing GSH to counteract reactive oxygen species produced during the seizure. Additional experiments need to be done in order to make further conclusions; however, it is evident that there is a correlation between seizures and oxidative stress.

Finally, Appendix I describes a small *in vitro* pharmacokinetic project using microdialysis sampling to measure plasma protein binding values of commercially available drugs with the ultimate goal of applying the technique for *in vivo* studies.

Acknowledgments

Where do I even start? I have to start, with my Lord Jesus Christ. Without His everlasting and forgiving love I would not have been able to survive these past four and a half years. I am so thankful to God that He stood by my side through it all and for bringing people to support me. I have made countless friends over these years, many of whom I will be friends with for a lifetime, many of whom have already left my life, but still had a great impact for the moment.

Next, to my family. Thank-you Mom and Dad for listening and giving me unending support. (Even though you tell people "my daughter kills rats for a living!") I learned that there is nothing more powerful than praying parents. (And boy, did you have to pray!) I would not have made it without you both. I love you! Also, thank-you Eric, my favorite brother, for being there for me forever and always.

One of my favorite quotes is "There is family, there are friends, and occasionally those friends become family." I do not believe there is any quote that is more appropriate for my relationship with Mary and Cal. From day one Mary and I started as friends, and they quickly embraced me as family. Thank-you both so much for everything you have ever done for me. Your unconditional love and support is something that I have never truly felt before, and it is something I pray is in my life forever. I do not think either of you will ever understand how much you did for me emotionally, financially, and spiritually. Cal, you were always there to keep it real, and Mary you were always there to pick up the pieces. And of course there was martini night when nothing else worked. You both have really helped develop me into the person I am today and I am forever grateful for you. Give me a few years and I will get that costal cottage ready for you, or should I say "y'all"!

Next, to all of my professors that have helped me get here. Mrs. Reed, you are truly my inspiration to chemistry. Your passion for science resounded through your teaching, even in high school. You are really the reason I even thought I could pursue a degree, and eventual career in chemistry (you and a silly cookie conversation with my cousin Kelly). Even though you gave me the only B I received in high school, the knowledge I gained from your class has impacted my life forever. There were so many times I wish I could come back and retake your course so I could benefit again. I hope that other students realize how amazing you are.

To my two chemistry profs in undergrad, Dr. Bryan and Dr. Weber, thank-you for teaching me how much I don't like synthetic chemistry! You both showed me a passion for analytical chemistry and a balance for grad school. It can't all be stress and work, but it can't all be fun and games. You both helped demonstrate that to me. Next, to my wonderful advisor Sue. Thank-you so much for taking me on. I know it had to have been hard, for so many reasons. I am sorry for being so stubborn, needy, and annoying! Thank-you for your support through it all.

Finally, to my advisor, Dr. Craig Lunte. This is one of the most difficult times for me, knowing you are not here for these moments. I miss your passion for life and science. Your banter with me was one of my favorite things, but you were always able to keep me in check. I will never forget one of our last conversations we had in New Orleans over coffee and beignets after an epic bar crawl. After enough hurricanes and grenades I had the guts to ask you why you were still working. What drives you to continue? Your answer will forever resonate in me, "I don't care about publishing. I have published. I don't need that anymore. I have made my name. What I care about is producing successful graduate students. I want my students to succeed and get good jobs and make a name for themselves so I can brag about them." Craig, I hope that I fall into that category. I hope that I have made you proud. You are forever missed.

Table of Contents

List of Figures

Chapter 1

Introduction

1.1 Oxidative Stress Overview

Oxidative stress is a result of the imbalance between the production of free radicals and the body's ability to counteract them through antioxidants. Oxidative stress can lead to a wide range of negative outcomes including cancer, neurodegeneration, DNA damage, and cell death[1]. There are many factors that can result in oxidative stress including exposure to chemicals, consumption of processed food, and neurological disorders[2, 3]. The brain is rich in fatty acids that are highly susceptible to oxidative damage, peroxidation and radical production[4]. One of the most common neurological disorders, epilepsy, is believed to cause oxidative stress in the brain[3, 5, 6]. Epilepsy is a result of an imbalance in the neurotransmitters in the brain that causes an activation of G-protein coupled receptors that change calcium ion concentrations at the neuronal membrane[7]. This change in membrane potential results in the production of reactive oxygen species (ROS) such as peroxides, superoxide, and the hydroxide radical through a variety of mechanisms. These ROS can lead to lipid peroxidation, neuronal damage, changes in neuronal plasticity, and cell death that can, in turn, result in subsequent seizures (Figure 1.1)[8]. Studies have shown that epileptic seizures tend to induce long-term hyperexcitability in neurons, making them more prone to future seizures[9]. This cycle of excitotoxicity continues until the damage is irreparable. Therefore, it is imperative to gain a better understanding of the biochemical pathways involved in the production of oxidative stress during seizures, in hopes that this cycle can be broken and therapeutic treatments can be developed.

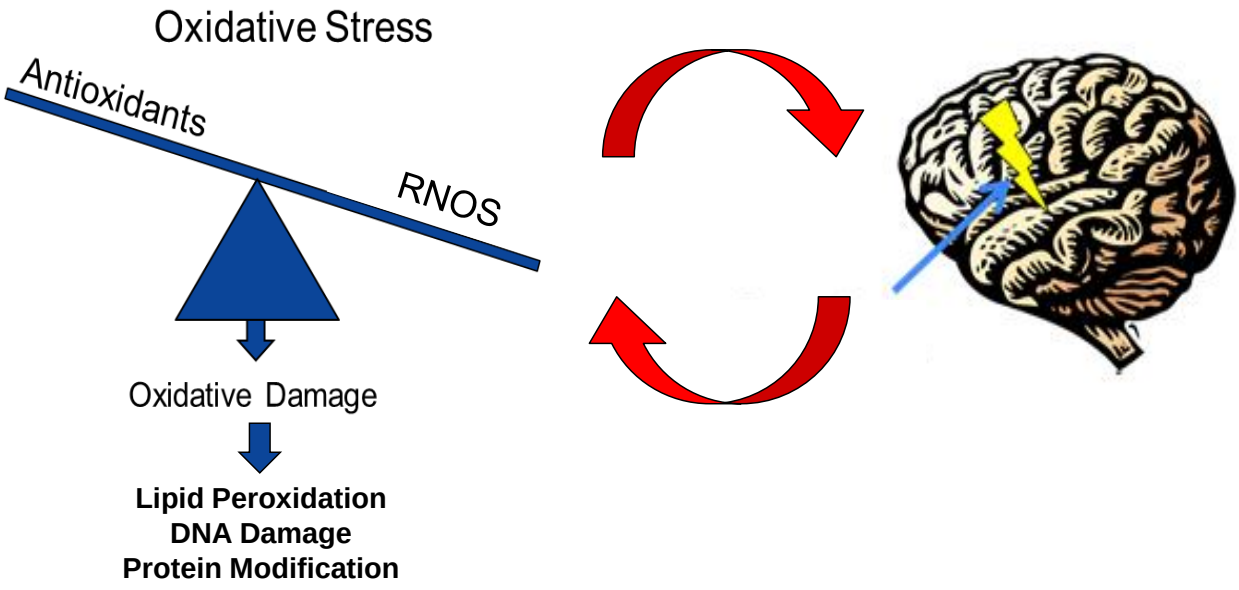

Figure 1.1: Relationship between oxidative stress and seizure induction

1.2 Epilepsy Overview

Epilepsy affects approximately one percent of the world population[10]. There is currently no known cure for epilepsy and only 70% of epileptic cases can be regulated with medication. This leaves nearly 30% of epileptic patients with a pharmacoresistant form of epilepsy that cannot be treated with medication[10]. There are several alternative treatments available for pharmacoresistant seizures including, special diets[11], surgery[12], and deep brain stimulation[13, 14]. Success has been achieved for all treatments; however, there are still cases that remain untreatable.

An epileptic event, or seizure, is caused by an imbalance of the neuronal firing in the brain. When the inhibitory responders are not able to offset the excitatory responders, a seizure is observed[7, 15]. There are two main categories of seizures, local and global (tonic-clonic). Seizures that occur locally affect only one region of the brain, whereas global seizures affect multiple brain regions. Nearly 70% of epileptic patients experience local seizures[6]. Local seizures, due to their specificity and unpredictability, are not as well understood as global seizures[16, 17]. Furthermore, symptoms of local seizures are not as severe as global seizures, thus making them harder to diagnose. There are many models available for global seizures, including knockout mice and the systemic dosing of the animal with convulsants[16, 18, 19]. However, there are only a few models that locally dose convulsants to a specific brain region to generate multiple local seizures. In some studies of epilepsy, single seizures were induced in the brain region of interest both chemically and electrically[20, 21]. However, patients are diagnosed with epilepsy after having experienced two or more unprovoked seizures[6, 9]. To date, there are no reported models that induce multiple local seizures within one experiment, meaning there is no model that represents local epilepsy. Generating multiple seizures in a localized brain region within the same experiment will provide

neurochemical insights into local epilepsy. Direct comparisons of analyte concentrations can be made between the first and second seizure as well as intraseizure neurochemical response.

1.3 Animal Seizure Models

There are two main types of animal models used to simulate epilepsy, stimulated and kindling models[7, 19]. With stimulated models, a convulsion is induced either electrically with electrode firing or chemically by dosing the animal with a convulsant, resulting in an instantaneous seizure. In kindling models, a subconvulsant dose of an epileptic agent, or a subthreshold electrical stimulus is administered over time until the animal develops a sensitivity to the stimulation that leads to spontaneous seizures. This approach induces unpredictable seizures[22]. While the kindling model more accurately represents epileptic seizures with the inherent unpredictability, these seizures are difficult to replicate in a laboratory setting. For this reason, stimulated seizures were used in this research. Kindling models are discussed further in Chapter 5.

1.3.1 Electrically Induced Seizures

Electrodes can be implanted directly into the brain region of interest. An electric current is deployed that disrupts the neurons and causes misfiring, resulting in a seizure[14, 23, 24]. A major advantage of electrically induced seizures is that they do not rely on a chemical to generate a seizure, removing an additional variable from the study, making them easier to validate. However,

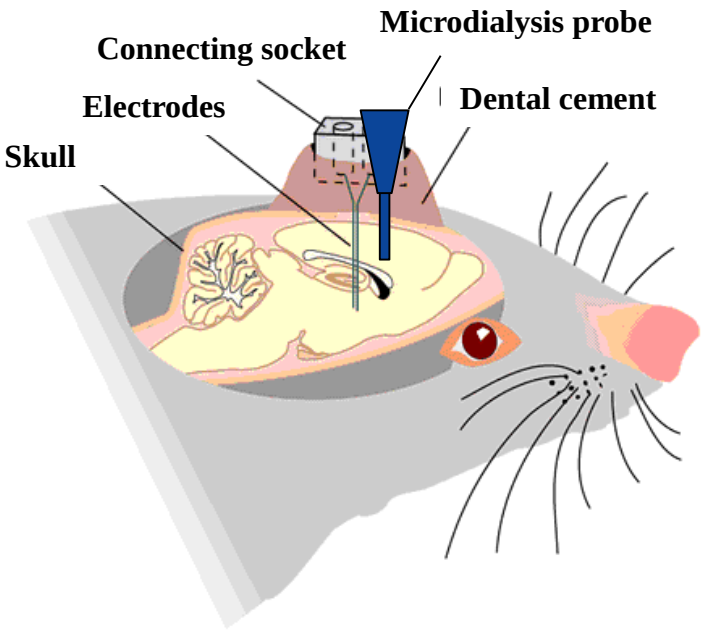

http://www.uni.edu/walsh/biolec.html

Figure 1.2: Example of loss of spatial resolution with electrically induced seizures.

as can be seen in Figure 1.2, the electrically stimulated model has a loss of spatial resolution associated with this type of stimulation. The brain of a rat is small and there is not much room to implant both electrodes for stimulation and microsampling probes for sample collection. The collection probe may not be in the same brain region as the stimulating electrodes, reducing spatial resolution and possibly resulting in measurement of false responses.

1.3.2 Chemically Induced Seizures

Chemically simulated models negate the need for electrode implantation. A convulsant dose of an epileptic agent is directly given to the animal, causing an imbalance in signaling of two of the most abundant excitatory and inhibitory neurotransmitters, glutamate and γ-aminobutyric acid (GABA), thereby resulting in a seizure[25, 26]. There are three main types of convulsants available including those that affect glutamate receptors, GABAergic receptors, and the synthesis and metabolism of GABA.

Agonists of glutamate receptors work by directly activating glutamate receptors that form the network of the major excitatory neurotransmitter in the brain, thus leading to abnormal electrical discharges[27, 28]. Drugs that work on GABAergic receptors ($GABA_A$ and $GABA_B$) act by blocking the GABA receptors, thus removing the activity of the main inhibitory neurotransmitter in the brain[29, 30]. The final category of convulsants alters the synthesis and metabolism of GABA. Glutamic acid decarboxylase (GAD) is the enzyme that converts glutamic acid to GABA via a decarboxylation reaction[25, 26, 31]. By using a chemically induced seizure model, both seizure duration and strength can be controlled by varying administration time and compound concentration. Additionally, experiments can be replicated with ease because the experimenter determines when the seizure occurs, making it ideal for the laboratory setting.

1.3.2.1 3-Mercaptopropionic Acid

3-Mercaptopropionic acid (3-MPA) is a well-established chemical convulsant that functions as a competitive inhibitor of GAD, creating an imbalance in glutamate and GABA concentrations[32, 33] (Figure 1.3). This results in an increase in extracellular glutamic acid concentrations and a decrease in GABA concentrations, simulating a seizure[34]. The exact mechanism of action has been previously described elsewhere[20, 32, 35, 36], but briefly, the structural similarity of 3-MPA and GABA makes 3-MPA an excellent competitive inhibitor of GAD. GAD metabolizes the 3-MPA in the same way that it would glutamic acid. It is a reversible inhibitor and, when there is no longer 3-MPA available to block the active site of the enzyme, then GAD continues to function normally, converting glutamic acid into GABA. Its reversible properties make it a good choice for a convulsant.

1.4 Methods

1.4.1 Microdialysis Sampling

The main sampling and delivery technique used in this research was microdialysis sampling. Microdialysis sampling involves a relatively simple system consisting of a probe, connecting tubing, and a perfusion pump[37]. The active area of the probe consists of a semipermeable membrane that provides chemical communication between the probe lumen and the surrounding tissue space. To perform microdialysis sampling, the probe is slowly perfused with a solution termed the perfusate that closely matches the composition of the extracellular fluid (ECF) of the target tissue[38, 39]. Small analytes cross the membrane by passive diffusion, driven by

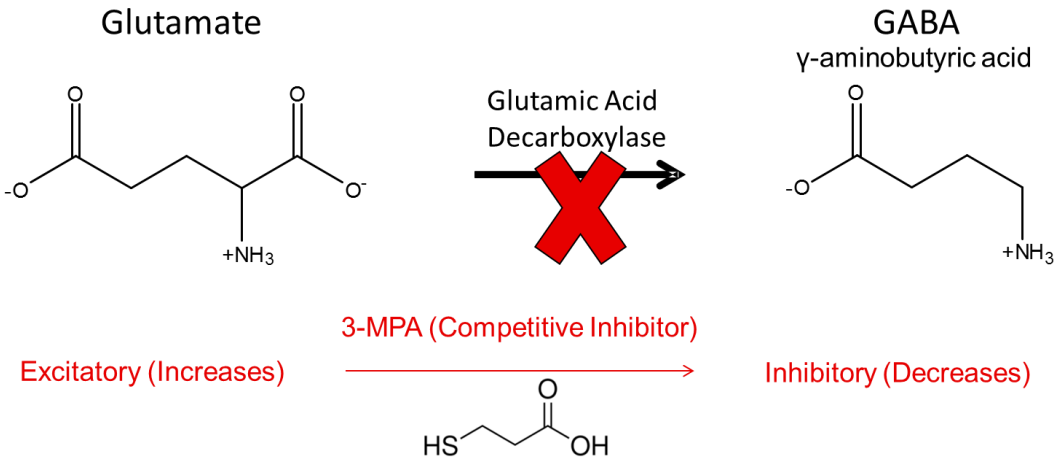

Figure 1.3: Mechanism of action of 3-Mercaptopropionic acid

any concentration difference across the membrane. Molecules can diffuse across the membrane in either direction depending on the direction of the concentration gradient allowing for both recovery/sampling of compounds from the target tissue as well as delivery of compounds to the tissue[37, 40]. Typical microdialysis membranes have molecular weight cutoffs between 10-100 kDa that prevent macromolecules, such as proteins, from crossing into the dialysate sample. Because large molecules are excluded from entering the probe, microdialysis samples are protein-free and typically require no additional sample clean up prior to analysis.

1.4.2 Type of Probes

There are several microdialysis probe designs available that allow for sampling in a variety of tissues and systems, which can be seen in Figure 1.4. The tissues and analytes being studied determine the type of probe to be used. The most common microdialysis probe for brain sampling is the concentric cannula style (Figure 1.5)[41, 42]. In the concentric style, the inlet and outlet tubing are on the same side of the probe and the membrane is on the other end. This style is favored in the brain because it allows for only one entry site, reducing tissue damage. In this set-up, a guide cannula containing a dummy probe is implanted into the region of interest and fixed to the skull using dental cement, guaranteeing that the probe remains in the correct region for the duration of the experiment. The dummy probe is then replaced with a stainless steel microdialysis probe for sampling.

Another probe type used for microdialysis studies is the flexible probe. Similar to the concentric cannula, the flexible cannula still allows for a single implantation site because the inlet and outlet are on the same side of the probe, however, it is not as rigid. Rather than the unyielding material of the concentric probe, the flexible probe is made up of a soft material like polyurethane

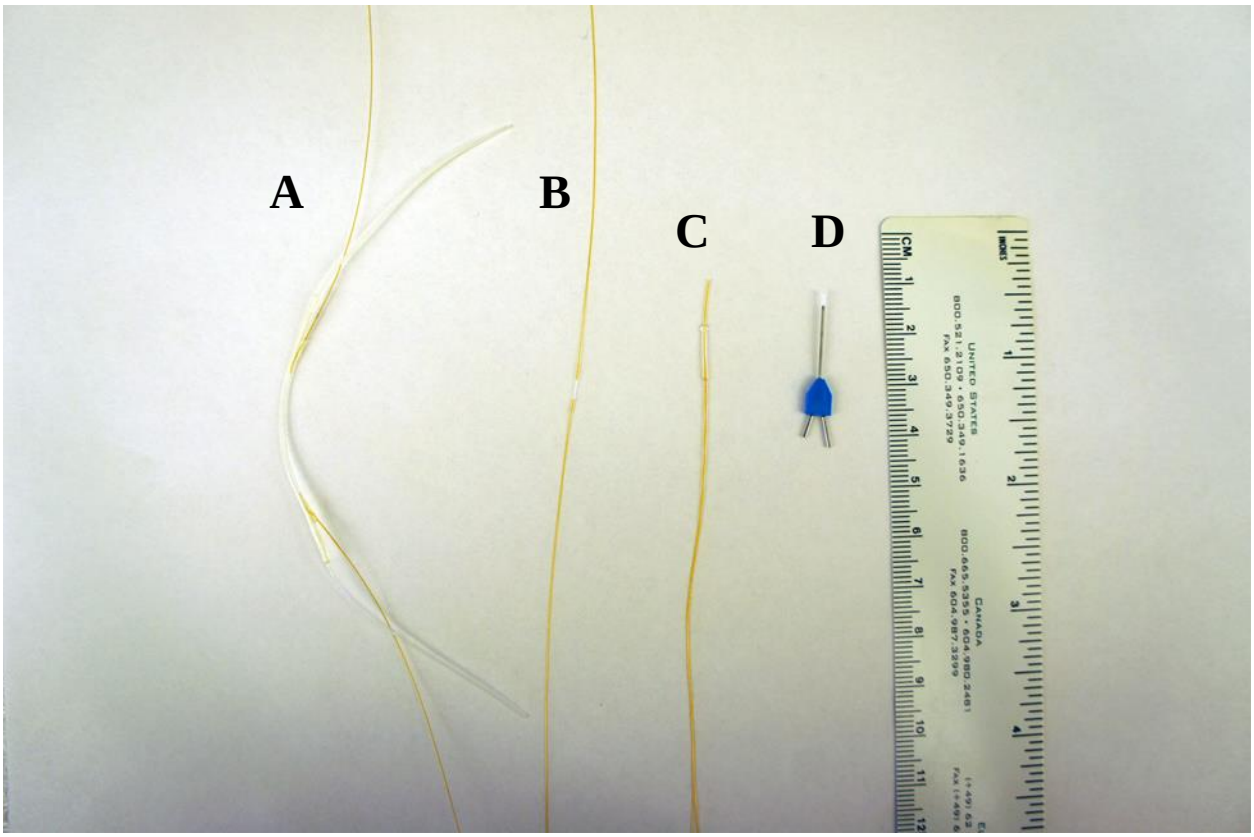

Figure 1.4: Four of the most common probe types. A) Shunt probe B) Linear probe C) Flexible probe D) Brain Probe

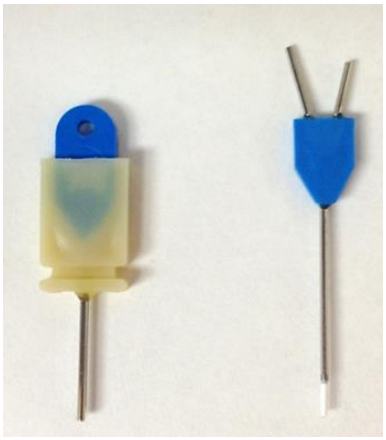

Figure 1.5: Concentric cannula probe system. CMA 12 Elite Microdialysis Probe

Membrane: OD, 0.5 mm; Length, 2 mm; Total Length, 14 mm

that is able to be implanted into vessels and other peripheral tissues[43]. In some experiments, a combination of a brain probe and flexible probe are used for blood brain barrier studies. A stainless steel concentric cannula probe is implanted into the brain to measure analyte concentration in the brain, while a flexible probe is implanted into a blood vessel to measure analyte concentrations in the blood. Simultaneous sampling from both the brain and blood can be done and direct concentration comparisons can be made[44].

The brain probe and flexible probe were the two main probes used in this research. Another common type of probe is the linear probe. Similar to the flexible probe, the linear probe is preferred for use in peripheral tissues due to its flexible property. It allows the animal to move freely while causing minimal damage to the tissue. In contrast to the concentric cannula and flexible probe designs, the linear probe has inlet and outlet tubing on opposite sides of the membrane[43, 45]. This allows for longer membrane lengths than other probe styles, which results in better sample recovery due to the increased surface area of the probe in the tissue. The last major type of probe style is the shunt probe. While not as common, the shunt probe is a good system for damage-free collection of fluids. A shunt is inserted into the desired location and then a linear probe is placed inside of the shunt. This microdialysis probe was specifically designed for sampling the bile while maintaining normal bile flow and volume[39].

1.4.3 Theory

Microdialysis is based on the same principles and concepts of large scale dialysis (Figure 1.6). Analytes passively diffuse across the semipermeable membrane down their concentration gradient according to Fick's Law[37, 46]. Unlike large scale dialysis, equilibrium is not achieved in microdialysis because of the constant perfusion. Rather, a steady-state concentration gradient is

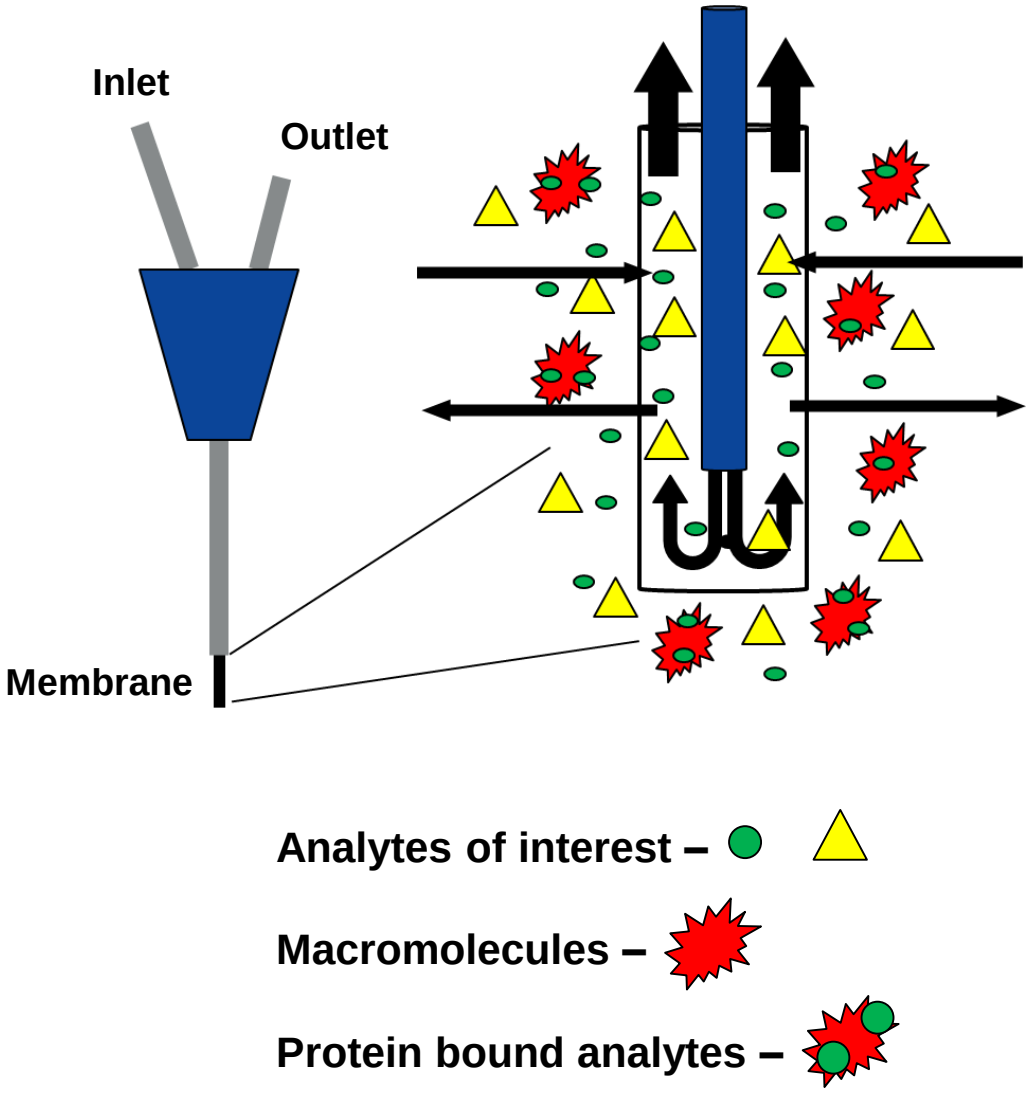

Figure 1.6: Schematic demonstrating microdialysis sampling mechanism

quickly established. There are several factors that affect how the steady-state is established including the perfusion fluid, perfusion rate, membrane type, membrane length, molecular weight cut-off, and composition of the tissue of implantation[40, 47].

Hydrophilicity of analytes must be taken into consideration when choosing a perfusion fluid and membrane type. Highly lipophilic compounds may have lower recovery if the perfusion fluid or membrane is highly hydrophilic. Higher flow rates of the perfusate allow for larger sample volumes, increasing the absolute recovery, but also results in dilution. The faster flow reduces the amount of time that analytes can diffuse across the probe and be collected, reducing overall relative recovery. An example plot of relative recovery versus flow rate is shown in Figure 1.7. Longer membrane lengths provide more room for analytes to cross but reduce spatial resolution for *in vivo* studies. Therefore, the shortest membrane length that provides adequate recovery is ideal for maintaining good spatial resolution. Choosing a membrane with a molecular weight cut-off that limits the amount of macromolecules in your sample reduces the need for extensive sample clean-up. Finally, composition of sample/tissue also affect recovery due to the complexity of the matrix and the possibility of analyte metabolism. All of these factors can lead to recoveries less than 100%, meaning the concentration of analyte in the dialysate is not the same as the true concentration of analyte in the tissue, but rather a relative amount.

1.4.3.1 Microdialysis Calibration Methods

In order to calibrate the microdialysis probe, recovery and delivery experiments performed *in vitro* can be used to determine the extraction efficiency of the probe; this efficiency can then be applied for use *in vivo*[48]. The relative recovery (EE_R) of the probe can be calculated using Equation

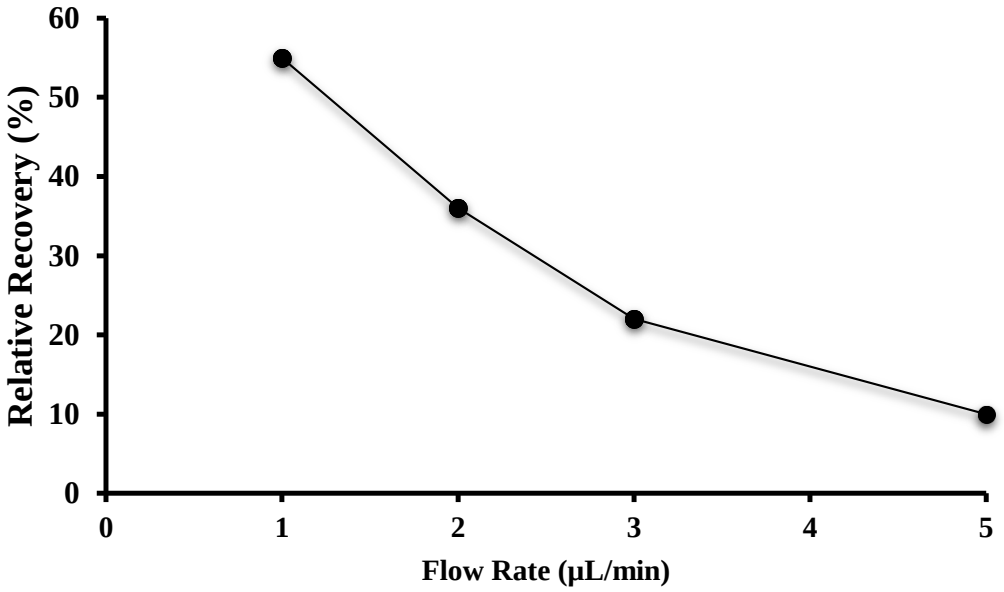

Figure 1.7: Relative recovery of probe versus flow rate

1. In a relative recovery experiment, a bath solution containing sample matrix is maintained at 37°C and stirred constantly. The bath solution is spiked with a known concentration of analyte. The probe is placed in the solution and blank sample matrix is perfused through the probe for a set length of time. As the perfusion occurs, analyte in the bath solution is allowed to passively diffuse across the membrane and be collected in the dialysate. The concentration of analyte in the dialysate is then determined analytically.

$$EE_R = \frac{(C_{dialysate})}{(C_{sample})}$$

Equation 1

In vitro delivery experiments can also be used as a form of probe calibration. In a similar set-up to recovery experiments, the probe is placed in a bath solution heated to 37°C and stirred constantly containing unspiked sample matrix. The perfusion fluid is spiked with a known concentration of analyte. Perfusion is allowed to occur for a set length of time, dialysate is collected, and analyte concentration is analytically determined. The delivery of the compound to sample can be calculated using Equation 2.

$$EE_D = \frac{(C_{perfusate} - C_{dialysate})}{(C_{perfusate})}$$

Equation 2

While these techniques work well for *in vitro* experiments where analyte concentration can be controlled, probe calibration is more difficult *in vivo* because the concentration of analyte in the sample is unknown and there are additional factors such as tortuosity and metabolism that can affect analyte recovery. Because of this, several methods for determining probe recovery *in vivo* have been developed.

Using the "no-net-flux" method described by Lonnroth et al., the expected *in vivo* analyte concentration is bracketed using varying concentrations of analyte in the perfusate[38]. Once the concentration of the analyte in the perfusate is greater than the *in vivo* concentration, the analyte will begin to diffuse into the tissue. Conversely, when the concentration of analyte in the perfusate is lower than the concentration in the tissue, the analyte will diffuse from the tissue into the dialysate. An example plot of concentration in perfusate versus concentration in dialysate is shown in Figure 1.8. The plot is then used to determine the concentration of analyte in the tissue, which is the point at which there is no-net-flux, represented in red in Figure 1.8. Unfortunately, this method is very time consuming and is not a practical method for monitoring analytes whose concentration can change rapidly *in vivo*.

Another, simpler method for determining probe recovery *in vivo* is using retrodialysis[49]. Retrodialysis is also known as relative delivery. In the same manner as determining delivery *in vitro*, retrodialysis employs spiking the perfusate with a known concentration of an internal standard. The recovery of the analyte is then estimated based on the concept that the delivery across the membrane is the same as recovery across the membrane. While this method is much simpler than no-net-flux, it does not take biological conditions (ischemia, reperfusion, metabolism, etc.) into consideration. Previous studies by the Lunte group have shown that there is little

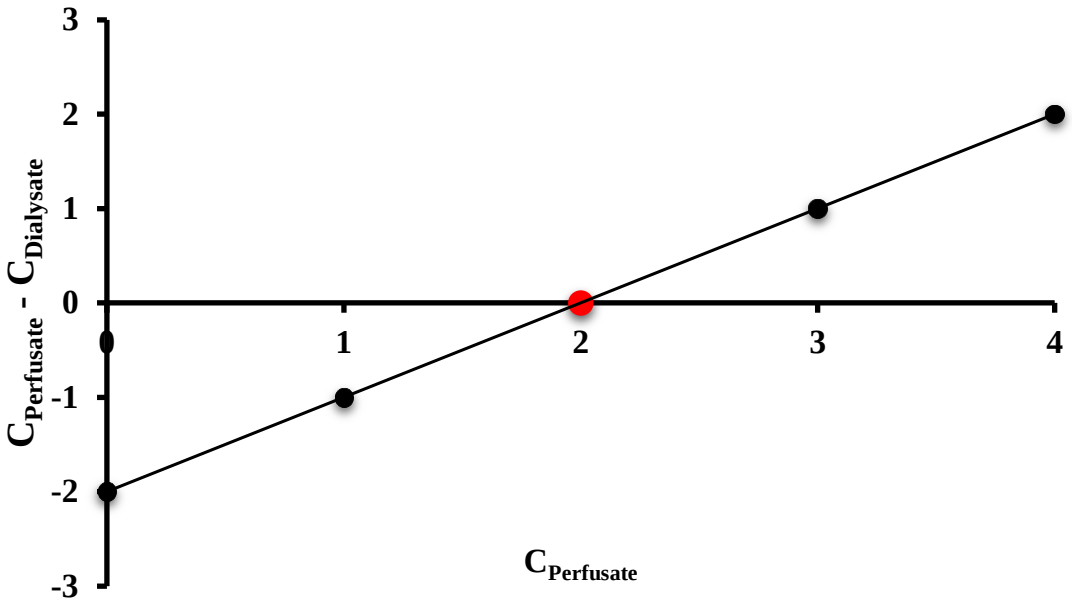

Figure 1.8: Sample plot of no-net-flux experiment

difference between no-net-flux and retrodialysis for a wide range of analytes[50, 51], and for this reason it was employed for all experiments in this research.

1.4.4 Other Sampling Techniques

While microdialysis sampling is currently the most common continuous *in vivo* microsampling technique, other microsampling techniques such as push-pull sampling, ultrafiltration, microextraction, and rapid equilibrium dialysis can also be used to achieve similar results. Each method has its own advantages and disadvantages. Some of these microsampling methods can be used to address certain limitations of microdialysis. While each of the aforementioned methods have been used for many years, recent developments have resulted in their increased utility for *in vivo* microsampling[46].

Ultrafiltration is an *in vivo* microsampling technique that is similar to microdialysis in that sampling occurs across a semipermeable membrane. For ultrafiltration sampling, a vacuum is applied to the probe and sampling occurs via bulk transport of ECF into the probe instead of via diffusion as with microdialysis sampling. Since bulk ECF is collected, the analyte concentration in the sample is the same as that in the tissue and calibration is not required. Like microdialysis, the ultrafiltration membrane excludes macromolecules making sample analysis easier[52]. Since ECF is removed from the sampling site, only tissues with high ECF volumes can be sampled without significant perturbation. The most common sampling sites for ultrafiltration have been the subcutaneous tissue or fluids such as blood. Denser tissues such as brain tissue are unsuitable for ultrafiltration sampling. Because of these limitations, ultrafiltration is not a very common method for *in vivo* sampling but is often used for environmental sampling[53].

The push-pull perfusion method is similar to microdialysis but does not use a membrane. Rather, two syringe pumps are employed with one delivering solution to the sampling site through one cannula and the other used to pull ECF sample from the second cannula[54]. The sample is thus collected via the pulling syringe and the ECF removed is replaced by the pushing syringe. Since bulk ECF is collected through the pull syringe, if the flow is not too high, the concentrations of the analytes in the sample are the same as in the tissue. Therefore, calibration can typically be avoided and because there is no membrane, all size molecules are collected. Thus, push-pull perfusion is directly amenable to sampling peptides and proteins. The major problems associated with the initial push-pull approaches resulted from the force of the push solution causing tissue damage and the pulling cannula being prone to clogging. However, new, low-perfusion push-pull techniques have been developed which allow for a decrease in sample volume while still maintaining good analyte recovery and reducing tissue damage[46].

Another alternative to microdialysis sampling is microextraction. Microextraction is a sampling technique that requires the insertion of a small, semipermeable probe into the desired system. Typically, the membrane is sheathed by a needle that is inserted into the tissue of interest. The membrane is on a solid support that is then ejected out of the needle into the tissue where diffusion of analytes into the probe is allowed to occur. After the allotted amount of time, the membrane is inserted back into the needle and then the needle is removed from the system[55]. Microextraction eliminates the need for excess solvent and also has a short sample collection time compared to push-pull perfusion. Possibly the biggest benefit to microextraction is the direct filtration and purification of the sample via solid-phase extraction. Generally, microextraction probes are connected to a filtration syringe that contains a solid phase purification system[55]. This

removes the need for sample preparation and allows for direct injection into an analytical instrument.

Microextraction can be performed on a small scale, which allows for the collection of samples in delicate *in vivo* systems such as blood capillaries. While microextraction is minimally invasive, not replenishing fluid can create problems in sample collection. The lack of perfusion through the probe can also result in clogged probes. Tissue dehydration and damage can result because fluid is being collected from the tissue and not being replaced. The microextraction method of microsampling allows for the collection of analytes of high molecular weights, which makes this method attractive for peptide and protein studies. Recent probe development has increased the number of semipermeable probes that are inserted into the tissue at one time[56]. This has increased sample through-put, allowing for more samples to be obtained at one time.

1.5 Liquid Chromatography Overview

Because microdialysis sampling produces clean, protein free sample, additional sample clean-up is usually not required, however, implementing a separation method is advantageous. This allows for the easy identification of multiple analytes within the complex *in vivo* samples. Liquid chromatography (LC) is a widely used separation technique that has been around since the 1960s[57]. LC separations are based on the interaction of the analyte with the stationary phase and the mobile phase. There are several different types of stationary phases that can be employed, which are discussed later. Compounds will partition between the stationary phase and the mobile phase based on their affinity for the phase. Retention time is based on the amount of time the compound spends in the stationary phase. A basic LC set-up is shown in Figure 1.9.

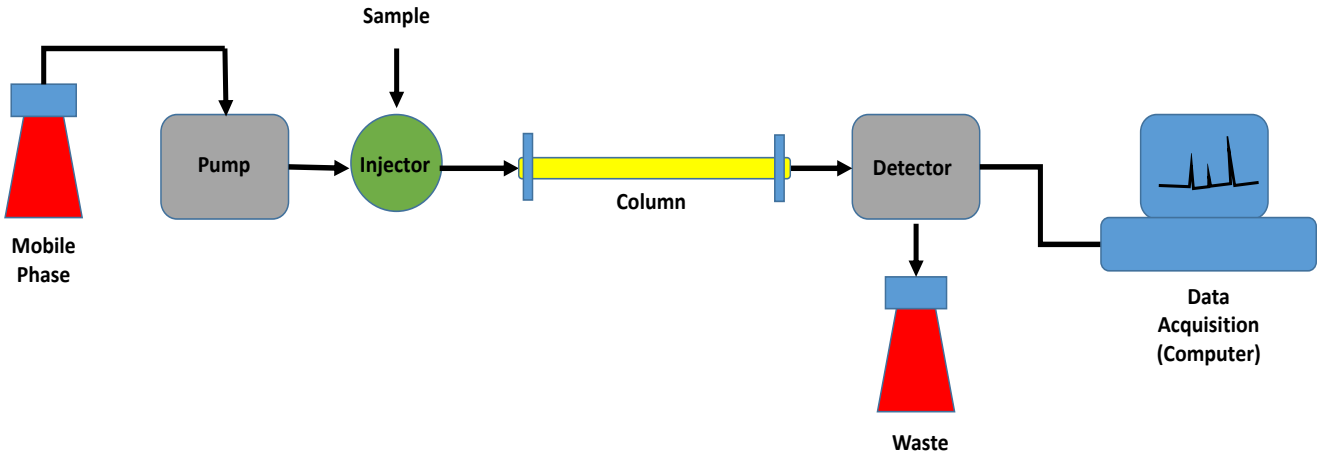

Figure 1.9: Schematic of isocratic liquid chromatography set-up

The mobile phase flows through the pump tubing and an injector port and then flows through the column for separation. The flow continues to allow the analytes to reach the detector that produces a signal that gets translated to the computer as output. The mobile phase is typically filtered and degassed to remove any contaminates, particulates, and oxygen. There are two main types of mobile phase separations, isocratic and gradient[57]. In an isocratic separation, a single pump is used with a single bottle of mobile phase. This is the simplest LC operation and works well for compounds with similar capacity factors and structures. When analytes have a wide range of capacity factors, structures, or chemical properties it becomes necessary to implement a gradient. In this LC operation mode, two pumps are used with two bottles of mobile phase, one containing a high aqueous composition and one containing a high organic composition. By using a gradient, the partitioning of compounds is altered quickly, causing highly retained compounds to elute earlier. This allows for the separation of a wide variety of compounds within one analysis run.

1.5.1 Theory

How long the analyte is retained on the column is mathematically described by the capacity factor k', Equation 3, where t_r is the retention time of the analyte and t_m is the retention time of non-retained compounds. The capacity factor of a compound is determined by the amount of time it spends in the stationary phase[58].

$$k' = \frac{t_r - t_m}{t_m}$$

Equation 3

The longer that compounds are retained on the column, the more time available for separation to occur. Because there is a set flow rate and run time, all compounds will spend the same amount of time in the mobile phase, meaning the separation of multiple compounds will depend on the amount of time spent in the stationary phase[58]. Selectivity, α, is mathematically determined in Equation 4. The capacity factors for two analytes are used to determine the stationary phase's ability to separate the compounds.

$$\propto = \frac{k'_1}{k'_2}$$

Equation 4

Additional chromatographic factors that affect separation include column efficiency (Equation 5), resolution (Equation 6), and theoretical plates (*N*) and plate height (*H*) (Equation 7). Column efficiency affects the width of the peaks.

$$N = 16\left(\frac{t_R}{w}\right)^2$$

Equation 5

A larger *N* value results in more narrow peaks. More narrow peaks means more space for more compounds to be separated. Resolution is the ability to distinguish two analytes based on their

retention time, represented at R_s in Equation 6. Ideally, compounds should be baseline resolved, having a resolution of 1.5, to have consistency in peak analysis.

$$R_s = \frac{1}{4}\sqrt{N}\frac{\propto -1}{\propto}\frac{k'_2}{1 + k'_{avg}}$$

Equation 6

Finally, theoretical plates and plate height represent a hypothetical zone of equilibrium between the mobile phase and the stationary phase[58]. *L* is the length of the column, represented in Equation 7. Longer columns allow for greater separation capacity but can also result in higher diffusion and band broadening.

$$H = \frac{L}{N}$$

Equation 7

The larger the number of theoretical plates (*N*), the more efficient the column. Similarly, the shorter the plate height (*H*), the more efficient the column, which can be observed in the Van Deemter equation (Equation 8). This equation demonstrates how band broadening determines plate height[59]. In this equation, the multiple paths term (A) represents Eddy Diffusion. Because the column is packed with material, there are going to be multiple path options that the analyte can take to make its way to the outlet. This will result in band broadening because a portion of the

analyte will take a faster path and a portion of the analyte will take a slower path. B represents longitudinal diffusion that occurs in the direction of the flow. The longitudinal diffusion considers that the compound will not only be moving horizontally with the flow, but also vertically within the column. Finally, C is the mass transfer term which represents the movement of the mobile phase through the stationary phase. The flow rate is represented by μ. Packing material, column parameters, flow rate, and mobile phase composition can all be adjusted and optimized in order to reduce these effects, thereby decreasing plate height and increasing separation efficiency.

$$H = A + \frac{B}{\mu} + C\mu$$

Equation 9

1.5.2 Stationary Phase

Analyte properties are used to help determine which type of column and mobile phase are required for separation. Normal phase, reverse phase, ion exchange, and size exclusion chromatography are the four most commonly used stationary phases. Reverse phase is by far the most common type of stationary phase and consists of a silica base with carbon chains, typically C-18 or C-8, making it a nonpolar stationary phase. Reverse phase C-18 columns were used in this thesis. Mobile phases with high aqueous content are used with this type of column so that hydrophilic compounds will elute first and hydrophobic compounds will be retained longer. Gradients can be used to increase organic concentration in the mobile phase and force the

hydrophobic compounds off the column. Modifiers can be added to both the mobile phase and stationary phase to improve retention and elution[60].

Normal phase chromatography involves a stationary phase that is more polar than the mobile phase, such as silica. Ion exchange chromatography uses either a cationic or anionic stationary phase to separate compounds based on their charge. Finally, size exclusion chromatography uses a stationary phase with pores that analytes are able to diffuse in and out of based on their size. All modes of separation have their benefits and it is critical to pick a stationary phase based on the analytes to be studied.

1.5.3 Fluorescence Detection of Amino Acid Neurotransmitters

There are many types of detection methods available to analytically determine analytes, each with its own benefits and drawbacks. Fluorescence detection was chosen for this study because it is a highly sensitive method that works for the analysis of many amino acids. According to Jablonski, fluorescence occurs when a molecule absorbs a photon at one wavelength and then emits that photon at a different wavelength due to the release of energy from the vibrational and rotational states[61]. Because energy is emitted from the compound, fluorescence is a direct measurement, making it more sensitive than UV-Vis which is a subtractive technique. Compounds that are highly conjugated are easily detected by fluorescence; because of their pi bonds, they have more orbitals into which the electrons may be excited and relaxed[62]. For compounds that are not highly conjugated, such as the amino acids measured in this thesis, a derivatization reagent such as naphthalene-2,3-dicarboxaldehyde or o-phthalaldehyde-2-mercaptoethanol may be used to form a fluorescent product with the analyte.

1.5.4 Electrochemical Detection of Catecholamine Neurotransmitters

Another mode of detection that provides the limits of detection required for neurochemical studies is electrochemical detection. Two of the most common electrochemical detection (EC) methods are voltammetry and amperometry. Both types of EC typically consist of a working electrode, a reference electrode, an auxiliary electrode, and a potentiostat and can be used for the analysis of electrochemically active compounds. A potential is applied by the potentiostat to the working electrode against a reference electrode. This ensures that the working electrode is experiencing consistent applied voltage. Additionally, because the faradaic current flows between the auxiliary electrode and the working electrode, a drop in potential, known as iR-drop, is avoided, further ensuring that the voltage being applied to the working electrode is correct [63, 64]. Working electrodes can be made of a variety of materials such as glassy carbon, carbon paste, gold, gold/mercury amalgam, and platinum. Reference electrodes are normally Ag/AgCl and the auxiliary electrode is typically made of electrochemically inert material like gold or platinum.

In cyclic voltammetry, the electrode potential is scanned over a range in a cyclic fashion. The applied voltage versus measured current is then plotted. In amperometry, the electrode potential is held constant through the duration of the run and is typically at a positive potential to encourage oxidation of analytes or a negative potential to encourage reduction of analytes. As the molecules interact with the surface of the electrode, current flows to or from the electrode based on the oxidation or reduction of the compound. This change in current produces a measureable signal[65]. The electrode serves as either an oxidizing agent or a reducing agent depending on the potential, making it a valuable detection method for all electrochemically active compounds, including catecholamines and their metabolites.

1.5.5 Mass Spectrometry – Commercially Available Drug Detection

The last detection method that was used in this research was mass spectrometry. Mass spectrometry (MS) provides a highly sensitive detection method based upon the mass-to-charge ratio and abundance of the analyte. Mass spectrometric analysis requires three main components: an ionizer, a mass analyzer, and a detector. The ionizer produces gas phase charged ions of the analyte. There are a variety of ionizers that can be used depending on the analyte and sample matrix. A few examples include fast atom bombardment, atmospheric-pressure chemical ionization, matrix-assisted laser desorption/ionization, and electrospray ionization[66]. In this research, electrospray ionization was used, which utilizes a high voltage spray of electrons to bombard the analyte, thereby creating an aerosol of ions which gets sent to the mass analyzer. Mass analyzers separate ions based on their mass-to-charge ratio. Some of the most common mass analyzers include time-of-flight, ion trap, and quadrupole. For the purpose of this research a triple quadrupole mass analyzer provided sufficient sensitivity for the study. A quadrupole mass analyzer uses oscillating electrical fields that either stabilize or destabilize the path of the ions toward the detector[67]. Ions will approach the detector depending on their mass-to-charge ratio and the potential of the 4 oscillating poles. In a triple quadrupole mass analyzer, the analyte must pass through three quadrupoles to reach the detector. The first functions as a mass analyzer to separate out the molecule with the mass-to-charge ratio of interest. This is known as the parent ion. The second quadrupole functions as a collision chamber, fragmenting the molecule into product or "daughter" ions. The final quadrupole also works as a mass analyzer and can be used to transmit the product ions of interest toward the detector. By fragmenting the parent ion and detecting the daughter ions, selectivity is greatly increased[68]. Finally, ions that reach the detector are then converted from charge/current to signal, typically using an electron multiplier.

1.6 Overview of the Research

The goal of the research was to develop and optimize a rat epilepsy model exhibiting multiple local seizures. Because patients are diagnosed with epilepsy after having two or more unprovoked seizures, two seizure episodes were induced within the same experiment. Only local seizures were explored, as they are not as well understood as global seizures. Chapter two discusses the development of an anesthetized, multiple-seizure rat model for epilepsy. In this model, two local seizures stimulations were induced by locally dosing 3-mercatopropionic acid directly into the hippocampus of an anesthetized rat using microdialysis. Samples were collected and analyzed for both catecholamine and amino acid neurotransmitters. Various time dosing regimens were explored to determine if time between seizures affected the biochemical responses to the epileptic agent. Upon development of the model, unexpected attenuation in glutamate release was observed in the second seizure stimulation. Because the ultimate goal of the research was to thoroughly investigate multiple seizures at a neurochemical level, a series of experiments were conducted to determine the cause of such attenuated glutamate release. Chapter three discusses these studies.

In Chapter 3, the same experimental procedures as in chapter two were followed; however, several neurochemical pathways were investigated to determine the cause of the glutamate release attenuation. Metabolic, energy, and transport pathways were investigated by spiking the perfusion fluid with either glucose, lactate, or dihydrokainic acid. Neuronal staining was also performed to determine the amount of viable neurons after the induction of the first seizure. Once the model was better understood, correlations between local epilepsy and oxidative stress could be made.

Chapter four discuss experiments that were performed to investigate the upregulation and downregulation of biomarkers of oxidative stress associated with epilepsy. Thiol levels were

depleted by buthionine sulfoxime or enhanced by ɣ-glutamylcysteine ethyl ester. Upregulation and downregulation of oxidative stress biomarkers during epileptic seizures allowed for conclusions to be made about the secondary oxidative effects of epilepsy. Chapter five is a summary of the research conducted, conclusions, and future directions of the research.

Finally, appendix one discusses a smaller *in vitro* pharmacokinetic project that was conducted using microdialysis. In this study, 12 different commercially available drugs were individually spiked in human plasma to determine plasma protein binding. Protein bound drugs ranging from 6% to 99.7% bound were explored to validate microdialysis as a plasma protein binding assay. This technique can also be applied for the *in vivo* determination of protein bound drugs.

1.7 References

1. Frantseva, M., Velazquez, J. P., Tsoraklidis, G., Mendonca, A., Adamchik, Y., Mills, L., Carlen, P., and Burnham, M. (2000) Oxidative stress is involved in seizure-induced neurodegeneration in the kindling model of epilepsy, *Neuroscience 97*, 431-435.
2. Love, S. (1999) Oxidative stress in brain ischemia, *Brain Pathology 9*, 119-131.
3. Emerit, J., Edeas, M., and Bricaire, F. (2004) Neurodegenerative diseases and oxidative stress, *Biomedicine & pharmacotherapy 58*, 39-46.
4. Uttara, B., Singh, A. V., Zamboni, P., and Mahajan, R. T. (2009) Oxidative Stress and Neurodegenerative Diseases: A Review of Upstream and Downstream Antioxidant Therapeutic Options, *Current Neuropharmacology 7*, 65-74.
5. (1981) *Neurotransmitters, seizures, and epilepsy*, New York : Raven Press, New York.
6. Engel, J. (2013) *Seizures and epilepsy*, Vol. 83, Oxford University Press.
7. (1993) *Epilepsy : models, mechanisms, and concepts*, Cambridge New York : Cambridge University Press, Cambridge New York.
8. Halliwell, B., and Gutteridge, J. M. (2015) *Free radicals in biology and medicine*, Oxford University Press, USA.
9. Hart, R. G. Seizure recurrence after a first, unprovoked seizure, *Archives of neurology (Chicago) 43*, 1289-1290.
10. Organization, W. H. (2016) Epilepsy Fact Sheet
11. Jiang, Y. Ketogenic diet protects against epileptogenesis as well as neuronal loss in amygdaloid-kindling seizures, *Neuroscience letters 508*, 22-26.

12. French, J. A. M. D., and Pedley, T. A. M. D. (2008) Initial Management of Epilepsy, *The New England Journal of Medicine 359*, 166-176.

13. Goddard, G. V. (1967) Development of Epileptic Seizures through Brain Stimulation at Low Intensity, *Nature 214*, 1020-1021.

14. Osorio, I. Automated seizure abatement in humans using electrical stimulation, *Annals of neurology 57*, 258-268.

15. Medical causes of seizures, *Lancet 352*, 383.

16. Sutula, T. P. (1990) Experimental models of temporal lobe epilepsy: new insights from the study of kindling and synaptic reorganization, *Epilepsia 31*, S45-S54.

17. Haneef, Z. Functional connectivity of hippocampal networks in temporal lobe epilepsy, *Epilepsia (Copenhagen) 55*, 137-145.

18. (2009) Animal models of epilepsy methods and innovations, (Baraban, S. C., Ed.), Totowa, NJ : Humana Press, Totowa, NJ.

19. Mares, P. Models of Epileptic Seizures in Immature Rats, *Physiological research 61*, S103-S108.

20. Mayer, A. (2010) Local Dosing in a 3-Mercaptopropionic Acid Chemically-Induced Epileptic Seizure Model with Microdialysis Sampling, (Lunte, C. E., Dunn, B., Johnson, M., Lunte, S., and Osorio, I., Eds.), ProQuest Dissertations Publishing.

21. Crick, E. (2007) In vivo microdialysis coupled with electrophysiology for the neurochemical analysis of epileptic seizures, (Lunte, C. E., Dunn, R., Johnson, M., Lunte, S., and Rivera, M., Eds.), ProQuest Dissertations Publishing.

22. McNamara, J. O., Byrne, M. C., Dasheiff, R. M., and Fitz, J. G. (1980) The kindling model of epilepsy: a review, *Progress in neurobiology 15*, 139-159.

23. Osorio, I., Frei, M. G., Manly, B. F., Sunderam, S., Bhavaraju, N. C., and Wilkinson, S. B. (2001) An introduction to contingent (closed-loop) brain electrical stimulation for seizure blockage, to ultra-short-term clinical trials, and to multidimensional statistical analysis of therapeutic efficacy, *Journal of Clinical Neurophysiology 18*, 533-544.

24. Siah, B. H. Suppression of acute seizures by theta burst electrical stimulation of the hippocampal commissure using a closed-loop system, *Brain research 1593*, 117-125.

25. Sastchenko, L. P. Inhibition of L-glutamic acid decarboxylase by cycloglutamates, *Biochemistry (Easton) 10*, 4888-4894.

26. Horton, R. W., and Horton, R. W. Seizures induced by allylglycine, 3-mercaptopropionic acid and 4-deoxypyridoxine in mice and photosensitive baboons, and different modes of inhibition of cerebral glutamic acid decarboxylase, *British journal of pharmacology 49*, 52-63.

27. Bradford, H. F. Glutamate, GABA and epilepsy, *Progress in neurobiology 47*, 477-511.

28. Sun, Y., and Yu, S. Mechanism of glutamate receptor desensitization, *Nature (London) 417*, 245-253.

29. Muthukumaraswamy, S. D. The effects of elevated endogenous GABA levels on movement-related network oscillations, *NeuroImage (Orlando, Fla.) 66*, 36-41.

30. Olsen, R. W. GABA and Epileptogenesis, *Epilepsia (Copenhagen) 38*, 399-407.

31. Cubells, J. F. In vivo action of enzyme-activated irreversible inhibitors of glutamic acid decarboxylase and gamma-aminobutyric acid transaminase in retina vs. brain, *The Journal of pharmacology and experimental therapeutics 238*, 508-514.

32. Fan, S., Wusteman, M., and Iversen, L. (1981) 3-Mercaptopropionic acid inhibits GABA release from rat brain slices in vitro, *Brain research 229*, 371-377.

33. Netopilov, aacute, and Miloslava. Inhibition of glutamate decarboxylase activity by 3-mercaptopropionic acid has different time course in the immature and adult rat brains, *Neuroscience letters 226*, 68-70.

34. Ma, D. Simultaneous determination of gamma-aminobutyric acid and glutamic acid in the brain of 3-mercaptopropionic acid-treated rats using liquid chromatography-atmospheric pressure chemical ionization mass spectrometry, *Journal of chromatography. B, Biomedical sciences and applications 726*, 285-290.

35. Crick, E. W. Correlation of 3-mercaptopropionic acid induced seizures and changes in striatal neurotransmitters monitored by microdialysis, *European journal of pharmaceutical sciences 57*, 25-33.

36. Crick, E. W. An investigation into the pharmacokinetics of 3-mercaptopropionic acid and development of a steady-state chemical seizure model using in vivo microdialysis and electrophysiological monitoring, *Epilepsy research 74*, 116-125.

37. Chaurasia, C. S. In vivo microdialysis sampling: theory and applications, *Biomedical chromatography 13*, 317-332.

38. Davies, M. I. Analytical considerations for microdialysis sampling, *Advanced drug delivery reviews 45*, 169-188.

39. (2011) *Applications of Microdialysis in Pharmaceutical Science*, Wiley, Hoboken, US.

40. Stenken, J. A. Factors that influence microdialysis recovery. Comparison of experimental and theoretical microdialysis recoveries in rat liver, *Journal of pharmaceutical sciences 86*, 958-966.

41. Boschi, G. Brain microdialysis in the mouse, *Journal of pharmacological and toxicological methods 33*, 29-33.

42. Petzold, A., and Petzold, A. In vivo monitoring of neuronal loss in traumatic brain injury: a microdialysis study, *Brain (London, England : 1878) 134*, 464-483.

43. Zuo, H., Ye, M., and Davies, M. (1995) The linear probe: a flexible choice for in vivo microdialysis sampling in soft tissues, *Current Separations 14*, 54-57.

44. Nicolazzo, J. A. Methods to assess drug permeability across the blood-brain barrier, *Journal of pharmacy and pharmacology 58*, 281-293.

45. Joukhadar, C. (2005) Microdialysis - Current applications in clinical pharmacokinetic studies and its potential role in the future, *Clinical pharmacokinetics 44*, 895-913.

46. Patricia, Z., and Gary, T. E. (2013) *Microsampling in Pharmaceutical Bioanalysis*, Future Science Ltd.

47. Buttler, T., ouml, and rn. Membrane characterisation and performance of microdialysis probes intended for use as bioprocess sampling units, *Journal of chromatography. A 725*, 41-56.

48. Menacherry, S. In vivo calibration of microdialysis probes for exogenous compounds, *Analytical chemistry (Washington) 64*, 577-583.

49. Melgaard, L., Hersini, K. J., Gazerani, P., and Petersen, L. J. (2013) Retrodialysis: a review of experimental and clinical applications of reverse microdialysis in the skin, *Skin pharmacology and physiology 26*, 160-174.

50. Song, Y. Comparison of calibration by delivery versus no net flux for quantitative in vivo microdialysis sampling, *Analytica chimica acta 379*, 251-262.

51. Davies, M. I. (1995) Microdialysis sampling for in vivo hepatic metabolism studies, Thesis (Ph. D.)--University of Kansas, Chemistry, 1995.

52. Lam, H., Davies, M., and E. Lunte, C. (1996) Vacuum ultrafiltration sampling for determination of plasma protein binding of drugs, *Journal of pharmaceutical and biomedical analysis 14*, 1753-1757.

53. Jensen, B., Chin, P., and Begg, E. (2011) Quantification of total and free concentrations of R- and S-warfarin in human plasma by ultrafiltration and LC-MS/MS, *Anal Bioanal Chem 401*, 2187-2193.

54. Wotjak, C. T. Release of vasopressin from supraoptic neurons within the median eminence in vivo. A combined microdialysis and push-pull perfusion study in the rat, *Brain research 726*, 237-241.

55. Scheppers Wercinski, S. A. (1999) *Solid Phase Microextraction : A Practical Guide*, CRC Press, New York.

56. Oca, ntilde, a, G., aacute, and lez, J. A. New developments in microextraction techniques in bioanalysis. A review, *Analytica chimica acta 905*, 8-23.

57. Snyder, L. R. (1974) *Introduction to modern liquid chromatography*, New York, Wiley, New York.

58. Xu, Q. A. (2013) *Ultra-High Performance Liquid Chromatography and Its Applications (1)*, Wiley, Somerset, US.

59. Gritti, F. (2016) General theory of peak compression in liquid chromatography, *Journal of Chromatography A 1433*, 114-122.

60. Shi, X., Qiao, L., and Xu, G. (2015) Recent development of ionic liquid stationary phases for liquid chromatography, *Journal of Chromatography A 1420*, 1-15.

61. Lakowicz, J. R. (2006) Principles of fluorescence spectroscopy, (SpringerLink, and Springer-Verlag, S., Eds.) 3rd ed.. ed., New York : Springer, New York.

62. (1990) *Practical fluorescence*, 2nd ed., rev. and expanded.. ed., New York : M. Dekker, New York.

63. Gilinsky, M. A. Determination of myocardial norepinephrine in freely moving rats using in vivo microdialysis sampling and liquid chromatography with dual-electrode amperometric detection, *Journal of pharmaceutical and biomedical analysis 24*, 929-935.

64. Thorr, eacute, and K. New antioxidant mixture for long term stability of serotonin, dopamine and their metabolites in automated microbore liquid chromatography with dual electrochemical detection, *Journal of chromatography. B, Biomedical sciences and applications 694*, 297-303.

65. Bard, A. J., and Murray, R. W. (2012) Electrochemistry, *Proceedings of the National Academy of Sciences of the United States of America 109*, 11484-11486.

66. Annesley, T. M. Ion suppression in mass spectrometry, *Clinical chemistry (Baltimore, Md.) 49*, 1041-1044.

67. Menet, M.-C. (2011) Mass spectrometry, *Revue Francophone des Laboratoires 2011*, 41.

68. Roboz, J. (1979) *Introduction to mass spectrometry : instrumentation and techniques*, Huntington, N.Y. : R. E. Krieger Pub. Co., Huntington, N.Y.

Chapter 2

Development of 3-Mercaptapropionic Acid Induced Multiple Seizure Animal Model

2.1 Background and Significance of Research

Epilepsy is a neurological disorder that is diagnosed when patients experience two or more seizure[1]. These seizures may occur as a result of a variety of factors including genetic disposition, excitotoxicity, and oxidative stress. However, the exact mechanism of action of seizure onset is unclear. Several hypotheses have been investigated as possible causes of seizures including disruption of pathways and excitatory neuronal emission[2-6]. Recent research has demonstrated that oxidative stress and the development of epilepsy have a cyclic relationship[7-9]. In order to better understand this relationship, we must first better understand epilepsy as a whole.

There are two main types of seizures that patients can experience, global seizures and local (focal) seizures. These categories can be broken down even further to simple local, complex local, myoclonic and tonic clonic. Previous members of the Lunte research lab developed animal models for global seizures[10] and local seizures[11]. However, by definition, patients must experience two or more seizures to be diagnosed with epilepsy; therefore, these models are seizure models and not true epilepsy models. Dr. Andrew Mayer performed preliminary experiments toward developing an animal model for local epilepsy[11]. The research discussed here further investigated and developed this model.

Microdialysis was used to locally dose the hippocampus of a rat with an epileptogenic agent, 3-MPA, while simultaneously collecting dialysate for analysis. The 3-MPA was administered at two separate time points within one experiment, simulating two consecutive seizure episodes that would define this outcome as fitting the definition of epilepsy. Various time

regimens were explored to investigate the animal's response to the epileptic agent. A statistical comparison between the first and second seizure event was done to demonstrate the neurochemical effect of inducing multiple seizure episodes.

2.1.1 Global Epilepsy – Previous Models

Global seizures are most commonly associated with epilepsy. These are also known as generalized seizures or tonic-clonic seizures because they affect the electrical activity in both hemispheres of the brain. There are two main phases in these seizures, the tonic phase and the clonic phase. In the tonic phase, the patient loses consciousness, muscles tense, and the body become rigid[12, 13]. This phase typically only lasts for a few seconds before the patient moves into the clonic phase. In the clonic phase, the neuronal misfiring causes the muscular system to rapidly contract and release repeatedly; this is known as convulsions. This phase can last for several minutes to hours. When the patient regains consciousness, nervous exhaustion often occurs, patients have difficulty breathing, and at times patients have no memory of the seizure[12-14]. Because these physiological symptoms are so severe, it is easy to diagnose patients with global seizures and in many cases the symptoms can be controlled with prescription medication.

An animal model to simulate global seizures was previously developed in the Lunte Lab by Eric Crick[15-17]. In this model, a systemic dose of 3-MPA was administered to the intraperitoneal cavity, followed by a constant intravenous infusion of 3-MPA to the femoral artery to maintain status epilepticus, or global seizure status, for 50 minutes. 3-MPA, glutamate, and GABA were all monitored via microdialysis using a probe that had been implanted into the CA3 region of the hippocampus (-5.6 A/P, +4.8 L/M, -7.0 D/V versus bregma). Following the induction of the

seizure, there was an increase in extracellular glutamate concentration and a decrease in GABA concentration in the dialysate, as was expected based on the mechanism of action of 3-MPA. Upon cessation of the 3-MPA infusion, both neurotransmitters returned to basal levels. The neurochemical response can be seen graphically in Figures 2.1.

2.1.2 Local Epilepsy – Previous Models

The second main type of seizures that patients can experience is local seizures, or partial seizures. As their name suggests, these seizures only affect the neuronal firing in one region of the brain, or in only one hemisphere[18, 19]. There are a wide range of symptoms that patients can experience from local seizures. Depending on the brain region being affected, seizures may cause sudden mood change, the feeling of *déjà-vu*, altered sense of hearing, smelling, or seeing, spatial distortion, muscle tremors, or hallucinations[18, 20]. Because these symptoms are not as severe, many times local seizures go undiagnosed and patients do not receive proper treatment. The specificity and unpredictability of these seizures make them difficult to investigate. For these reasons, a model for local seziures was developed by the Lunte group in the hopes of gaining a better understanding of the neurochemical processes that occur during a local seizure.

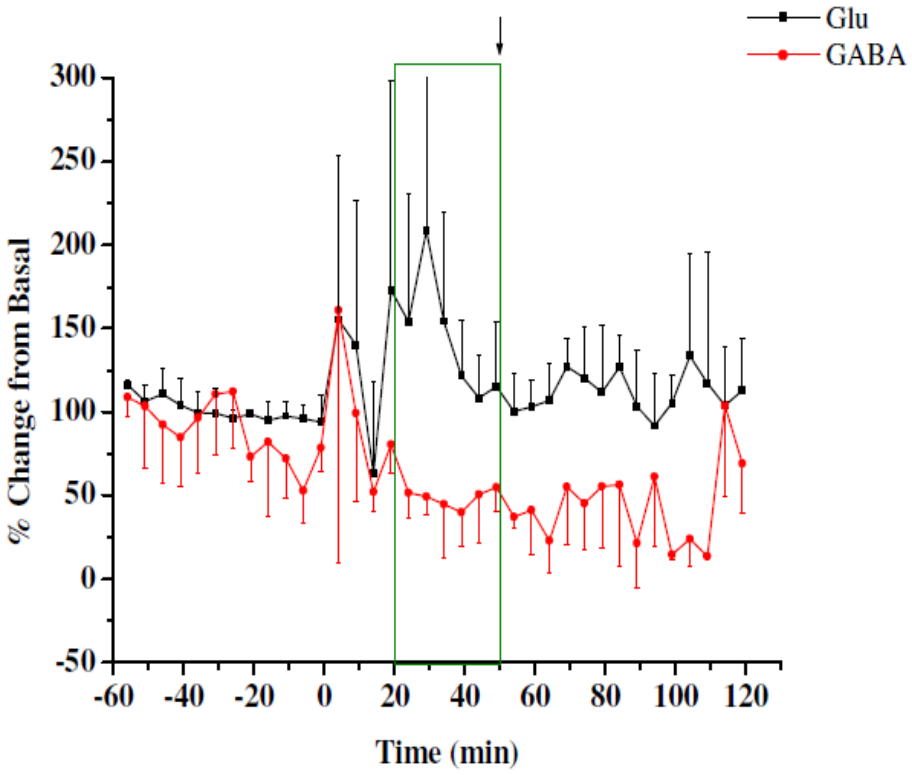

Figure 2.1: Glutamate and GABA response from systemically induced global seizure[15].

Reproduced from the thesis by Dr. Eric Crick. Bolus systemic dose of 3-Mercaptopropionic acid was administered at *t*=0 and constantly perfused through the femoral vein for 50 minutes (represented by green box) N=3

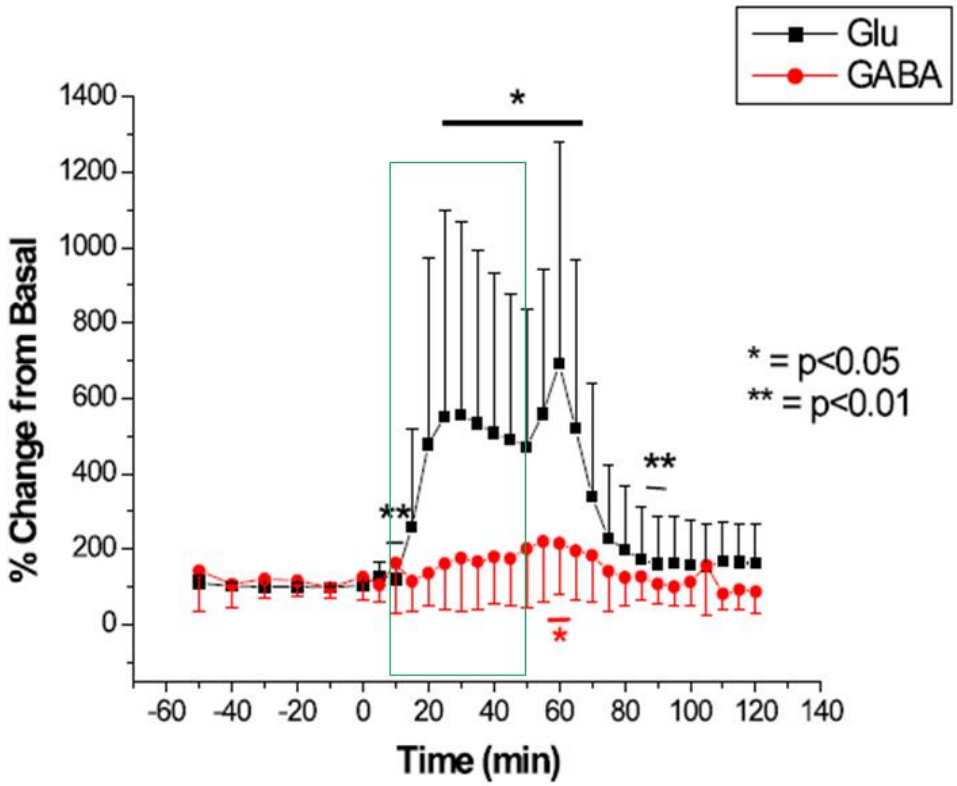

Figure 2.2: Glutamate and GABA response to locally induced seizure with perfusion of 3-MPA through the microdialysis probe.

Reproduced from the thesis by Dr. Andrew Mayer. Constant perfusion of 3-MPA through the probe occurred for 50 minutes starting at *t*=0, represented by the green box. (N=9)

Andrew Meyer directly dosed 3-MPA through the microdialysis probe to the CA1 region of the hippocampus (-3.3 A/P, +1.7 L/M, -3.7 D/V versus bregma)[21]. To mimic the conditions used by Crick, Meyer also constantly perfused the epileptic agent through the probe for 50 minutes (Figure 2.2). Once again, an increase in glutamate was observed, however a significantly higher percent change from basal occurred with the local dose in comparison to the systemic dose (Figure 2.1 versus Figure 2.2). Additionally, an increase in GABA was observed as opposed to the anticipated decrease. These results led us to add a second seizure episode to the model and investigate the time between the two seizure inductions to see if varying the time affected the neurochemical response.

2.1.3 Hippocampus

When human patients experience local seizures, the medial temporal network is typically affected. This network includes the hippocampus, amygdala, entorhinal cortex, lateral temporal neocortex, medial thalamus, and inferior frontal lobes of the brain[22]. The hippocampus is commonly associated with the local seizures observed in temporal lobe epilepsy. The hippocampus is part of the limbic system, which is responsible for both short and long-term memory and spatial navigation[5, 23, 24]. The tissue is curved (typically referred to as seahorse-shaped) and can be divided into three main regions: the dentate gyrus, the hippocampus proper, and the subiculum[18]. The hippocampus proper is also known as the Cornu Ammonis (CA) region and can be broken down even further into three sub-fields, CA1, CA2, and CA3. All three regions contain pyramidal neurons; however, the size of neurons varies depending on the region. Neurons increase in size from CA1 to CA3. Because CA1 is comprised of smaller neurons, they form a

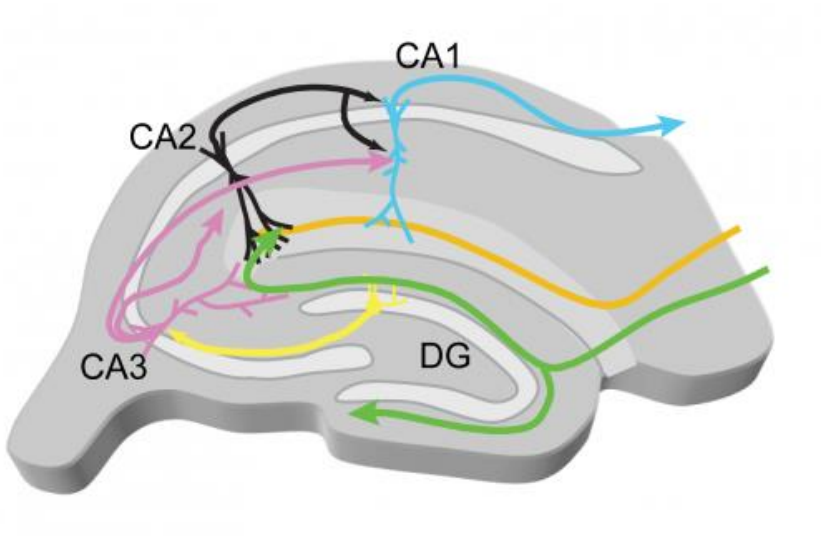

Figure 2.3: Neuronal pathways in the hippocampus

http://www.biomedicale.parisdescartes.fr/physiocer/?page_id=2942

dense network. The CA3 region contains pyramidal cells and commissural fibers that are responsible for transmitting signals to other areas of the hippocampus and the brain[25, 26]. Hippocampal signaling is unidirectional and follows the pathways shown in Figure 2.3. Because the hippocampus is one of the most electrically excitable parts of the brain, it can be easily damaged by repeated seizure induction[19, 26, 27]. The hippocampus has a highly dense network of neurons, and these neurons are constantly being regenerated throughout a lifetime, unless they are permanently damaged. For this reason, the hippocampus has been studied in a wide variety of rodent models for neurological disease[2, 28, 29].

2.1.4 Amino Acid Neurotransmitters

Amino acid neurotransmitters are small molecules that transmit information across the synapses in the brain. There are two main categories of amino acid neurotransmitters, inhibitory and excitatory. They can either be taken up into the cell through transport carriers or be released from the cell via exocytosis[30-32]. During exocytosis, the neurotransmitters are released into the synapse where they can bind to receptors. Excitatory amino acids bind to G-protein coupled receptors that may contain ion channels and allow positively charged ions such as Na^+ to enter the cell[30, 33]. This results in a depolarization and generates an excitatory response. Conversely, amino acids that open ion channels to allow negatively charged ions flow into the cells are known as inhibitory neurotransmitters. The most common excitatory neurotransmitter is glutamate and the most common inhibitory neurotransmitter is GABA[34-37]. It is essential to have a balance between the two in order to maintain normal polarization in brain neurons. If there is an imbalance between the two, a seizure can occur. In the present experiments, glutamate and GABA were monitored to

determine to what extent 3-MPA is capable of inducing such an imbalance and if this results in a seizure[38].

2.1.5 Catecholamine Neurotransmitters

Monoamine or catecholamine neurotransmitters are compounds that contain a catechol group with an amino acid. In the brain, they are synthesized from aromatic amino acids such as tyrosine and tryptophan. Norepinephrine and dopamine function as neuromodulators that regulate a variety of neuronal processes such as stress, hormones, and blood circulation by spending a long time in the extracellular space[39-41]. In these studies, norepinephrine (NE) and dopamine (DA) were measured in the brain to investigate their involvement in oxidative stress and seizure induction. Additionally, analyzing a class of neurotransmitters that are not directly affected by the epileptic agent, the extent of neuronal damage during a seizure can be determined[42-44].

2.2 Materials and Methods

2.2.1 Chemicals and Reagents

Monobasic sodium phosphate, dibasic sodium phosphate, sodium chloride, potassium chloride, magnesium chloride, calcium chloride, disodium ethylenediaminetetraacetate (Na2EDTA), 85% o-phosphoric acid, and 0.3-μm alumina powder were purchased from Fisher Scientific (Pittsburgh, PA). L-aspartic acid, L-glutamic acid, L-arginine, L-alanine, γ-aminobutyric acid, 3-mercaptopropionic acid, ammonium acetate, 1-octanesulfonic acid, HPLC-grade methanol, and HPLC-grade tetrahydrofuran were purchased from Sigma-Aldrich (St. Louis,

MO). ARC/ARG3.1 Antibody was purchased from Novus Biologics (Littleton, CO) and Anti-Synaptophysin antibody was purchased from Abcam (Cambridge, MA). Ketamine HCl was obtained from Fort Dodge Animal Health (Fort Dodge, IA). Xylazine was obtained from Lloyd Laboratories (Shenandoah, IA). All solutions in water were prepared with 18.2-MΩ distilled, deionized water (Labconco, Kansas City, MO). Artificial cerebral spinal fluid (aCSF) was prepared in house and sterile filtered before use. (145 mM NaCl, 2.7 mM KCl, 1.0 mM $MgCl_2$, 1.2 mM $CaCl_2$, 0.45 mM NaH_2PO_4, and 2.33 mM Na_2HPO_4).

2.2.2 Liquid Chromatography-Fluorescence Detection

A liquid chromatographic system with fluorescence detection was used for the analysis of the amino acid neurotransmitters in the microdialysis samples. The method was adapted from Shah et al.[45]. The system consisted of two Shimadzu LC-10ADvp pumps, a 100 µL Shimadzu mixer, and a Rheodyne 9725i PEEK sample injector connected to a Phenomenex Synergi 4-µm Hydro-RP column (150 × 2.0 mm, Phenomenex, Torrance, CA) with a Phenomenex C18 guard cartridge. The binary gradient was controlled by a Shimadzu SCL-10vp system controller. Mobile phase A was a 95% 50 mM ammonium acetate buffer:5% THF (v:v), pH 6.4. Mobile phase B was 100% methanol. The gradient was as follows: 1-6 min, 45-60% B; 6-9 min, 60% B; 9-11.5 min, 60-90% B; 11.5-12 min, 90-45% B; 12-15 min, 45% B. The Shimadzu 10AXL fluorescence detector was operated at an excitation wavelength of 442 nm and an emission wavelength of 490 nm.

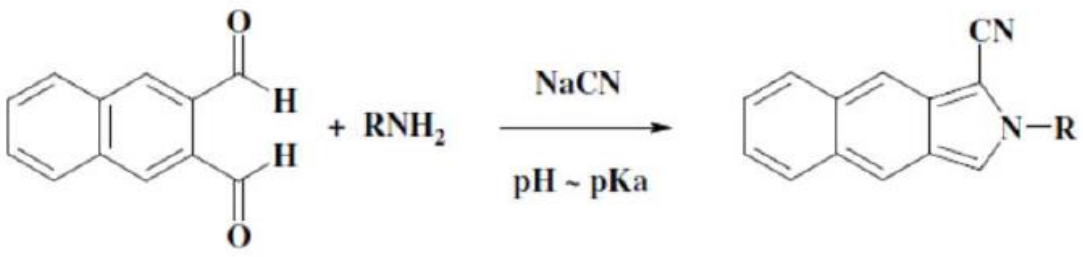

NDA **CBI derivative**

Figure 2.4: Derivatization of primary amines with NDA/CN

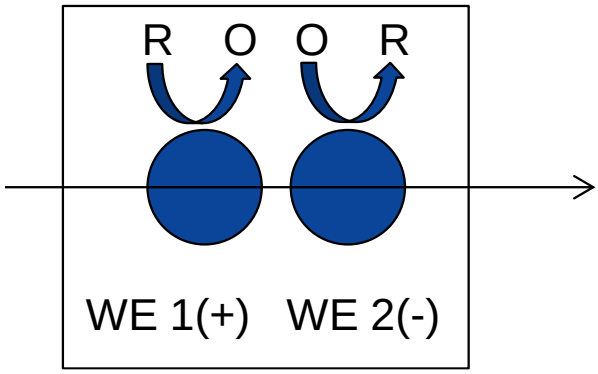

Figure 2.5: Dual electrode series configuration for electrochemical detection of catecholamines.

Working Electrode 1: +0.75V, Working Electrode 2: -0.20V vs. Ag/AgCl reference electrode

2.2.3 Derivatization Mechanism

Since the amino acids of interest are not naturally fluorescent, derivatization was carried out prior to sample analysis. The primary amines were derivatized with naphthalene-2,3-dicarboxyaldehyde (NDA) following the reaction in Figure 2.4 described by De Montigny[46]. Briefly, 1.0 μL of 500-mM borate with 87 mM CN^- (100:20 v:v) and 1.0 μL of 3 mM NDA in a methanol:water solution (50:50, v:v) was added to 3 μL of microdialysate. The samples were allowed to react for 30 minutes in the dark. After the derivatization was complete, 4.0 μL of the sample was injected for analysis. Samples are stable for up to 12 hours, however, they were analyzed as soon as possible to prevent any possible degradation.

2.2.4 Liquid Chromatography-Electrochemical Detection

A liquid chromatographic system with electrochemical detection was used for the analysis of the catecholamine neurotransmitters dopamine and norepinephrine in brain microdialysate. The system consisted of a Shimadzu LC-20AD pump, a Rheodyne 9725i PEEK sample injector, and an LC-4C potentiostat (Bioanalytical Systems, West Lafayette, IN) with an Agilent ZORBAX 3.5-μm SB-C18 column (1 × 50 mm, Agilent Technologies, Santa Clara, CA). The mobile phase was adapted from Stenken et al. and consisted of a phosphate buffer with methanol (90:10, v:v)[47, 48]. Specifically, 100 mM NaH_2PO_4, 2 mM Na_2EDTA, and 0.75 mM SOS, adjusted to pH 3.5 with 85% o-phosphoric acid.

Electrochemical detection was performed in series using the glassy carbon working electrode set-up shown in Figure 2.5. Preparation and use of the electrodes have been described previously[49, 50]. Briefly, a 3 mm glassy carbon electrode embedded in a PEEK block (Bioanalytical

Systems, West Lafayette, IN) was polished with various grit size diamond polish (Bioanalytical Systems, West Lafayette, IN) followed by 0.3-μm alumina powder. The electrode was then rinsed with methanol and water. The surface of the electrode was carefully dried with a KimWipe and placed into the electrochemical flow cell. The electrode was allowed to equilibrate with the mobile phase and charging current for a minimum of one hour after applying the potential. The detection of the catecholamine neurotransmitters were observed at working electrode 1 at an oxidation potential of +750 mV versus an Ag/AgCl reference electrode. The data were collected at 10 Hz with a range of 10 nA and processed using a Chrom&Spec chromatography data system (Ampersand International, Beachwood, OH).

2.2.5 Determination of Neuronal Activation

Physiological recordings such as electrocorticography (ECoG) recordings may be used to measure the changes in neuronal activity associated with seizures. Electrocorticography, or ECoG, recordings are a type of electrophysiological monitoring in which electrodes are placed directly on the exposed surface of the brain[51]. Small holes are drilled into the skull so that the electrodes can make contact with the cortex. Dr. Meyer noticed that with the systemic dosing of the epileptic agent 3-MPA, changes in electrical activity were observed. This indicates that the animal is experiencing a global seizure because the entire brain is being affected. With locally induced seizures, only a minimal change in electrical activity was observed using the ECoG recordings in his studies. According to his analysis, this was not enough to confirm seizure activity. Examples of both systemic and local dosing ECoG recordings taken by Dr. Meyer can be seen in Figure 2.6[11]. It is hypothesized that because such a small region and so few neurons are being affected

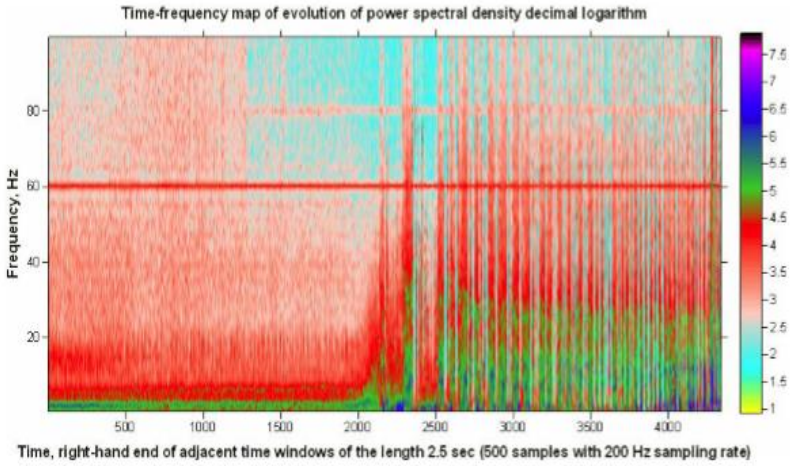

Systemic Dosing

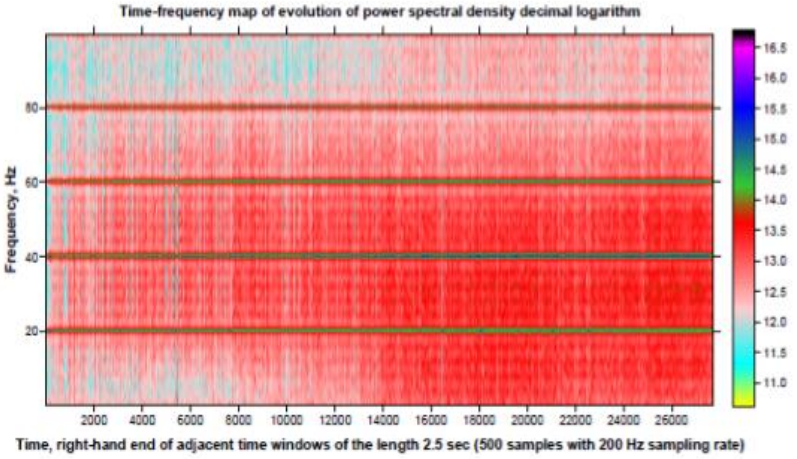

Local Dosing

Figure 2.6: Sample electrocorticographs from both systemic and locally induced seizures.

Reproduced by the thesis by Dr. Meyer[11]

by the local dosing, there is not a large enough change in electrical activity to be detected by the ECoG electrodes. In order to verify that the local perfusion of 3-MPA was in fact inducing seizures, we chose to use immunohistochemical staining to measure the amount of neuronal activation.

2.2.5.1 ARC Staining

Activity-regulated cytoskeleton-associated protein (ARC) is a marker for synaptic activation and synaptic plasticity. ARC is part of a rapidly activated class of genes that are categorized by their ability to be transcribed in the presence of protein synthesis inhibitors[52, 53]. ARC is localized in activated synaptic sites dependent on glutamate-NMDA receptors. The presence of newly transcribed protein signifies neuronal activation and plasticity. ARC regulates the endocytosis of AMPA receptors. AMPA receptors are glutamate receptors that mediate fast synaptic transmission in the central nervous system. By quantifying ARC, we are able to quantify the amount of glutamate-driven synaptic activity, in this case representing a seizure. ARC is localized to the synapses, making it easy to stain using antibodies and therefore quantify. In order to confirm that the local perfusion of the 3-MPA led to neuronal activation and synaptic transcription, animals were sacrificed after 15 minutes of the start of 3-MPA perfusion, brains were harvested for immunohistochemical staining, described in detail later.

2.2.5.2 Synaptophysin

Synaptophysin is a synaptic vesicle glycoprotein that is present in neuronal cells and all other cells involved in synaptic transmission[54, 55]. Its exact function is not known; however,

knockout studies in mice show behavioral changes, specifically dealing with spatial learning. Its presence at the synapse allows for immunostaining which can be used for quantification of total synapses. Antibodies for both ARC and synaptophysin were used to quantify both total and activated synapses to determine what percent of synapses have been activated. Further explanation of tissue staining protocols as well as quantitative results are describe later in this chapter.

2.3 Surgical Procedures

2.3.1 Animal and Instrumentation Preparation

Surgical tools were sterilized using ROCCAL® prior to every experiment. Because these were not survival surgeries, autoclave sterilization was not necessary. Male Wistar Rats weighing 300-450 grams, purchased from Charles River (Charles River Laboratories, Wilmington, MA) or Harlan (Harlan Laboratories, Indianapolis, Indiana) were used in this study. Rats were housed communally with free access to food and water until the time of the study. Rats were placed in an isoflurane chamber and pre-anesthetized via isoflurane inhalation for 5 minutes. The anesthetic cocktail of ketamine(80mg/kg)/xylazine(10mg/kg) was administered I.P. and allowed to take effect. Once the rat was fully anesthetized via, the hair on the skull was shaved as closely as possible. Booster doses of ketamine (40 mg/kg) were administered as needed to maintain adequate anesthesia. The animal's body temperature was maintained at approximately 37 °C using a PhysioSuite automatic heating unit (Kent Scientific Corporation, Torrington, Connecticut). All animal experiments were done using approved animal use protocols adhering to IACUC regulations.

2.3.2 Microdialysis Brain Probe Implantation

Once the rat was fully anesthetized, it was then placed in the stereotaxic frame using the ear bars and incisor bar. The skull was made level and centered within the frame. Once the rat was securely in place, an incision approximately 3 cm in length was made in the midline of the skull using a 10 blade scalpel. Four tissue clamps were used to hold the skin to the side, and excess tissue was removed using cotton tip applicators. Once the skull was removed of excess tissue and blood, the bregma coordinates were determined. The appropriate stereotaxic coordinates were calculated for the area of interest, the hippocampus (posterior 5.6 mm, lateral +4.8 mm, and ventral 5.0 mm). Two 1 mm holes were drilled arbitrarily around the desired probe location and anchor screws were inserted to serve as stability for the cannula. Next, a 3 mm hole was drilled at the calculated probe site. Once the hole had been drilled, the guide cannula was lowered to the appropriate depth and fixed to the skull with dental cement, covering the anchor screws. After the dental cement solidified, the dummy probe was removed from the cannula and replaced with a CMA 12 microdialysis probe, with a 2 mm PAES membrane length. The probe was perfused with aCSF/3-MPA for the duration of the experiment. The rat was maintained under anesthesia for the duration of the experiment using 40-50mg/kg supplemental does of ketamine injected I.P. or I.M. At the termination of the experiment, the rat was euthanized using isoflurane overdose followed by decapitation and the brain was harvested for histological analysis.

2.4 Experimental Design

Post operatively, animals were allowed to recover for one hour, during which time aCSF was constantly perfused through the microdialysis probe at a flow rate of 1.0 μL/min with a

CMA/100 microinjection pump (Harvard Apparatus, Holliston, Massachusetts). After a 60 minute recovery period, aCSF was perfused for one hour and collected in ten minute intervals to serve as basal level samples. After the basal collection, a solution of 10 mM 3-MPA in aCSF was administered through the probe at a rate of 1.0 µL/min. For all experiments, samples were collected in ten minute intervals.

2.4.1 Immunohistochemical Staining

A set of 3 dosed animals and 3 control animals were used for immunochemical staining with both ARC and Synaptophysin antibodies. The surgical procedure and probe implantation were the same as describe above. For the dosed animals, after basal collection, 10 mM 3-MPA was perfused through the probe for 15 minutes to ensure neuronal activation. For the control experiments, the animal was only administered aCSF but was sacrificed at the same time point as the dosed animal. One control and one dosed animal were performed on the same day to reduce any experimental variability. The animals were sacrificed and the brain was harvested. Brains were cut into three equal sections, rostral to caudal, using a razor blade, and ensuring not to cut through the hippocampus. Each section was placed in 4% paraformaldehyde in phosphate buffered saline (PBS) until solidified, approximately one week. The tissues were then preserved in 30% sucrose-PBS solution and allowed to become saturated, signified by the flotation of the tissues. Once saturated, the middle section containing the hippocampus was rinsed with PBS. Hippocampal-containing sections were then flash-frozen using liquid nitrogen for 30 seconds then placed on dry ice. The sections were fixed to chilled cryostat platforms using OTC compound. The fixed sections were allowed to equilibrate to -40 °C for approximately 45 minutes and then to -20 °C for approximately 30 minutes. Sections were cut in 20 µm thickness and placed in 2 mM

EDTA PBS buffer in 12-well plates. Samples were stored at 4°C until they were ready to be stained using antibodies.

Three sections from each rat were selected to be stained and fixed for imaging. To stain the sections with the ARC and Synaptophysin antibodies, the sections were permeabilized with 0.2% Triton X-100 for 10 minutes at room temperature. Sections were then rinsed with PBS to remove any excess detergent. A few drops of Image-IT signal enhancer was added to the wells, and then the sections were allowed to incubate for 30 minutes in a humid chamber. Sections were once again rinsed and then placed in 3% gelatin-PBS solution to solidify the slices. The anti-ARC antibody was diluted 1:200 in PBS and the anti-Synaptophysin was diluted 1:250 in PBS. 500 µL of each antibody solution was added to each well and allowed to incubate overnight at 4°C. Slices were rinsed with PBS to remove excess antibody. Secondary antibodies of goat anti-rabbit and rat anti-mouse were diluted 1:500 in PBS and added to each well for the labeling of ARC and synaptophysin, respectively. Sections were incubated for 2 hours at 37°C. Finally, the sections were rinsed to remove any excess secondary antibody and were mounted to glass slides using 70% glycerol-PBS solution. The slides were imaged using a Leica SPE2 confocal microscope.

2.4.2 Animal Experiments – Induction of Two Seizures

In order to replicate the preliminary studies done by Dr. Andrew Meyer, experiments involved the induction of two 30 minute local seizures with 40 minutes between seizure inductions. A 30 minute local seizure was induced by perfusing 10 mM 3-MPA through the probe directly into the hippocampus. The rat was allowed to recover for a period 40, 60, or 180 minutes after the

3-MPA perfusion stopped, during which time blank aCSF was perfused through the probe. A second 30 minute local seizure stimulation was then induced and aCSF was perfused for one hour post second perfusion of 3-MPA.

2.4.2.1 Control Experiments

In order to confirm that the neurochemical response being observed was due to the epileptic agent and not the surgical procedure or the anesthetic agent, control experiments were performed. All experimental manipulations done in the seizure experiments were replicated in the control experiments, the only difference being the epileptic agent was not administered and instead replaced with perfusion of blank aCSF.

2.5 Results and Discussion

The goal of this research was to development of a rat model for locally induced epilepsy by inducing two seizure episodes within one experiment. Because we were unable to measure seizure activity through ECoG monitoring, the seizure induction was confirmed with immunohistochemical staining using ARC and Synaptophysin to measure neuronal activation.

2.5.1 Immunohistochemical Staining Results

Images of both CA1 and CA3 regions of all 18 sections were taken. Examples images are shown in Figure 2.7. Average pixel density counts for both ARC and Synaptophysin staining were made using Leica software for the CA1 and CA3 regions of both control and dosed animals (Table

2.1 and 2.2). There was 49% more neuronal activation in the dosed experiments than in the control experiments in the CA1 region and 66% more activation in the CA3 region, quantified by the ARC expression. The synaptophysin expression was essentially the same for both dosed and control experiments in all regions. This was expected. The Synaptophysin quantified total synapses which should not change between dosed versus control. Likewise, there was minimal difference in both ARC and Synaptophysin expression on the contralateral side of the brain in the dosed versus the control. This is to be expected because in both the dosed and control experiments no perturbation was experienced on the contralateral side of the brain. T-tests were performed on this data comparing the dosed versus the control in both the CA1 and CA3, producing a p value of 0.08 and 0.03 respectively, making the difference in neuronal activation significantly different. The statistically significant change in neuronal activation as a result of the 3-MPA dose confirms that that the neurons were being activated, signifying seizure induction.

2.5.2 Multiple Dosing Results

Control experiment data is included in the corresponding time interval graphs. The yellow and black plots on Figures 2.8-2.10 represent the glutamate and GABA data for the control animals. All three experimental conditions show no significant change in glutamate or GABA for the controls, meaning the experimental and surgical procedures were not the cause of neurological response, but it was in fact caused by the epileptic agent.

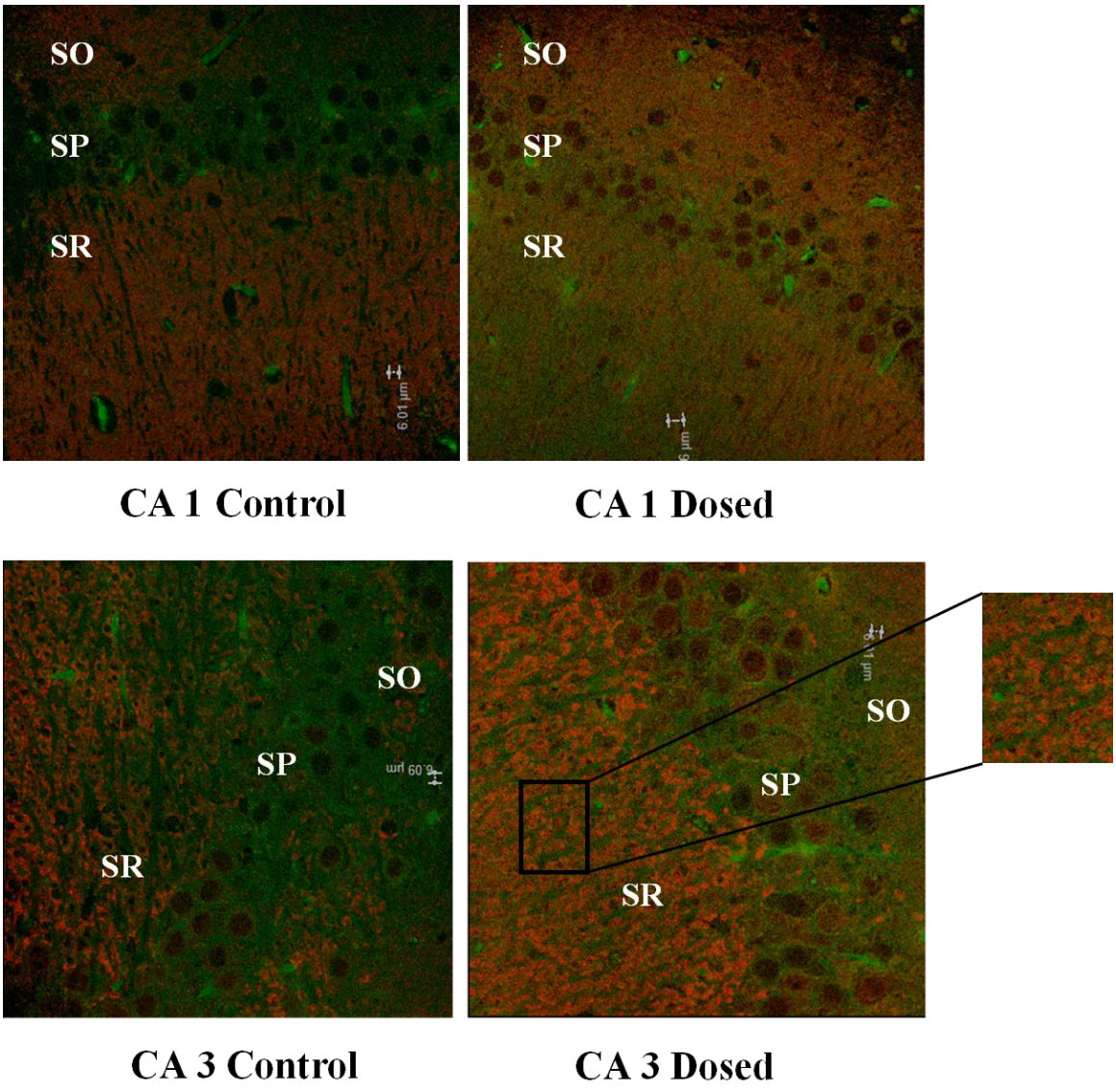

Figure 2.7: Example confocal microscopy images of hippocampal slices taken after ARC (red) and Synaptophysin (green) staining

Stratum oriens (SO), stratum pyramidale (SP), and stratum radiatum (SR) regions are labeled accordingly. The zoomed-in section more clearly shows the dendrites and synaptic staining.

ARC	CA 1		CA 3	
	Dosed	Control	Dosed	Control
Ipsilateral (pixel density)	41 ± 5	21 ± 3	91 ± 8	33 ± 5
Contralateral (pixel density)	29 ± 3	21 ± 4	44 ± 3	37 ± 3

Table 2.1: Comparison of pixel density values for ARC staining from CA1 vs. CA3 regions for dosed and control animals. Numbers represent raw pixel density counts taken from the LAS data processing program. (N=3 control, N=3 dosed)

Syn	CA 1		CA 3	
	Dosed	Control	Dosed	Control
Ipsilateral (pixel density)	25 ± 6	26 ± 2	37 ± 5	34 ± 3
Contralateral (pixel density)	24 ± 5	26 ± 4	36 ± 3	40 ± 4

Table 2.2: Comparison of pixel density values for Synaptophysin staining from CA1 vs. CA3 regions for dosed and control animals Numbers represent raw pixel density counts taken from the LAS data processing program. (N=3 control, N=3 dos

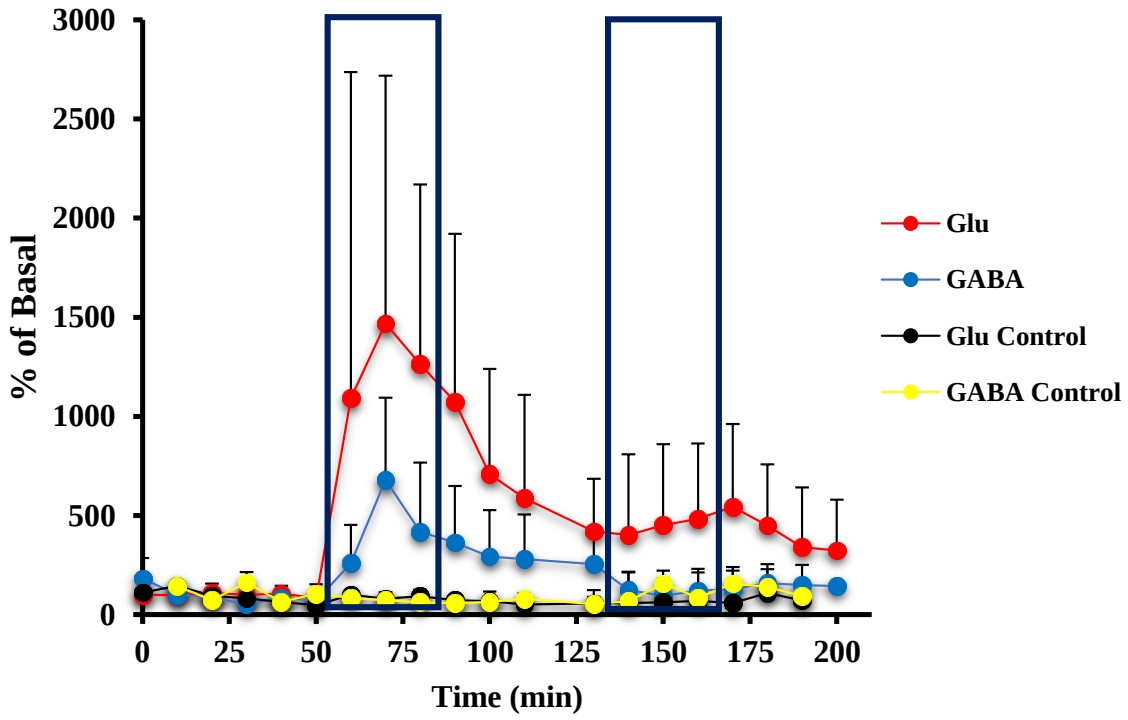

Figure 2.8: Change in glutamate and GABA concentrations over time following delivery of 10 mM 3-MPA: 40-min interval between seizures (N = 7).

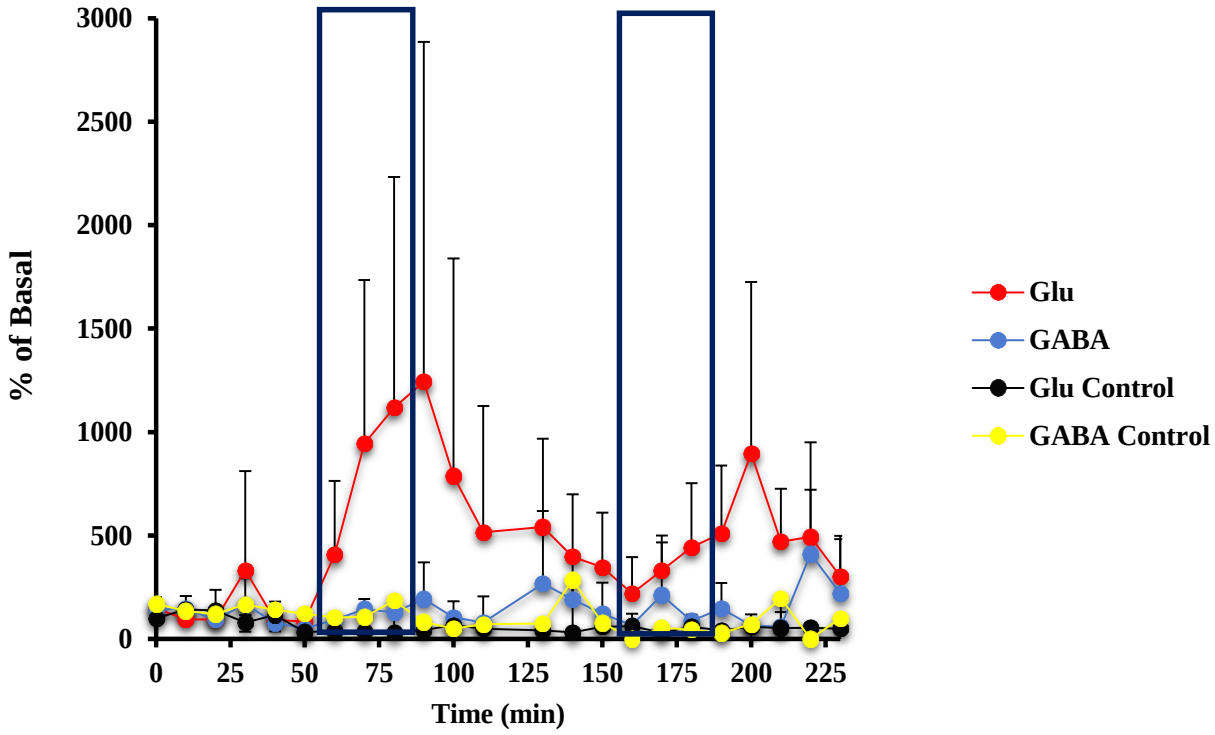

Figure 2.9: Change in glutamate and GABA concentrations following delivery of 10 mM 3-MPA: 60-min interval between seizures (N = 5).

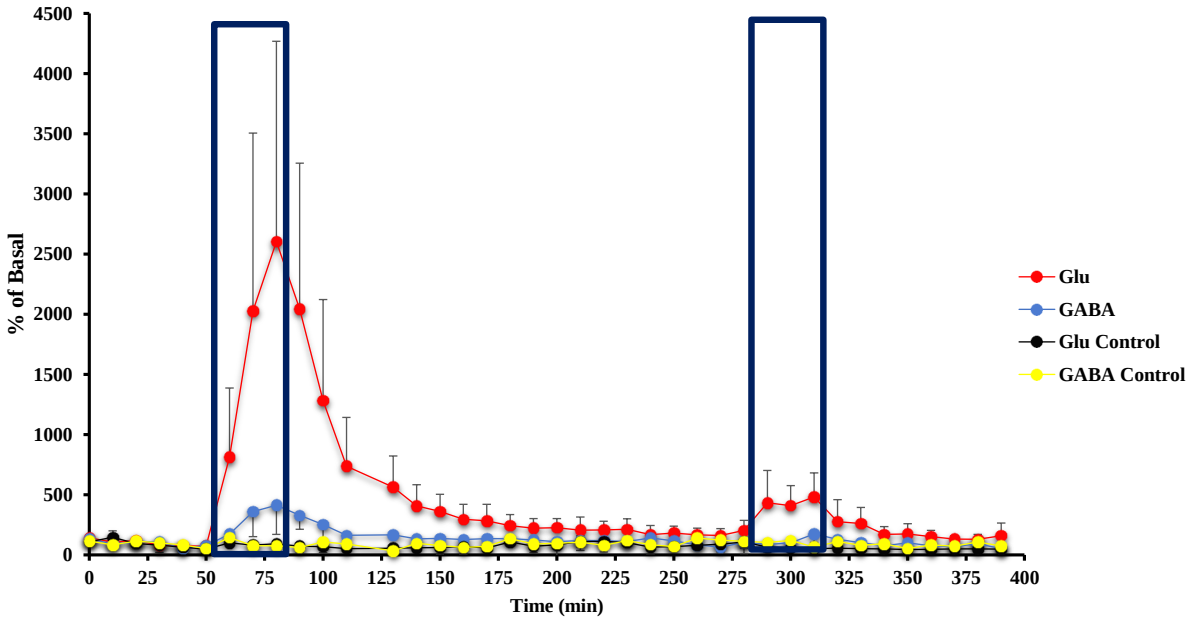

Figure 2.10: Change in glutamate and GABA concentration following delivery of 10 mM 3-MPA: 180-min interval between seizures (N = 5).

When only 40 minutes recovery time was allowed between dosing with epileptic agent, basal levels of glutamate and GABA were not reestablished before the second seizure induction. This indicates that at the level of neurochemicals released, there were not two separate seizure stimulations (Figure 2.8). In order to ensure that there were two separate seizure events, time between seizure inductions was varied to determine the recovery time necessary for glutamate and GABA to return to basal levels prior to the second seizure induction (Figures 2.9, 2.10). Glutamate and GABA concentrations returned to basal levels at approximately 150 minutes after the end of the first seizure induction. This return to initial baseline signifies that each seizure induction was a separate episode and that two seizures are induced within one experiment, thereby developing the equivalent of an animal model for local epilepsy.

In all three experiments, a significant attenuation of extracellular glutamate was observed during the second seizure episode even though the same concentration of 3-MPA was administered for the same length of time to induce each seizure (Figures 2.8-2.10). By extending the time between seizures, more time was available for glutamate recovery after the induction of the first seizure. Two analyses of the data were done. The first using the baseline prior to the first seizure induction to determine glutamate attenuation observed in the second seizure, and the second analysis used the baseline directly before the second seizure to determine the glutamate attenuation. The results of both statistical analyses are discussed below. Possible causes of this decrease in glutamate release include glutamate depletion, desensitization to the epileptic agent, or excitotoxicity leading to synaptic depression.

2.5.3 Statistical Analysis

In the first analysis of the data, the baseline established prior to the first seizure was used to calculate the percent of basal for both seizures. In this analysis, a 62 ± 3% decrease in glutamate response was observed with the stimulation of the second seizure episode after a 40 minute recovery period. A 59 ± 4% decrease in release after 60 minute recovery period and 80 ± 7% decrease in release after 180 minute recovery were also observed.

In the second analysis of the data, the baseline prior to the first seizure was used to calculate the percent of basal for the first seizure and the baseline prior to the second seizure induction was used to calculate the percent of basal for the second seizure. It was necessary to calculate the response this way since the glutamate concentration never fully returned to the initial baseline prior to the second seizure induction, making the baseline prior to the second seizure significantly different than the initial baseline. In this analysis, a 92 ± 3% decrease in glutamate response was observed with the stimulation of the second seizure episode after a 40 minute recovery period. An 89 ± 4% decrease in release after 60 minute recovery period and 90 ± 7% decrease in release after 180 minute recovery were also observed. When using this analysis, significantly higher attenuation in glutamate release is being observed. This is to be expected since the baseline is never fully able to recover prior to the second induction. The cells do not have time nor nutrients to release the same amount of glutamate in both stimulations. Interestingly, there was not a statistically significant difference between the analyses in the 180 minute results, further confirming that 180 minutes was enough time for baseline to essentially be reestablished prior to the second induction.

Experimental Interval	Attenuation (%)	p Value
40 min	62 ± 3 (N=7)	0.005*
60 min	59 ± 4 (N=5)	0.021**
180 min	80 ± 7 (N=5)	0.019**

Table 2.3: Percent attenuation in glutamate release for each experiment using initial baseline for both seizures.

Experimental Interval	Attenuation (%)	p Value
40 min	92 ± 3 (N=7)	0.00042***
60 min	89 ± 4 (N=5)	0.00037***
180 min	90 ± 7 (N=5)	0. 0005***

Table 2.4: Percent attenuation in glutamate release for each experiment using individual baseline for each seizure.

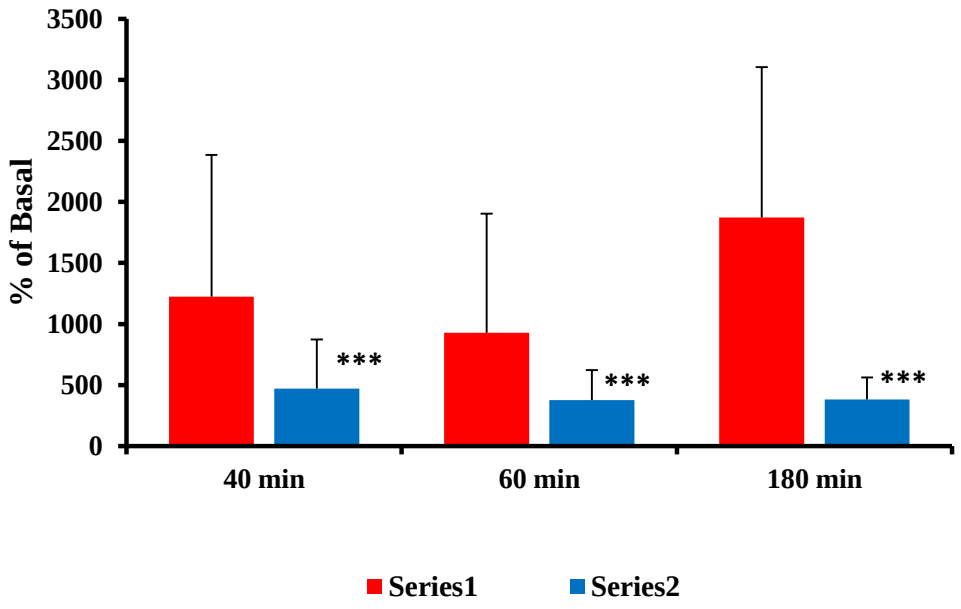

Figure 2.11: Graphical comparison of glutamate release between first and second seizure episodes for each experimental condition.

40 min, N=7; 60 min, N=5; 180 min, N=5

*** $p<0.0005$

To demonstrate statistical significance and determine the difference in neurotransmitter response in the first and second seizure episodes, t-tests were performed on all data (Table 2.3 and 4). For the first analysis method, the 60 min and 180 min intervals had confidence levels of $p<0.05$ and the 40 min interval experiments had a confidence interval of $p<0.01$. For the second analysis, all experiments had a confidence interval of $p<0.0005$. This confidence interval implies that thereis a significant difference in the glutamate response between the first and second seizure. Figure 2.11 graphically represents these differences for each of the time interval.

2.5.4 Glutamate Attenuation Hypotheses

The initial hypothesis as to the cause of attenuated glutamate release in the second seizure that was investigated was glutamate depletion. During the seizure, the vesicles release glutamate into the synaptic cleft. As can be seen in the above data, glutamate concentrations steadily increase and then remain elevated for the duration of the thirty minute seizure. Once the seizure is over, the concentration approaches basal levels again, but the reservoir of glutamate has already been depleted. It is possible that a 60 minute delay was still not enough time after the first seizure for the glutamate supply to regenerate, so the time was extended to 180 minutes between seizures[56]. Because such a severe decrease in glutamate release was still observed even after 180 minutes recovery time, it is believed that the cells are being starved for nutrients such as glucose and lactate that are necessary for the production of glutamate[57-59]. A series of experiments to further investigate this hypothesis were conducted and are discussed in Chapter 3.

Desensitization to the epileptic agent could also lead to the attenuated glutamate release. Desensitization results when binding of the ligand to a receptor leads to a decrease in the effectiveness of the receptor. When this happens, the receptor is no longer able to allow the release

or reuptake of the neurotransmitters. High concentrations of post-synaptic neurotransmitters can act upon the pre-synaptic terminals depressing further release, resulting in an apparent decrease in neurochemical response[60, 61]. This affects communication between glial cells and neurons. Furthermore, if desensitization occurs it can result in excitotoxicity that can result in neuronal damage and death.

Finally, the last hypothesis discussed here is glutamate excitotoxicity. Unfortunately, glutamate excitotoxicity can occur at relatively low concentrations and has been observed with extracellular levels of glutamate as low as 2-5 μM[62-64]. Cellular swelling and apoptosis have been observed with glutamate concentrations around 25 μM and necrosis occurs with concentrations of approximately 100 μM extracellular glutamate[65, 66]. Excitotoxicity is an important factor to consider when studying epilepsy because many times the effects of the excitotoxicity are more damaging than the seizures themselves. Neuronal damage is also a possible cause of the attenuated glutamate response. However, the catecholamine data in Figure 2.12 suggests that there is no significant reduction in NE and DA release during the second seizure episode. Interestingly, there was no significant increase in NE during the seizure stimulations, but there was in DA. In a recent study by Rocchetti et al. DA fibers were located and labeled in the CA1 region of the hippocampus[67]. This could be the reason for the increase in DA with stimulation. Because there was no significant difference in DA release between the two seizure inductions, this leads to the conclusion that the dopaminergic neurons are not being severely damaged. In this study, the GAD inhibitor produced such a large increase in glutamate that it is possible that a feedback mechanism is occurring, where glutamate itself is acting on the pre-synaptic terminal, thus depressing further release of glutamate[68-71]. Glutamate concentrations during the seizure stimulation ranged from 5-12 μM, making excitotoxicity a highly plausible cause of the attenuated response.

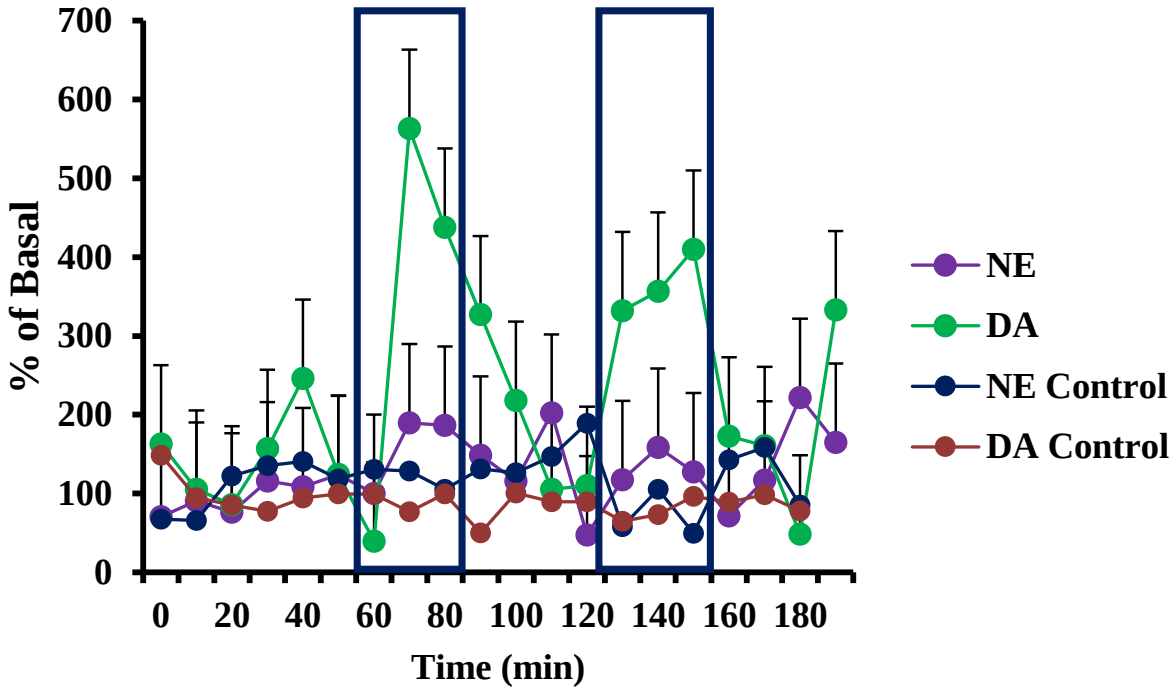

Figure 2.12: Change in norepinephrine and dopamine concentrations over time following delivery of 10 mM 3-MPA: 40-min interval between seizures (N = 7).

2.6 Conclusions

In this chapter, an animal model for locally induced epilepsy was developed by the induction of two seizure episodes within the same experiment. A 40 and 60 minute delay between seizures was not sufficient for basal levels of neurotransmitters to be reestablished, meaning these were not two separate events. It required 150 minutes of recovery time after the first seizure before basal levels were reestablished. By allowing 180 minutes of recovery time, the second seizure induction was truly a separate event. Significant attenuation in glutamate release was observed in the second seizure induction for all investigated time regimes. It was originally hypothesized that there was not enough time for recovery of glutamate levels, but 180 minutes of recovery should have been enough time. Several hypotheses as to the cause of attenuation have been investigated and are discussed in the next chapter.

2.7 References

1. Organization, W. H. (2016) Epilepsy Fact Sheet
2. (2009) Animal models of epilepsy methods and innovations, (Baraban, S. C., Ed.), Totowa, NJ : Humana Press, Totowa, NJ.
3. Bertram, E. H., Lothman, E. W., and Lenn, N. J. (1990) The hippocampus in experimental chronic epilepsy: a morphometric analysis, *Annals of neurology 27*, 43-48.
4. Bradford, H. F. Glutamate, GABA and epilepsy, *Progress in neurobiology 47*, 477-511.
5. Cavus, I., Kasoff, W. S., Cassaday, M. P., Jacob, R., Gueorguieva, R., Sherwin, R. S., Krystal, J. H., Spencer, D. D., and Abi-Saab, W. M. (2005) Extracellular metabolites in the cortex and hippocampus of epileptic patients, *Annals of neurology 57*, 226-235.
6. Clinckers, R. Pharmacological and neurochemical characterization of the involvement of hippocampal adrenoreceptor subtypes in the modulation of acute limbic seizures.(Report), *Journal of neurochemistry 115*, 1595.
7. Emerit, J., Edeas, M., and Bricaire, F. (2004) Neurodegenerative diseases and oxidative stress, *Biomedicine & pharmacotherapy 58*, 39-46.
8. Frantseva, M., Velazquez, J. P., Tsoraklidis, G., Mendonca, A., Adamchik, Y., Mills, L., Carlen, P., and Burnham, M. (2000) Oxidative stress is involved in seizure-induced neurodegeneration in the kindling model of epilepsy, *Neuroscience 97*, 431-435.
9. Lopez, J., González, M. E., Lorigados, L., Morales, L., Riveron, G., and Bauza, J. Y. (2007) Oxidative stress markers in surgically treated patients with refractory epilepsy, *Clinical biochemistry 40*, 292-298.
10. Crick, E. W., Osorio, I., Bhavaraju, N. C., Linz, T. H., and Lunte, C. E. (2007) An investigation into the pharmacokinetics of 3-mercaptopropionic acid and development of

a steady-state chemical seizure model using in vivo microdialysis and electrophysiological monitoring, *Epilepsy research 74*, 116-125.

11. Mayer, A. (2010) Local Dosing in a 3-Mercaptopropionic Acid Chemically-Induced Epileptic Seizure Model with Microdialysis Sampling, (Lunte, C. E., Dunn, B., Johnson, M., Lunte, S., and Osorio, I., Eds.), ProQuest Dissertations Publishing.
12. (1993) *Epilepsy : models, mechanisms, and concepts*, Cambridge New York : Cambridge University Press, Cambridge New York.
13. Engel, J. (2013) *Seizures and epilepsy*, Vol. 83, Oxford University Press.
14. (1981) *Neurotransmitters, seizures, and epilepsy*, New York : Raven Press, New York.
15. Crick, E. (2007) In vivo microdialysis coupled with electrophysiology for the neurochemical analysis of epileptic seizures, (Lunte, C. E., Dunn, R., Johnson, M., Lunte, S., and Rivera, M., Eds.), ProQuest Dissertations Publishing.
16. Crick, E. W. An investigation into the pharmacokinetics of 3-mercaptopropionic acid and development of a steady-state chemical seizure model using in vivo microdialysis and electrophysiological monitoring, *Epilepsy research 74*, 116-125.
17. Crick, E. W. Correlation of 3-mercaptopropionic acid induced seizures and changes in striatal neurotransmitters monitored by microdialysis, *European journal of pharmaceutical sciences 57*, 25-33.
18. Haneef, Z. Functional connectivity of hippocampal networks in temporal lobe epilepsy, *Epilepsia (Copenhagen) 55*, 137-145.
19. McDonald, J. W., and McDonald, J. W. Altered excitatory and inhibitory amino acid receptor binding in hippocampus of patients with temporal lobe epilepsy, *Annals of neurology 29*, 529-541.

20. Aultman, J. M. Distinct contributions of glutamate and dopamine receptors to temporal aspects of rodent working memory using a clinically relevant task, *Psychopharmacology (Berlin, Germany) 153*, 353-364.

21. Mayer, A. P. (2010) Local Dosing in a 3-Mercaptopropionic Acid Chemically-Induced Epileptic Seizure Model with Microdialysis Sampling, (University of, K., Lawrence . University of, K., Kansas, U., Ku, and Universitas, K., Eds.), Thesis (Ph.D.)--University of Kansas, 2010.

22. (2014) From molecules to networks : an introduction to cellular and molecular neuroscience, (Byrne, J. H. e., Heidelberger, R. e., and Waxham, M. N. e., Eds.) Third edition.. ed., London, UK Waltham, MA : Academic Press.

23. Andersen, P. Recurrent inhibition in the hippocampus with identification of the inhibitory cell and its synapses, *Nature (London) 198*, 540-542.

24. Bertram, E. H. The hippocampus in experimental chronic epilepsy: A morphometric analysis, *Annals of neurology 27*, 43-48.

25. Wang, X., Pal, R., Chen, X.-w., Limpeanchob, N., Kumar, K. N., and Michaelis, E. K. (2005) High intrinsic oxidative stress may underlie selective vulnerability of the hippocampal CA1 region, *Molecular Brain Research 140*, 120-126.

26. Lebovitz, R., Dichter, M., and Spencer, W. (1971) Recurrent excitation in the CA3 region of cat hippocampus, *International Journal of Neuroscience 2*, 99-107.

27. Raza, M., Blair, R. E., Sombati, S., Carter, D. S., Deshpande, L. S., and DeLorenzo, R. J. (2004) Evidence that injury-induced changes in hippocampal neuronal calcium dynamics during epileptogenesis cause acquired epilepsy, *Proceedings of the National Academy of Sciences of the United States of America 101*, 17522-17527.

28. Brueh, C., Kloiber, O., Hossman, K., Dorn, T., and Witte, O. (1995) Regional hypometabolism in an acute model of focal epileptic activity in the rat, *European Journal of Neuroscience 7*, 192-197.

29. Mares, P. Models of Epileptic Seizures in Immature Rats, *Physiological research 61*, S103-S108.

30. Cherubini, E. Excitatory amino acids in synaptic excitation of rat striatal neurones in vitro, *The Journal of physiology 400*, 677-690.

31. Hamberger, A., Nyström, B., Sellström, Å., and Woiler, C. (1976) Amino acid transport in isolated neurons and glia, In *Transport Phenomena in the Nervous System*, pp 221-236, Springer.

32. Meldrum, B., and Garthwaite, J. (1990) Excitatory amino acid neurotoxicity and neurodegenerative disease, *Trends in pharmacological sciences 11*, 379-387.

33. (1995) *Excitatory amino acids and synaptic transmission*, 2nd ed.. ed., London San Diego : Academic Press, London San Diego.

34. Pocock, G., and Richards, C. (1993) Excitatory and inhibitory synaptic mechanisms in anaesthesia, *British journal of anaesthesia 71*, 134-147.

35. Sarhan, S. (1979) Metabolic inhibitors and subcellular distribution of GABA, *Journal of neuroscience research 4*, 399-421.

36. Gulledge, A. T., and Stuart, G. J. (2003) Excitatory Actions of GABA in the Cortex, *Neuron 37*, 299-309.

37. Naylor, D. E. (2010) Glutamate and GABA in the balance: Convergent pathways sustain seizures during status epilepticus, *Epilepsia 51*, 106-109.

38. Mayer, A. P., Osorio, I., and Lunte, C. E. (2013) Microperfusion of 3-MPA into the brain augments GABA, *Epilepsy & Behavior 29*, 478-484.

39. Gross, R., and Ferrendelli, J. (1982) Relationships between norepinephrine and cyclic nucleotides in brain and seizure activity, *Neuropharmacology 21*, 655-661.

40. Herman, J. P. Norepinephrine–gamma-aminobutyric acid (GABA) interaction in limbic stress circuits: effects of reboxetine on GABAergic neurons, *Biological psychiatry (1969) 53*, 166-174.

41. Hirota, K. (2000) Inhibitory effects of intravenous anaesthetic agents on K evoked norepinephrine and dopamine release from rat striatal slices: possible involvement of PQtype voltagesensitive Ca 2 channels, *British journal of anaesthesia : BJA 85*, 874-880.

42. August, J. T., Murad, F., Anders, M., Coyle, J. T., Goldstein, D. S., Eisenhofer, G., and McCarty, R. (1997) *Catecholamines: bridging basic science with clinical medicine*, Vol. 42, Academic Press.

43. Berod, A. Catecholaminergic and GABAergic anatomical relationship in the rat substantia nigra, locus coeruleus, and hypothalamic median eminence: immunocytochemical visualization of biosynthetic enzymes on serial semithin plastic-embedded sections, *The journal of histochemistry and cytochemistry 32*, 1331-1338.

44. Morales-Villagrán, A., López-Pérez, S., Medina-Ceja, L., and Tapia, R. (1999) Cortical catecholamine changes and seizures induced by 4-aminopyridine in awake rats, studied with a dual microdialysis-electrical recording technique, *Neuroscience letters 275*, 133-136.

45. Shah, A. J. Amino acid neurotransmitters: separation approaches and diagnostic value, *Journal of chromatography. B, Analytical technologies in the biomedical and life sciences 781*, 151-163.

46. De Montigny, P., Stobaugh, J. F., Givens, R. S., Carlson, R. G., Srinivasachar, K., Sternson, L. A., and Higuchi, T. (1987) Naphthalene-2,3-dicarboxyaldehyde/cyanide ion: a rationally designed fluorogenic reagent for primary amines, *Analytical chemistry 59*, 1096-1101.

47. Bowser, M. T. In vivomonitoring of amine neurotransmitters using microdialysis with on-line capillary electrophoresis, *Electrophoresis 22*, 3668-3676.

48. Lunte, S. M., Mohabbat, T., Wong, O. S., and Kuwana, T. (1989) Determination of desmosine, isodesmosine, and other amino acids by liquid chromatography with electrochemical detection following precolumn derivatization with naphthalenedialdehyde/cyanide, *Analytical biochemistry 178*, 202-207.

49. Dorris, M. (2013) Development of Dual-Electrode Amperometric Detectors for Liquid Chromatography and Capillary Electrophoresis, (Lunte, C., Johnson, M., Lunte, S., Rivera, M., and Scott, E., Eds.), ProQuest Dissertations Publishing.

50. Gilinsky, M. A. Determination of myocardial norepinephrine in freely moving rats using in vivo microdialysis sampling and liquid chromatography with dual-electrode amperometric detection, *Journal of pharmaceutical and biomedical analysis 24*, 929-935.

51. Osorio, I. Automated seizure abatement in humans using electrical stimulation, *Annals of neurology 57*, 258-268.

52. Bloomer, W. (2007) Post-transcriptional regulation and localization of the activity - regulated cytoskeleton -associated protein Arc/Arg3.1, (VanDongen, A., Ed.), ProQuest Dissertations Publishing.

53. Lv, X.-F. Expression of activity-regulated cytoskeleton-associated protein (Arc/Arg3.1) in the nucleus accumbens is critical for the acquisition, expression and reinstatement of morphine-induced conditioned place preference, *Behavioural brain research 223*, 182-191.

54. Korzhevskii, D. E., and Korzhevskii, D. Simultaneous Detection of Glutamate Decarboxylase and Synaptophysin in Paraffin Sections of the Rat Cerebellum, *Neuroscience and behavioral physiology 46*, 106-109.

55. Yong, Z. Effects of thienorphine on synaptic structure and synaptophysin expression in the rat nucleus accumbens, *Neuroscience 274*, 53-58.

56. Stevens, C. F. Estimates for the pool size of releasable quanta at a single central synapse and for the time required to refill the pool, *Proceedings of the National Academy of Sciences - PNAS 92*, 846.

57. Chuang, Y. C., Chang, A. Y., Lin, J. W., Hsu, S. P., and Chan, S. H. (2004) Mitochondrial Dysfunction and Ultrastructural Damage in the Hippocampus during Kainic Acid–induced Status Epilepticus in the Rat, *Epilepsia 45*, 1202-1209.

58. Liang, L.-P., and Patel, M. (2006) Seizure-induced changes in mitochondrial redox status, *Free Radical Biology and Medicine 40*, 316-322.

59. Patel, M. (2004) Mitochondrial dysfunction and oxidative stress: cause and consequence of epileptic seizures, *Free Radical Biology and Medicine 37*, 1951-1962.

60. Sun, Y., and Yu, S. Mechanism of glutamate receptor desensitization, *Nature (London) 417*, 245-253.

61. Trussell, L. O. Desensitization of AMPA receptors upon multiquantal neurotransmitter release, *Neuron (Cambridge, Mass.) 10*, 1185-1196.

62. Biasini, E., Unterberger, U., Solomon, I. H., Massignan, T., Senatore, A., Bian, H., Voigtlaender, T., Bowman, F. P., Bonetto, V., Chiesa, R., Luebke, J., Toselli, P., and Harris, D. A. (2013) A Mutant Prion Protein Sensitizes Neurons to Glutamate-Induced Excitotoxicity, *The Journal of Neuroscience 33*, 2408-2418.

63. Mehta, A., Prabhakar, M., Kumar, P., Deshmukh, R., and Sharma, P. L. (2013) Excitotoxicity: Bridge to various triggers in neurodegenerative disorders, *European Journal of Pharmacology 698*, 6-18.

64. Wang, W., Zhang, F., Li, L., Tang, F., Siedlak, S. L., Fujioka, H., Liu, Y., Su, B., Pi, Y., and Wang, X. (2015) MFN2 Couples Glutamate Excitotoxicity and Mitochondrial Dysfunction in Motor Neurons, *Journal of Biological Chemistry 290*, 168-182.

65. Cheung, N. S. Micromolar l-glutamate induces extensive apoptosis in an apoptotic-necrotic continuum of insult-dependent, excitotoxic injury in cultured cortical neurones, *Neuropharmacology 37*, 1419-1429.

66. Davis, W., Ronai, Z. e., and Tew, K. D. (2001) Cellular thiols and reactive oxygen species in drug-induced apoptosis, *Journal of Pharmacology and Experimental Therapeutics 296*, 1-6.

67. Rocchetti, J., Isingrini, E., Dal Bo, G., Sagheby, S., Menegaux, A., Tronche, F., Levesque, D., Moquin, L., Gratton, A., Wong, T. P., Rubinstein, M., and Giros, B. (2015) Presynaptic

D2 Dopamine Receptors Control Long-Term Depression Expression and Memory Processes in the Temporal Hippocampus, *Biological Psychiatry 77*, 513-525.

68. Araque, A. Glutamate-dependent astrocyte modulation of synaptic transmission between cultured hippocampal neurons Astrocytes modulate synaptic transmission, *The European journal of neuroscience 10*, 2129-2142.

69. Howells, F. M. Glutamate-stimulated release of norepinephrine in hippocampal slices of animal models of attention-deficit/hyperactivity disorder (spontaneously hypertensive rat) and depression/anxiety-like behaviours (Wistar–Kyoto rat), *Brain research 1200*, 107-115.

70. McAdoo, D. J., Xu, G.-Y., Robak, G., Hughes, M. G., and Price, E. M. (2000) Evidence that reversed glutamate uptake contributes significantly to glutamate release following experimental injury to the rat spinal cord, *Brain research 865*, 283-285.

71. Sun, Y., Olson, R., Horning, M., Armstrong, N., Mayer, M., and Gouaux, E. (2002) Mechanism of glutamate receptor desensitization, *Nature 417*, 245-253.

Chapter 3

Neurochemical Investigation of Glutamate Depletion and Oxidative Stress Observed in the Multiple Seizure Model

3.1 Background and Significance

Chapter 2 discussed the development of an animal model for local epilepsy. By definition, epilepsy is diagnosed after the patient experiences two or more seizures. For this reason, a single seizure stimulation is not sufficient to constitute an epileptic model. Local seizure-like stimulations were induced in the CA1 region of the hippocampus for 30 minutes each. Because the same concentration of epileptic agent was administered for the same length of time in each episode, it was anticipated that the neurochemical response would be the same in both stimulations. Significant attenuation in glutamate response was observed during the second stimulation. There are several hypotheses available as to the cause of the decrease in glutamate release. This chapter discusses the investigation of four of the most likely hypotheses: glutamate depletion by metabolic and energy pathways, neuronal protective response, neuronal damage, and the mechanism of action of the epileptic agent.

3.1.1 Glutamate Depletion

The vesicles at the nerve terminals contain different pools of neurotransmitters, including the readily releasable pool, the recycling pool and the reserve pool[1]. The readily releasable pool is located close to the membrane and contains the first group of neurotransmitters to be released into the extracellular space, in this case glutamate[2]. When stimulation occurs via the epileptic agent, the glutamate in the readily releasable pool is quickly released. Once this pool has been drained,

continuous stimulation mobilizes the glutamate in the recycling pool for release. Only with intense stimulation does the glutamate in the reserve pool get released. In the case of a 30 minute seizure stimulation, it is likely that all three pools are mobilized and release all available glutamate into the extracellular space. If this occurs during the first seizure, there may not be enough time or nutrients for the glutamate pools to be replenished prior to the second seizure episode[3, 4]. This could completely deplete the glutamate supply. We predicted that 180 minutes would be enough time for the pools to be replenished, however, attenuation in glutamate release was still observed after that time delay (Chapter 2). For this reason, it was hypothesized that the lack of nutrients available to the mitochondria is the cause of the glutamate diminution, specifically glucose and lactate. Once the pools are depleted, glutamate must be synthesized to replenish them through the KREBS cycle (Figure 3.1). The mitochondrial enzyme, glutaminase metabolizes glutamine into glutamate. Additionally, glutamate is taken up by glia to be converted to glutamine, which is then released and taken up by neurons to be converted back from glutamine to glutamate.

Glucose is a key precursor to glutamate synthesis, and therefore adding it to the system would enhance glutamate production. Similarly, when neurons are stressed, glial cells release lactate to enhance glutamate synthesis which can lead to potential neuronal damage[5, 6]. It is possible that the first seizure episode depleted the surrounding glia of lactate, thus diminishing a major source of mitochondrial KREBS nutrients. Therefore, lactate supplementation might enhance the energy pathway of glutamate production[7-9].

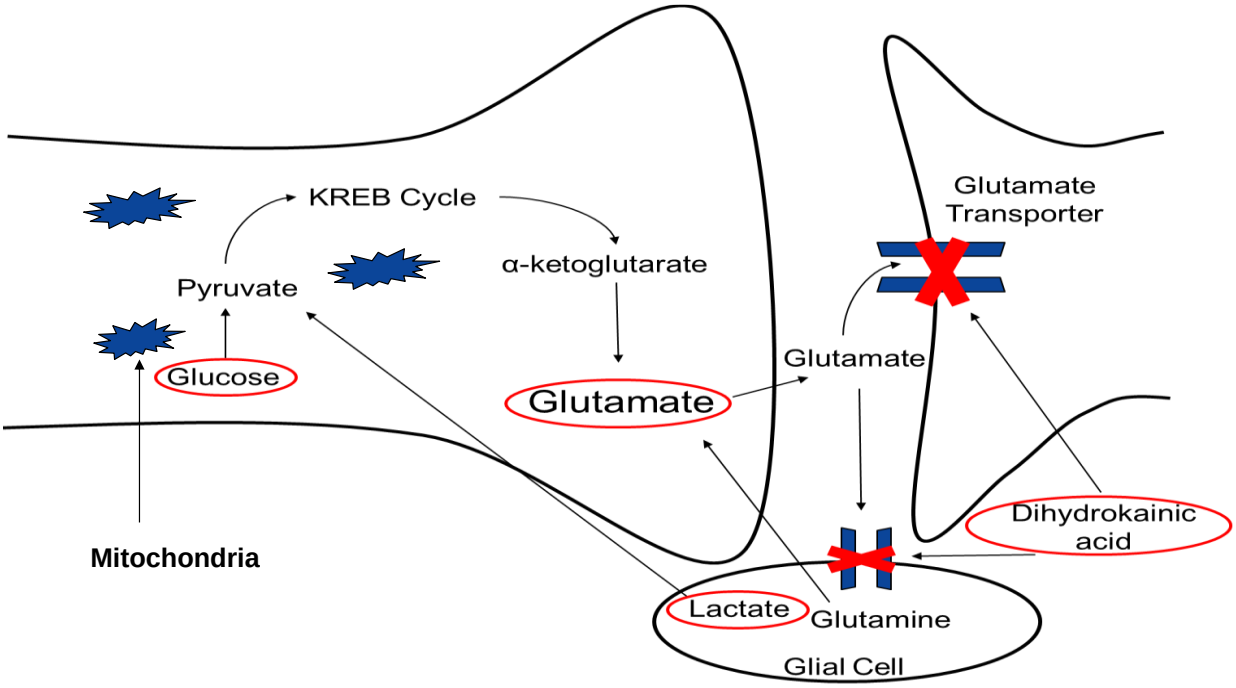

Figure 3.1: Biochemical pathways for glutamate synthesis.

3.1.2 Neuronal Protective Responses

Upon extensive stimulation, the brain has a natural tendency to self-preserve neuronal structure and function, i.e., neuronal protection[10]. The overall goal of the self-preservation is to slow the rate of neuronal loss caused by repeated disruption of the system. While the body does this naturally, induced neuroprotection has also recently been explored as a form of treatment for neurodegenerative diseases such as traumatic brain injury, Alzheimer's disease and Huntington's disease[11]. The natural neuronal protective response is triggered when imbalances in the brain occur as a result of oxidative stress, mitochondrial dysfunction, or excitotoxicity[11-14]. Excitotoxicity caused by glutamate is the most common cause of neurodegeneration. When glutamate receptors are hyperactivated, the calcium ion channels remain open. This results in oxidative damage. The induction of a seizure may cause the hyperactivation of glutamate transporters as a form of neuronal protection. Glutamate transporters function to remove glutamate from the synaptic cleft to be taken up by neurons and glia. There are glutamate transporters on both glial cells and neurons and they are essential in maintaining the balance of extracellular glutamate and preventing excitotoxicity[15, 16]. When extracellular glutamate concentrations reach excitotoxic levels, the transporters go into overdrive as a neuronal protective response to the stimulant. They begin to take up all and any available glutamate, which could be a reason for the attenuated glutamate response in the second seizure episode. If all extracellular glutamate is taken up by the transporters, reduced amounts of glutamate would remain in the extracellular space for collection by microdialysis sampling.

3.1.3 Neuronal Death and Damage

As mentioned above, high levels of extracellular glutamate can lead to excitotoxicity and eventual cell death[11,17-19]. Unfortunately, glutamate-induced excitotoxicity can occur at relatively low concentrations of extracellular glutamate (2-5 μM)[11]. Excitotoxicity-induced cell death is an important consideration in seizures because after an initial seizure, the cells become more easily excitable due to damage and sensitization, which can lead to subsequent seizures and damage. Studies have shown that often the excitotoxicity is more damaging than the seizures themselves[20,21]. If significant cell death occurs before the induction of the second seizure, then there are not enough viable neurons and glial cells available for glutamate release in the second seizure induction.

3.1.3.1 Detection of Neuronal Damage

Propidium iodide (PI) is a fluorescent molecule that intercalates between the bases in DNA[22]. It does not have sequence preference and exhibits a stoichiometric ratio of one PI molecule to 4-5 base pairs in DNA[23]. PI is not able to permeate viable cell membranes and therefore will not stain viable cells. However, if the cell membrane has been damaged, the PI will penetrate and be able to reach the nucleus for binding. This selective permeability allows for PI to be used as a marker for cell viability.

3.1.4 Other Epileptic Agents

Various chemical agents may be used to alter the excitatory/inhibitory balance in the brain. The biggest benefit to using a chemical stimulation model is that seizure duration and intensity can be easily controlled and reproduced. The work in Chapter 2 utilized the GAD inhibition mechanism of action of 3-MPA to develop an animal model for local epilepsy[24, 25]. While this epileptic agent has been used in previous studies both in this lab and in the literature[30-33], it could be the cause of the glutamate attenuation being observed during the second stimulation.

It is well-known that 3-MPA can damage and kill glial cells[34]. Specifically, 3-MPA damages ionotripic glutamate receptors such as the *N*-methyl-D-aspartate receptor[35]. These receptors play a crucial role in synapse formation and neuronal plasticity. This damage could be the reason for the decreased glutamate in the second seizure episode. Additionally, the damage to the glial cells could result in higher extracellular glutamate concentrations, leading to neuronal damage and death.

Other types of convulsants can act as either agonists or antagonists of either the glutamate or GABA receptors[26, 27]. Agonists of glutamate receptors open glutamate channels and can lead to abnormal electrical discharges. Two of the most common glutamate receptor agonists are kainic acid (KA), which acts on the ionotropic glutamate receptors, and homocysteic acid, which acts on the metabotropic glutamate receptors[28, 29]. To rule out 3-MPA as the cause of the glutamate attenuation, a different epileptic agent with a different mechanism of action was utilized. Kainic acid (KA) is a well-known epileptic agent that activates the kainate glutamate receptors[28, 29, 36]. KA is an agonist for the kainate receptors, the receptors that control Na^+ channels responsible for producing excitatory postsynaptic potentials. This hyperactivation of the excitatory responders will result in a seizure.

3.2 Materials and Methods

3.2.1 Chemical Reagents

Glucose, lactate, dihydrokainic acid, and kainic acid were all purchased from Sigma-Aldrich (St. Louis, MO). Propidum iodide was purchased from Abcam (Cambridge, MA). All other reagents purchased for use in this study are listed in Chapter 2.

3.2.2 Liquid Chromatography- Fluorescence Detection

Sample analysis was carried out as described in Chapter 2. The same analytical systems, mobile phases, and sample preparation that was describe in the earlier chapter were implemented in this chapter as well. Because only glutamate diminution was observed, samples were only analyzed for amino acid neurotransmitters. Briefly, 3.0 µL of sample was derivatized following the NDA/CN^- mechanism describe by De Montigny et. al[37]. Derivatized samples were then injected on to an LC-Fl system consisting of a reverse phase column, two Shimadzu pumps, and a Shimadzu 10A-XL fluorescence detector at an excitation wavelength of 442 nm and an emission wavelength of 490 nm.

3.2.3 Surgical Procedures

Similar to the analytical methods, the same surgical and animal procedures describe in Chapter 2, Section 3 were followed for all experiments carried out in this chapter as well. Male Wistar Rats weighing 300-450 grams, purchased from Charles River (Charles River Laboratories, Wilmington, MA) or Harlan (Harlan Laboratories, Indianapolis, Indiana) were used in this study. Rats were housed communally with free access to food and water until the time of the study. Rats

were anesthetized with a cocktail of ketamine and xylazine and maintained under anesthesia with booster doses of ketamine for the duration of the experiment.

Once the rat was fully anesthetized, it was then placed in the stereotaxic frame, an incision made, and the bregma located. The appropriate stereotaxic coordinates were calculated for the CA1 region of the hippocampus (posterior 5.6 mm, lateral +4.8 mm, and ventral 5.0 mm). Anchor screws and the probe were implanted. The probe was perfused with aCSF/3-MPA for the duration of the experiment. At the termination of the experiment, the rat was euthanized using isoflurane overdose followed by decapitation and the brain was harvested for histological analysis.

3.3 Experimental Design

3.3.1 Mitochondrial Starvation

3.3.1.1 Glucose and Lactate Supplementation

Both glucose and lactate are important precursors of glutamate that may have been depleted during the first seizure, leading to a reduction in intracellular glutamate[5, 6, 9, 38, 39]. In this set of experiments, either 15 mM glucose or 10 mM lactate was added to the perfusate during the inter-seizure period to determine whether glutamate depletion following the first episode of seizures was caused by a reduction in glutamate synthesis[7, 9].

3.3.2 Transporter Pathway

In another set of experiments the transporter pathway was investigated to determine if a neuronal protective response is occurring. To test this hypothesis, a glutamate transport blocker,

1.0 mM dihydrokainic acid, was administered simultaneously through the MD probe with the second dose of the epileptic agent[40]. Blocking the transporters counteracts this hyperactivation and protective response, leaving all available glutamate in the extracellular space to be measured via microdialysis sampling.

3.3.3 Neuronal Death and Damage

To determine the amount of cell death occurring during and after the first seizure, propidium iodide (PI) was used to stain slices of the brain tissue to determine cell viability[22]. Brain slices were stained with PI, and the number of dead (PI-positive) cells were counted. For the histochemical staining experiments, surgical procedures were the same as described above. Experiments followed the same protocol as in the 180-min time regime. Both control and 3-MPA dosing experiments were performed for histochemical staining. Animals were sacrificed immediately before the induction of the second seizure stimulation to determine the amount of viable cells at that time point. The brain was harvested and cut into 1 mm thick slices which were incubated in aCSF with 10 mM glucose to keep them viable. Slices were incubated with 1.5 mL of 10 µg/mL PI for 30 min at 37 °C. After the staining was complete, slices were rinsed with aCSF and read on a Nikon Eclipse TE2000-S inverted microscope. Images were captured using a 1X objective lens and NIS-Elements software.

3.3.4 Epileptic Agent Mechanism of Action

To determine if the mechanism of action of 3-MPA is the cause of the glutamate diminution or cell damage, preliminary experiments using KA as an epileptic agent as opposed to 3-MPA

were done. The experimental procedures were identical to those previously described above. Two 30-minute seizure inductions were made by delivering 500 µM KA in aCSF through the microdialysis probe rather than the 3-MPA. The same 180 minute recovery period with blank aCSF was allow between the two inductions.

3.4 Results and Discussion

3.4.1 Statistical Analysis

Similar to the statistical analyses performed in Chapter 2, analysis of this data was done twice, once using the initial baseline for both seizures, and once using the baselines before each individual seizure for calculation. Numbers obtained from the second set of calculations are represented in parentheses below. Statistical analysis was performed using t-tests that were run on each set of experiments to demonstrate if there was a statistically significant difference in glutamate response between the two seizure episodes and are shown in Table 3.1 and Table 3.2. Graphical representation to summarize the difference in glutamate release between seizure episodes one and two for all of the experimental conditions is shown in Figure 3.2. The error bar on the first seizure for the DHK experiments is extremely large because one animal did not experience a first seizure.

3.4.2 Transporter Inhibition

DHK had very little effect on the amount of glutamate released during the second seizure episode compared to control. As can be seen in Figure 3.3, a 70 ± 4 % (83 ± 4 %) decrease in

Medium Supplementation	Attenuation (%)	p Value
aCSF	80. ± 7 (N=5)	0.019
15 mM Glucose	57 ± 3 (N=5)	0.039
10 mM Lactate	50. ± 4 (N=6)	0.016
1.0 mM DHK	70. ± 4 (N=5)	0.022

Table 3.1: Percent attenuation in glutamate release for each experiment using initial baseline for both seizures.

Medium Supplementation	Attenuation (%)	p Value
aCSF	90. ± 7 (N=5)	0.0005
15 mM Glucose	79 ± 3 (N=5)	0.0007
10 mM Lactate	19 ± 4 (N=6)	0.28
1.0 mM DHK	83 ± 4 (N=5)	0.03

Table 3.2: Percent attenuation in glutamate release for each experiment using individual baseline for each seizure.

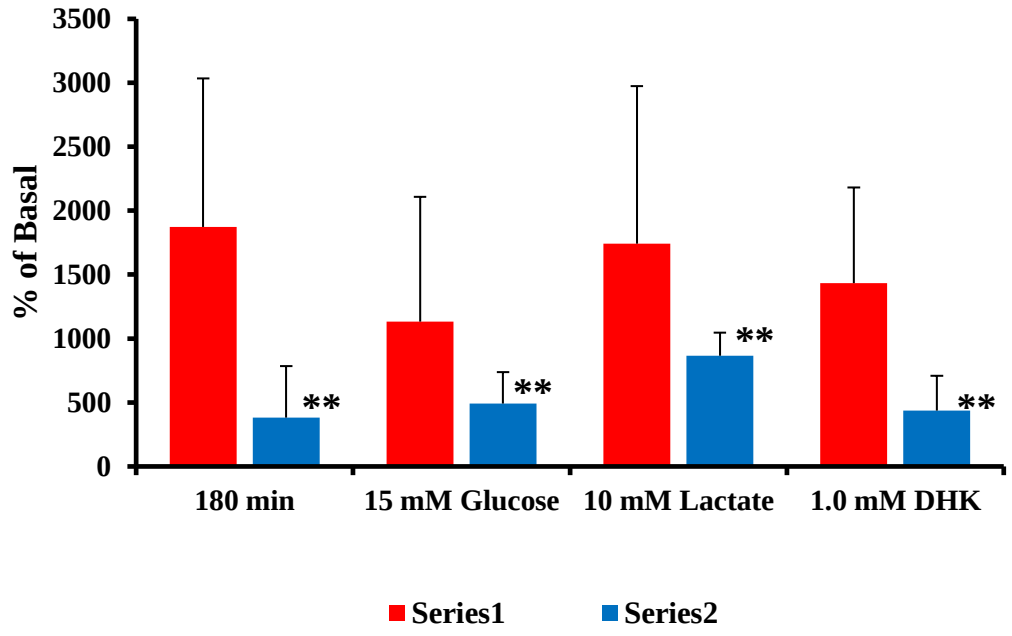

Figure 3.2: Graphical comparison of glutamate release between first and second seizure episodes for each experimental condition.

**p<0.05

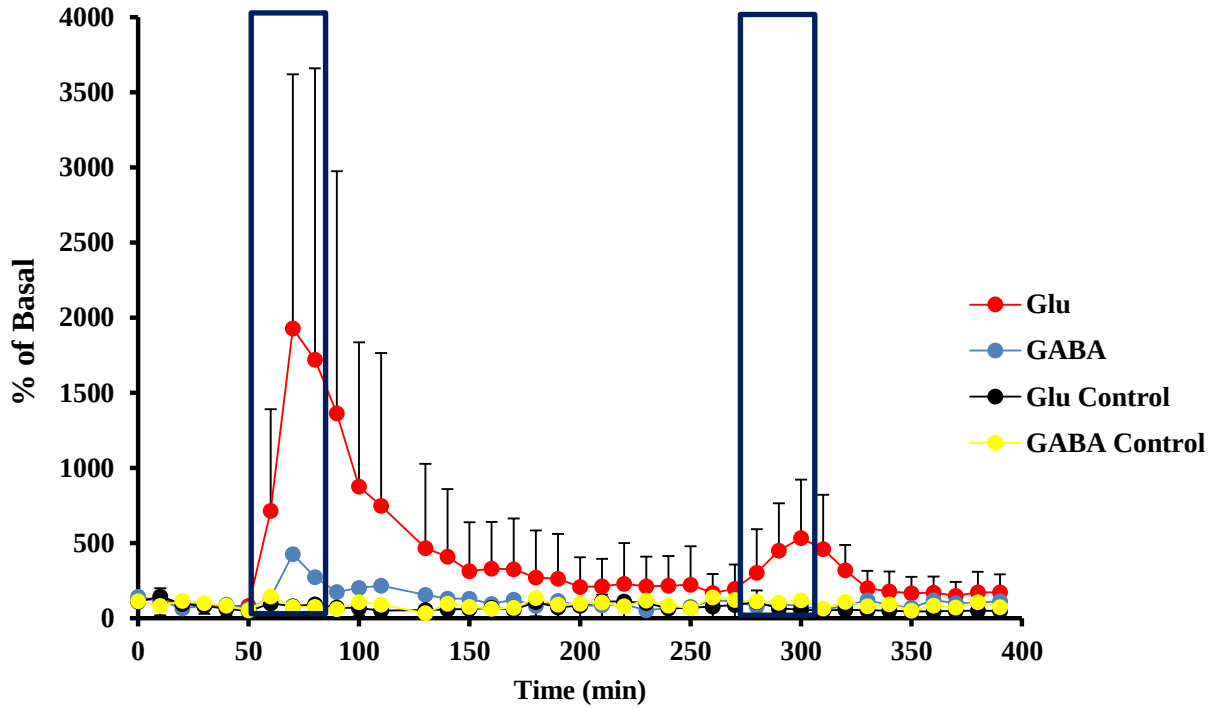

Figure 3.3: Glutamate transporter inhibition by dihydrokainic acid during second seizure episode (N = 5).

glutamate release was observed during the second seizure-like stimulation, which was less than the 80 ± 7% (90 ± 7 %) observed in experiments performed in the absence of DHK. However, this was not a statistically significant improvement compared to control, leading us to believe that the increase in glutamate reuptake is most likely not the mechanism responsible for the diminution of glutamate release during the second seizure episode.

3.4.3 Mitochondrial Starvation

Another set of experiments involved supplementing the perfusate with 15 mM glucose between the two seizure events (Figure 3.4). Under these conditions, a 23 ± 3% (11 ± 3%) increase in extracellular glutamate concentrations was observed during the second episode compared to the 180-min control experiment without glucose. However, these glutamate levels were still significantly attenuated compared to those in the first seizure, an indication that additional factors were possibly affecting glutamate production.

Interestingly, there was a 30 ± 4% (71 ± 4%) increase in glutamate release observed during the second seizure episode with lactate supplementation compared to 180-min control experiments without lactate (Figure 3.5). According to the first calculation, an attenuation in glutamate release was still observed during the second episode when compared with the first. However, when the true baseline is used for the second seizure induction, there is only at 19 ± 4% attenuation in glutamate release in the second seizure episode. After a t-test analysis comparing the first seizure to the second seizure, there was no statistically significant difference in the glutamate release between seizures when the perfusate was supplemented with lactate ($p=0.28$). This increase can most likely be explained by the direct connection of lactate to the KREBS cycle. During stimulation, the glia act to replenish the source of lactate so it can be converted to pyruvate to

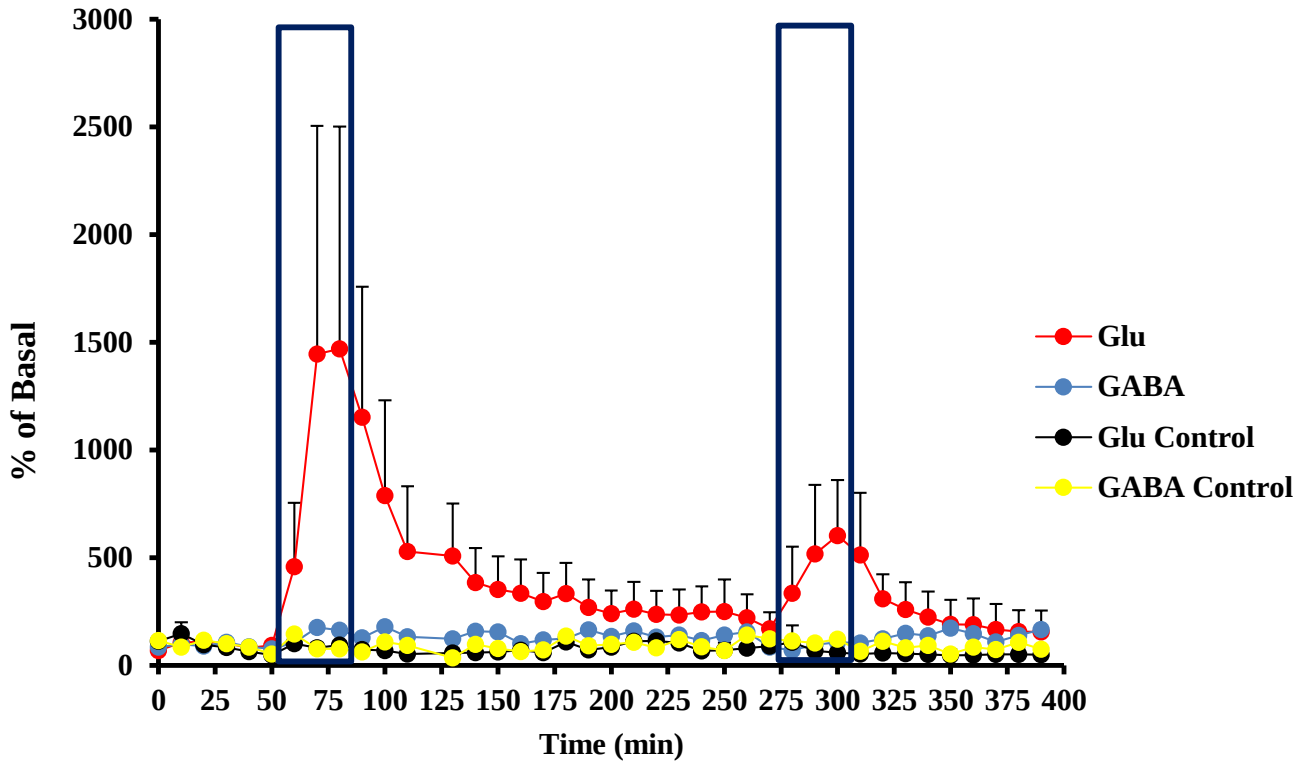

Figure 3.4: Supplementation of inter-seizure perfusion fluid with 15 mM glucose (N = 5).

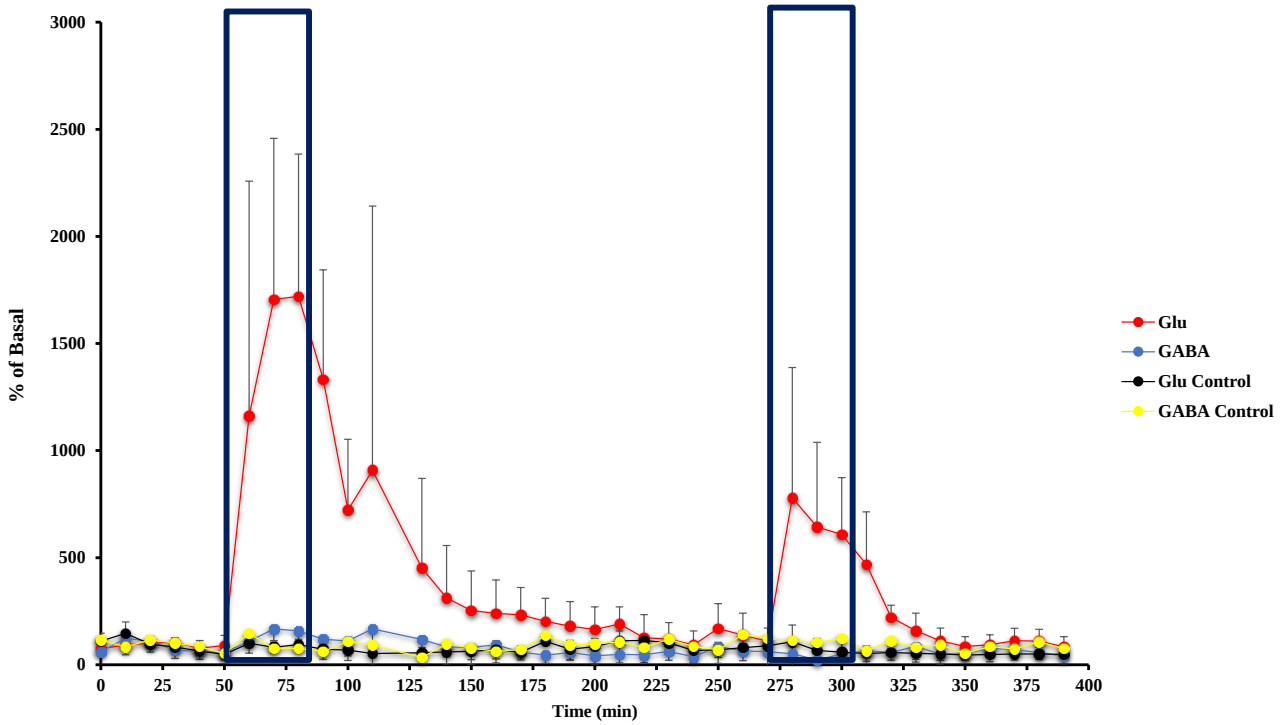

Figure 3.5: Supplementation of inter-seizure perfusion fluid with 10 mM lactate (N = 6).

encourage the KREBS cycle. By flooding the system with supplemental lactate, this process can occur quicker. The conversion of lactate to glutamate is a much faster process than glucose to glutamate. Lactate can directly supplement the production of α-ketoglutarate to increase glutamate. The keto-acids are transported out of the mitochondria to be used for glutamate synthesis which can then be release from the vesicles or by cell damage.

It is apparent from both the glucose and lactate experiments that the surrounding glial cells were being depleted of the nutrients needed for glutamate biosynthesis. Supplementing the perfusate with lactate yielded a significant increase in glutamate release in the second seizure episode. A slight increase in glutamate release was observed when the perfusate was supplemented with glucose. Both of these observations confirm mitochondrial starvation, however, the fact that the glutamate concentration never reached the same level in the second seizure suggests that other factors must also be affecting glutamate production or release.

3.4.4 Neuronal Death and Damage

Figure 3.6 shows PI-stained histological slices representing the contralateral and ipsilateral sections of a control hippocampus and a hippocampus subjected to the administration of 3-MPA. There was statistically significantly more damage to the ipsilateral side of dosed rats compared to that of the control rats (Table 3.3). It was determined that 37 ± 8% more CA1 and 30 ± 9% more CA3 cells in the ipsilateral hippocampus had died in the dosed rats than in the control rats prior to the second seizure episode. No significant difference in damage was observed in the contralateral side. Additionally, there was overall more damage in the ipsilateral side of the hippocampus for both CA1 and CA3 regions in comparison to the contralateral side, demonstrated in Figure 3.7.

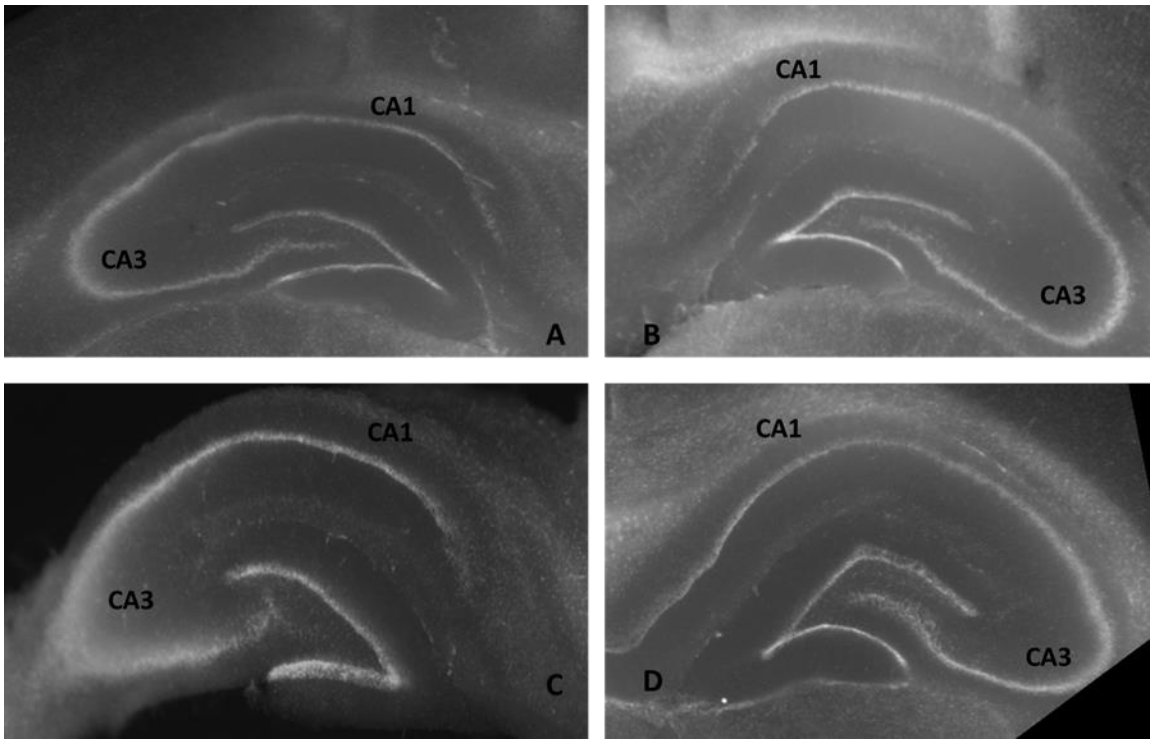

Figure 3.6: Propidium iodide staining of hippocampal slices after the first seizure induction and 180-min recovery period.

A) Ipsilateral dosed, B) contralateral dosed, C) ipsilateral control, D) contralateral control.

Table 3.3

Region	**Damage Diff (%) N=6**	**p Value**
CA1	39 ± 1	0.056^{***}
CA3	30 ± 1	0.075^{***}

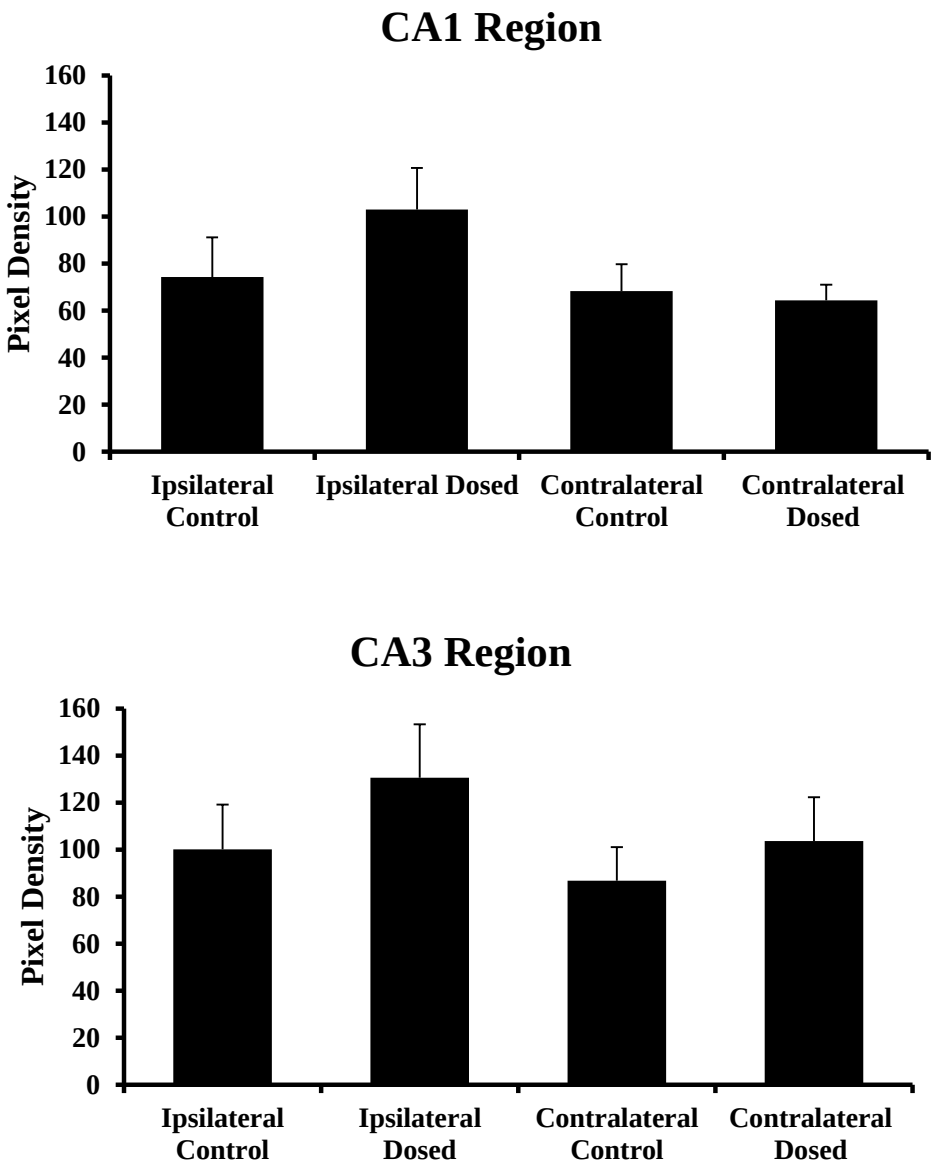

Figure 3.7: Graphical representation of cell death from PI staining.

This is to be expected because the probe was implanted on the ipsilateral side and the contralateral side remained undisturbed in both dosed and control rats. From these experiments, it can be concluded that there is substantial neuronal death during the first seizure, which would lead to a significant reduction in glutamate release during the second seizure episode. However, this reduction was not the sole cause of glutamate attenuation during the second seizure episode, since an increase in glutamate release with both lactate- and glucose-supplemented systems was observed using this same seizure model.

3.4.5 Kainic Acid

The CA1 region of the hippocampus is not as rich in kainate receptors as other regions of the hippocampus, therefore using KA as an epileptic agent in this region would be difficult to get the same level of excitation as that observed with the 3-MPA. Figure 3.8 shows preliminary results for the induction of successive seizure episodes, 180 min apart, within the same experiment using KA as the epileptic agent instead of the 3-MPA. An opposite trend was observed using KA compared with 3-MPA. There was a greater glutamate release in the second induction, compared to the first induction. It is possible that because there are not very many kainate receptors in CA1, the few that are there are becoming sensitized to the epileptic agent. Sensitization refers to an increase in response caused by repeated exposure to a stimulus. Similar to the kindling effect for inducing seizures, the animal becomes sensitized to the epileptic agent following the first application and experiences seizures, or more severe seizures, during the second application of KA. The different trend could also be explain by the different mechanisms of action for seizure induction by KA and 3-MPA. Because these are only preliminary results, it is difficult to arrive

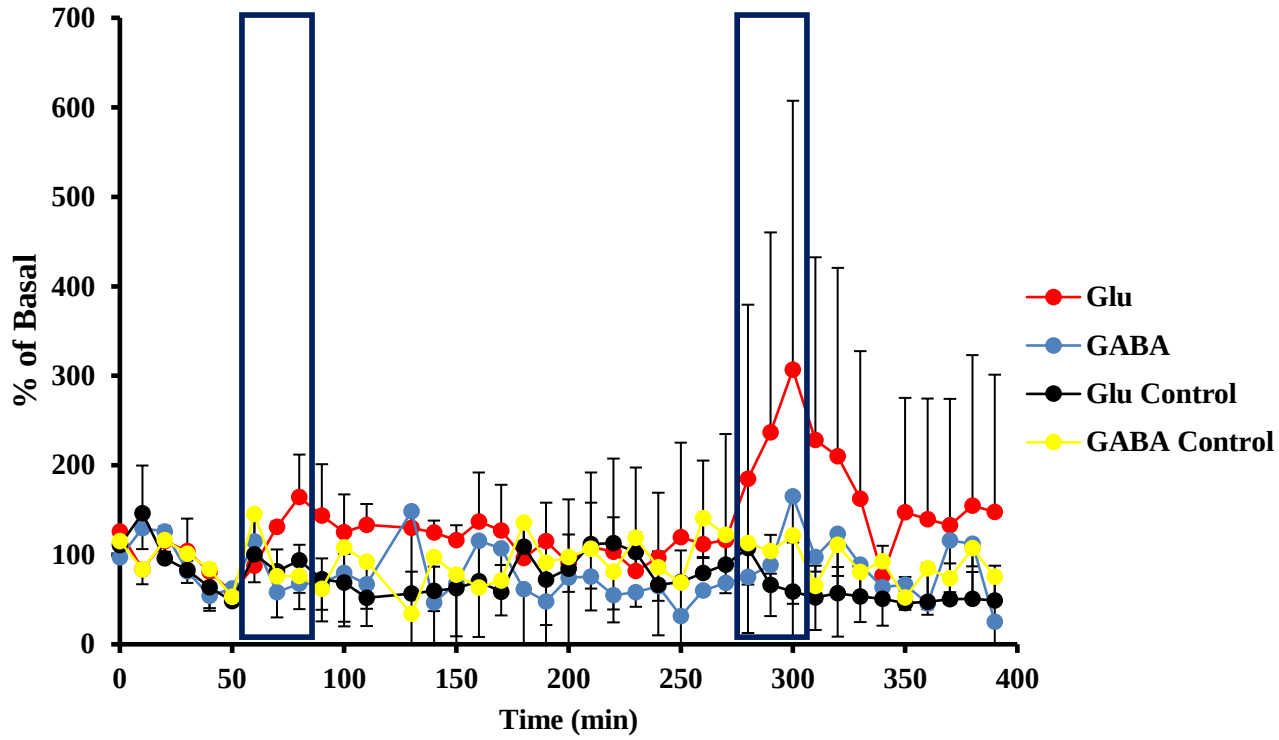

Figure 3.8: Multiple seizure induction by kainic acid (N=3).

at any concrete conclusions regarding the meaning of these results, however, it would be beneficial to add additional seizure episodes to this model to determine if the increase in extracellular glutamate release is compounded with additional seizure episodes. Furthermore, a brain region in which kainate receptors are more highly expressed, such as the CA3 region, should also be studied.

3.5 Conclusions

Based on the results presented here, it is proposed that deficits of glutamate biosynthesis leading to glutamate depletion and cell/neuronal damage/death are the major contributors to the diminution in glutamate release during the second period of seizures induced by 3-MPA. Supplementing the perfusate with lactate proved to have a significant effect on the biosynthesis of glutamate, most likely by encouraging the KREBS cycle. In the future, other epileptic agents should be investigated to determine the specificity of action of 3-MPA-induced seizures in causing depletion of glutamate levels and neuronal damage. More seizures should be added to the model to determine if subsequent seizures lead to compounding glutamate diminution.

3.6 References

1. Rosenmund, C. Definition of the Readily Releasable Pool of Vesicles at Hippocampal Synapses, *Neuron (Cambridge, Mass.) 16*, 1197-1207.
2. Von Gersdorff, H. Depletion and replenishment of vesicle pools at a ribbon-type synaptic terminal, *The Journal of neuroscience 17*, 1919-1927.
3. Stevens, C. F. Estimates for the pool size of releasable quanta at a single central synapse and for the time required to refill the pool, *Proceedings of the National Academy of Sciences - PNAS 92*, 846.
4. Wang, L.-Y., and Kaczmarek, L. K. (1998) High-frequency firing helps replenish the readily releasable pool of synaptic vesicles, *Nature 394*, 384-388.
5. Lama, S., Auer, R. N., Tyson, R., Gallagher, C. N., Tomanek, B., and Sutherland, G. R. (2014) Lactate Storm Marks Cerebral Metabolism following Brain Trauma, *Journal of Biological Chemistry 289*, 20200-20208.
6. Uehara, T., Sumiyoshi, T., Itoh, H., and Kurachi, M. (2007) Role of glutamate transporters in the modulation of stress-induced lactate metabolism in the rat brain, *Psychopharmacology 195*, 297-302.
7. Maddock, R. J., Buonocore, M. H., Miller, A. R., Yoon, J. H., Soosman, S. K., and Unruh, A. M. (2013) Abnormal Activity-Dependent Brain Lactate and Glutamate+Glutamine Responses in Panic Disorder, *Biological Psychiatry 73*, 1111-1119.
8. Tholance, Y. Analytical validation of microdialysis analyzer for monitoring glucose, lactate and pyruvate in cerebral microdialysates, *Clinica chimica acta 412*, 647-654.
9. Wakabayashi, K. T., Myal, S. E., and Kiyatkin, E. A. (2015) Fluctuations in nucleus accumbens extracellular glutamate and glucose during motivated glucose-drinking

behavior: dissecting the neurochemistry of reward, *Journal of neurochemistry 132*, 327-341.

10. Verma, P., Augustine, G. J., Ammar, M.-R., Tashiro, A., and Cohen, S. M. (2015) A neuroprotective role for microRNA miR-1000 mediated by limiting glutamate excitotoxicity, *Nat Neurosci 18*, 379-385.
11. Mehta, A., Prabhakar, M., Kumar, P., Deshmukh, R., and Sharma, P. L. (2013) Excitotoxicity: Bridge to various triggers in neurodegenerative disorders, *European Journal of Pharmacology 698*, 6-18.
12. Biasini, E., Unterberger, U., Solomon, I. H., Massignan, T., Senatore, A., Bian, H., Voigtlaender, T., Bowman, F. P., Bonetto, V., Chiesa, R., Luebke, J., Toselli, P., and Harris, D. A. (2013) A Mutant Prion Protein Sensitizes Neurons to Glutamate-Induced Excitotoxicity, *The Journal of Neuroscience 33*, 2408-2418.
13. Liang, L.-P., and Patel, M. (2006) Seizure-induced changes in mitochondrial redox status, *Free Radical Biology and Medicine 40*, 316-322.
14. Patel, M. (2004) Mitochondrial dysfunction and oxidative stress: cause and consequence of epileptic seizures, *Free Radical Biology and Medicine 37*, 1951-1962.
15. Gunduz, O., Oltulu, C., and Ulugol, A. (2011) Role of GLT-1 transporter activation in prevention of cannabinoid tolerance by the beta-lactam antibiotic, ceftriaxone, in mice, *Pharmacology Biochemistry and Behavior 99*, 100-103.
16. Miller, B. R. Up-regulation of GLT1 expression increases glutamate uptake and attenuates the Huntington's disease phenotype in the R6/2 mouse, *Neuroscience 153*, 329-337.

17. Liubinas, S. V., O'Brien, T. J., Moffat, B. M., Drummond, K. J., Morokoff, A. P., and Kaye, A. H. (2014) Tumour associated epilepsy and glutamate excitotoxicity in patients with gliomas, *Journal of Clinical Neuroscience 21*, 899-908.

18. Sodero, A. O., Vriens, J., Ghosh, D., Stegner, D., Brachet, A., Pallotto, M., Sassoè-Pognetto, M., Brouwers, J. F., Helms, J. B., Nieswandt, B., Voets, T., and Dotti, C. G. (2012) Cholesterol loss during glutamate-mediated excitotoxicity, *The EMBO Journal 31*, 1764-1773.

19. Wang, W., Zhang, F., Li, L., Tang, F., Siedlak, S. L., Fujioka, H., Liu, Y., Su, B., Pi, Y., and Wang, X. (2015) MFN2 Couples Glutamate Excitotoxicity and Mitochondrial Dysfunction in Motor Neurons, *Journal of Biological Chemistry 290*, 168-182.

20. Cheung, N. S. Micromolar l-glutamate induces extensive apoptosis in an apoptotic-necrotic continuum of insult-dependent, excitotoxic injury in cultured cortical neurones, *Neuropharmacology 37*, 1419-1429.

21. Levy, R. Status Epilepticus: Mechanisms of Brain Damage and Treatment, *Archives of neurology (Chicago) 41*, 252-252.

22. Newbold, A., and Newbold, A. Detection of Apoptotic Cells Using Propidium Iodide Staining, *Cold Spring Harbor protocols 2014*, pdb.prot082545-pdb.prot082545.

23. Hezel, M. Propidium iodide staining: A new application in fluorescence microscopy for analysis of cytoarchitecture in adult and developing rodent brain.(Report), *Micron (Oxford, England : 1993) 43*, 1031.

24. Horton, R. W., and Horton, R. W. Seizures induced by allylglycine, 3-mercaptopropionic acid and 4-deoxypyridoxine in mice and photosensitive baboons, and different modes of

inhibition of cerebral glutamic acid decarboxylase, *British journal of pharmacology 49*, 52-63.

25. Netopilová, M., Dršata, J., Haugvicová, R., Kubová, H., and Mareš, P. (1997) Inhibition of glutamate decarboxylase activity by 3-mercaptopropionic acid has different time course in the immature and adult rat brains, *Neuroscience letters 226*, 68-70.
26. Olsen, R. W., and Avoli, M. (1997) GABA and epileptogenesis, *Epilepsia 38*, 399-407.
27. Sarhan, S. (1979) Metabolic inhibitors and subcellular distribution of GABA, *Journal of neuroscience research 4*, 399-421.
28. Babb, T. L., and Babb, T. Kainic acid induced hippocampal seizures in rats: comparisons of acute and chronic seizures using intrahippocampal versus systemic injections, *Italian journal of neurological sciences 16*, 39-44.
29. eacute, and vesque, M. The kainic acid model of temporal lobe epilepsy, *Neuroscience and biobehavioral reviews 37*, 2887-2899.
30. Crick, E. W. Correlation of 3-mercaptopropionic acid induced seizures and changes in striatal neurotransmitters monitored by microdialysis, *European journal of pharmaceutical sciences 57*, 25-33.
31. Crick, E. W., Osorio, I., Bhavaraju, N. C., Linz, T. H., and Lunte, C. E. (2007) An investigation into the pharmacokinetics of 3-mercaptopropionic acid and development of a steady-state chemical seizure model using in vivo microdialysis and electrophysiological monitoring, *Epilepsy research 74*, 116-125.
32. Mayer, A. (2010) Local Dosing in a 3-Mercaptopropionic Acid Chemically-Induced Epileptic Seizure Model with Microdialysis Sampling, (Lunte, C. E., Dunn, B., Johnson, M., Lunte, S., and Osorio, I., Eds.), ProQuest Dissertations Publishing.

33. Mayer, A. P., Osorio, I., and Lunte, C. E. (2013) Microperfusion of 3-MPA into the brain augments GABA, *Epilepsy & Behavior 29*, 478-484.

34. Netopilov, aacute, and Miloslava. Differences between immature and adult rats in brain glutamate decarboxylase inhibition by 3-mercaptopropionic acid, *Epilepsy research 20*, 179-184.

35. Girardi, E. 3-Mercaptopropionic Acid-Induced Seizures Decrease NR2B Expression in Purkinje Cells: Cyclopentyladenosine Effect, *Cellular and molecular neurobiology 30*, 985-990.

36. Ueda, Y., Yokoyama, H., Niwa, R., Konaka, R., Ohya-Nishiguchi, H., and Kamada, H. (1997) Generation of lipid radicals in the hippocampal extracellular space during kainic acid-induced seizures in rats, *Epilepsy research 26*, 329-333.

37. De Montigny, P., Stobaugh, J. F., Givens, R. S., Carlson, R. G., Srinivasachar, K., Sternson, L. A., and Higuchi, T. (1987) Naphthalene-2,3-dicarboxyaldehyde/cyanide ion: a rationally designed fluorogenic reagent for primary amines, *Analytical chemistry 59*, 1096-1101.

38. Di Sebastiano, K. M., Bell, K. E., Barnes, T., Weeraratne, A., Premji, T., and Mourtzakis, M. (2013) Glutamate supplementation is associated with improved glucose metabolism following carbohydrate ingestion in healthy males, *The British Journal of Nutrition 110*, 2165-2172.

39. Koska, J., Blazicek, P., Marko, M., Grna, J., Kvetnansky, R., and Vigas, M. (2000) Insulin, catecholamines glucose and antioxidant enzymes in oxidative damage during different loads in healthy humans, *Physiological Research 49*, S95-S100.

40. Gynther, M., Petsalo, A., Hansen, S. H., Bunch, L., and Pickering, D. S. (2015) Blood–Brain Barrier Permeability and Brain Uptake Mechanism of Kainic Acid and Dihydrokainic Acid, *Neurochemical Research 40*, 542-549.

41. Dunleavy, M., Provenzano, G., Henshall, D. C., and Bozzi, Y. (2013) Kainic Acid-Induced Seizures Modulate Akt (SER473) Phosphorylation in the Hippocampus of Dopamine D2 Receptor Knockout Mice, *Journal of Molecular Neuroscience 49*, 202-210.

Chapter 4

Effect of Glutathione Upregulation and Downregulation on Oxidative Damage

4.1 Background and Significance

A major secondary effect of seizures is oxidative stress that occurs when there is an imbalance in the body's endogenous antioxidants and reactive oxygen and nitrogen species (ROS and RNS)[1-4]. Several rodent models have been developed to study the secondary effect of oxidative damage associated with epilepsy[5]. The body can scavenge ROS both enzymatically, for example through superoxide dismutase (SOD), or glutathione peroxidase (GPx) or nonenzymatically, through compounds like antioxidants [5].

Glutathione (GSH) is one of the most prominent natural antioxidants in the brain[6]. GSH contains a thiol group that can act as a reducing agent to neutralize ROS. When GSH is oxidized, it can readily react with another oxidized GSH to form stable glutathione disulfide (GSSG). This reaction is catalyzed by GPx. It is hypothesized that higher levels of GSH in the brain would reduce the amount of oxidative damage by neutralizing the ROS[7, 8]. Similarly, decreased GSH would lead to an increase in oxidative damage. The brain accounts for nearly 20% of the aerobic metabolism for the body. It is the organ that consumes the highest amount of oxygen and is rich in polyunsaturated fatty acids[5]. These factors make brain cells highly susceptible to ROS-induced damage, specifically lipid peroxidation.

Arachidonic acid (ARA) is a fatty acid that is responsible for maintaining neurological health and hippocampal cell membrane structure[9]. It can help protect the brain from oxidative damage by activating lipid receptors[10, 11]. When cell membranes become damaged during oxidative stress, ARA undergoes lipid peroxidation, producing fatty acid radicals and eventually

stable end products, like malondialdehyde (MDA). Previous research in the Lunte lab by Dr. Carl Cooley demonstrated a significant increase in MDA production with the induction of a local seizure using 3-MPA[12]. His results are shown in Figure 4.1. Increasing doses of 3-MPA resulted in an increase in extracellular MDA production. As discussed in Chapter 3 of this thesis, cell damage occured with seizure induction, which was confirmed with PI staining. When a significant amount of stress occurs to the cells, the ARA cannot counteract the ROS and gets broken down, producing MDA, which can be used as a quantitative biomarker of seizure induced oxidative damage. In this research, seizures were locally induced to one region of the brain. Because the seizure induction was so localized, the imbalance was focused to a small region, leading to concentrated neurotoxicity. This localized imbalance and subsequent neurotoxicity can affect a multitude of oxidative pathways. It is evident that there is a correlation between seizures and oxidative damage; however, the specific pathways and brain regions that account for this damage are still unclear.

This chapter describes a study in which the amount of an antioxidant, GSH, was modulated prior to the induction of seizures. Extracellular MDA and GSH levels were measured before, during, and after the induction of a single seizure to determine the role of GSH on seizure induced oxidative damage. Control experiments were performed by measuring basal concentrations of GSH and MDA before the induction of a seizure. GSH synthesis was then upregulated to see if an increase in GSH leads to a decrease in MDA, signifying a decrease in oxidative damage. Conversely, GSH synthesis was also downregulated to determine if a decrease in antioxidants leads to an increase in oxidative damage.

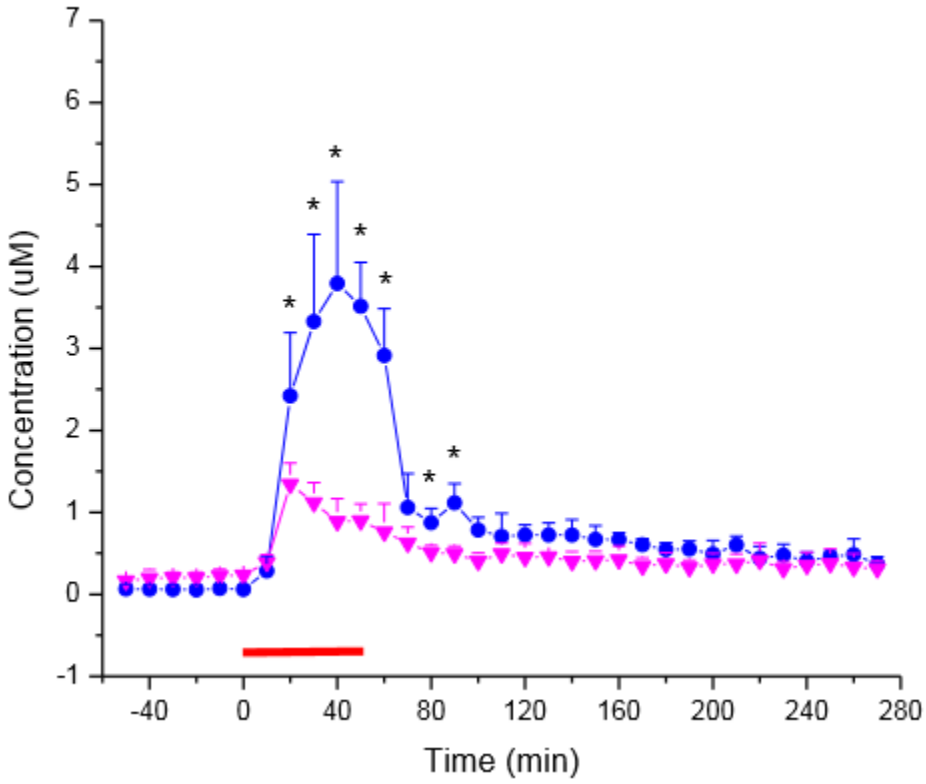

Figure 4.1: Extracellular MDA concentration versus time from CA1 region of the hippocampus as determined by microdialysis sampling.

The red bar represents the period when 3-MPA was being perfused through the probe, starting at time zero, ending at time 50. Two concentrations were tested, 10mM (blue plot) (n=5), and 1 mM (pink plot) (n=3). (* $p<0.001$ for 10 mM perfusion t-test)

Reproduced from the thesis by Dr. Carl Cooley[12].

4.1.1 Glutathione as an Antioxidant

The body has a series of defense mechanisms to protect itself from oxidative stress. Glutathione (GSH) is a natural antioxidant tripeptide containing glutamate, cysteine, and glycine. It functions as a reducing agent and ROS scavenger[6, 13, 14]. GSH is present in the millimolar range intracellularly and the micromolar range extracellularly[5]. Under normal physiologic conditions, GSH is oxidized by hydrogen peroxide in the presence of GPx to form GSSG[15]. GSH plays a key role in the body's defense against oxidative stress through two mechanisms: scavenging free radicals and acting as a cofactor for oxygen damage-protecting enzymes. GSSG can be reduced back to GSH by glutathione reductase using NADPH as an electron donor[16]. Because GSH exists in both the oxidized and reduced forms, it can serve as a redox agent to prevent oxidative damage[8]. It has been reported that, during a seizure, there is a decrease in glutathione reductase enzymatic activity[5]. When this happens, there is a decrease in GSH and an increase in GSSG. Less GSH available means less antioxidants to neutralize the ROS, leading to further damage and hyperexcitabilty[17]. This cycle continues until the damage is irreparable. Therefore, in this chapter, it is hypothesized that neurotoxicity, specifically seizure induced oxidative damage, can be modulated by either upregulating or downregulating the amount of GSH. Encouraging GSH synthesis or GPx activity may have mitigating effects for seizure induced oxidative damage.

4.1.2 Biomarkers of Oxidative Damage

The most direct way to measure the amount of oxidative stress is to quantify the amount of ROS and RNS in the body[1, 18, 19]. Various pathways and resulting damage of oxidative stress are shown in Figure 4.2. Superoxide and hydroxyl radicals are the most common ROS. Half-lives

of these free radicals are typically between 10^{-6} to 10^{-9} seconds with basal levels of 90 nM for superoxide to 60 nM for hydroxyl radical, so it is important to find other, more stable markers to measure the amount of oxidative damage occurring to the body.

4.1.2.1 Lipid Peroxidation

Lipid peroxidation occurs when oxidative free radicals react with lipids in the body. Phospholipase A_2 is responsible for the hydrolysis of phospholipids, which causes the release of arachidonic acid from neural membranes during oxidative stress[10-12]. When membrane lipids are oxidized by free radicals, their structure changes and the cell is damaged. There are three steps to this process: initiation, propagation, and termination. These end with the formation of lipid oxidation products (LOPs) that are shown in Figure 4.3. In the initiation step, a fatty acid radical is produced by the reaction of fatty acids with ROS. These fatty acid radicals are unstable and therefore quickly react with oxygen to produce peroxyl-fatty acid radicals. These radicals are also highly unstable and readily react with other free fatty acids to produce additional radicals, lipid peroxides, or cyclic peroxides[20, 21]. This propagation cycle continues as new fatty acid radicals are produced and continue to react with one another. Finally, when two fatty acid radicals react with each other, they produce an unreactive non-radical species in a process known as termination. This only happens when the radical species concentration is high enough to encourage the collision of two radicals rather than a radical with a non-radical. After termination occurs, lipid hydroperoxides are formed that quickly decompose into more stable compounds such as isoprotanes and reactive aldehydes like MDA or 4-hydroxynonenal (HNE)[22, 23].

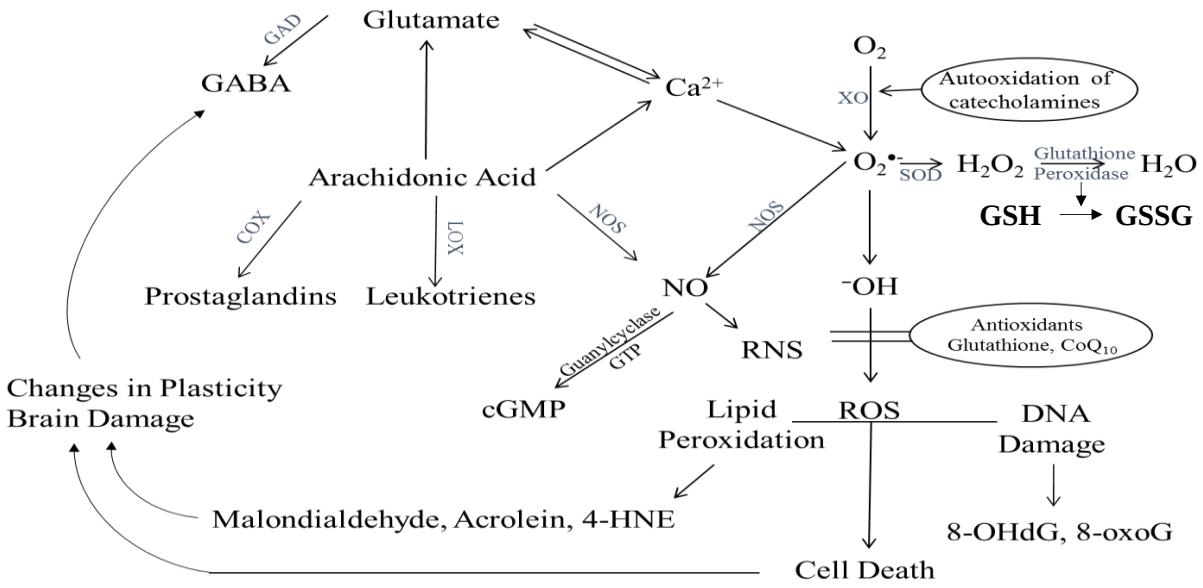

Figure 4.2: Key pathways and biomarkers of oxidative stress

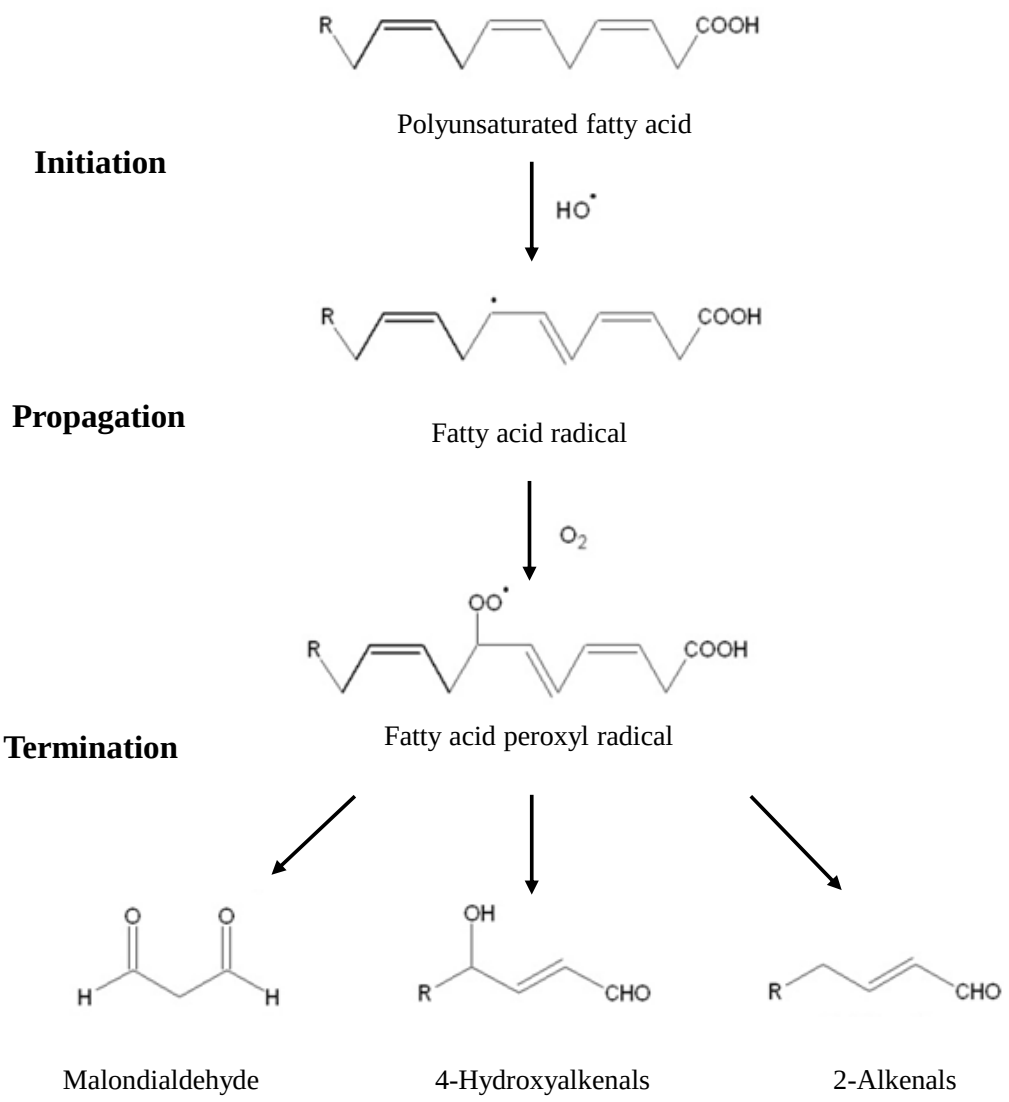

Figure 4.3: Schematic of lipid peroxidation mechanism.

4.1.2.2 Malondialdehyde

As stated above, lipid peroxidation leads to the formation of lipid hydroperoxides and bicyclic endoperoxides. These peroxides breakdown further into secondary products like acrolein, HNE and MDA. It was shown in Chapter 3 that cell damage was occurring from the propidium iodide staining. In these studies, MDA was selected as the biomarker to quantify the amount of oxidative stress induced lipid peroxidation. MDA is a more stable biomarker for the determination of lipid peroxidation induced oxidative damage than acrolein or HNE. In this study, MDA was quantified using a commercially available fluorescence assay. Thiobarbituric acid (TBA) reacts with MDA to form a fluorescent TBA-MDA adduct that can be quantitated spectrophotometrically.

4.1.3 Upregulation and Downregulation of Glutathione

4.1.3.1 Buthionine Sulfoximine – Downregulation of GSH

Because GSH functions as a reducing agent and ROS scavenger, depletion of GSH should make the cells more susceptible to the effects of oxidative damage. Buthionine sulfoximine (BSO) has been shown to function as an inhibitor of ɣ-glutamylcysteine synthase, the rate-limiting enzyme in GSH synthesis[24]. A study by Vanella *et al.* has shown that the intravenous dosing of BSO depletes total GSH in the striatum by up to 59% within 24 hours of the dose[14, 25]. BSO takes 24 hours to take full effect and remains in the system, depleting GSH for up to 48 hours. Furthermore, BSO does not affect other biological thiols, keeping the rest of the system essentially unaltered. By administering BSO prior to the induction of a seizure, the amount of GSH would be

downregulated. It was anticipated that by decreasing the amount of the antioxidant available there would be an increase in the amount of observed oxidative damage.

4.1.3.2 ɣ-Glutamylcysteine Ethyl Ester – Upregulation of GSH

An important precursor to GSH, ɣ-glutamylcysteine is the rate limiting substrate in GSH biosynthesis[26]. It is anticipated that, by increasing the amount of natural antioxidant GSH in the system prior to seizure induction, the brain would suffer less oxidative damage. Studies have shown that the administration of ɣ-glutamylcysteine ethyl ester increases the total levels of ɣ-glutamylcysteine by protecting the substrate for GSH synthesis[27]. The conversion from ɣ-glutamylcysteine to GSH goes to completion quickly. By administering the precursor to GSH synthesis, there should be an increase in total GSH in the system and a reduction in oxidative damage.

4.2 Materials and Methods

4.2.1 abcam© GSH/GSSG Ratio Detection Assay Kit (Fluorometric Green)

Samples were analyzed for GSH using a commercially available, abcam© GSH/GSSG Ratio Detection Assay Kit, purchased from abcam© (Cambridge, MA). Samples and standards were prepared according to the user guide. The derivatization reagent was Thiol Green Indicator. Unfortunately, the exact structure of this compound is proprietary, and is therefore not reported in the literature. The molecular weight of the reagent is 419 Da and it contains a fluorophore masked

by a quencher. Upon reaction with a thiol, the quencher is released, increasing the fluorescence intensity (This information was provided by Dr. Paul, the Scientific Support Manager at abcam©)

Because microdialysis produces essentially protein-free samples, no additional sample clean-up or preparation was required prior to the derivatization of the real samples. According to the kit instructions for low volume sample analysis, 25 µL of sample or standard was to be added to a 384-microwell plate. Because only 5 µL of dialysate sample was available for analysis, 20 µL of phosphate buffered saline was added to the sample to make the total sample volume 25 µL. To that, 25 µL of 100X Thiol Green Indicator in Assay Buffer was added to each well. Samples were allowed to incubate in the dark at room temperature for 50 minutes. Samples were then analyzed using a SpectraMax Plus Microplate Reader at Ex: 490 nm, Em: 520 nm.

4.2.2 abcam© GSH/GSSG Ratio Detection Kit Validation via LC-Fl

In order to validate that the GSH assay kit would have linearity and limits of detection comparable to that of the more robust liquid chromatography-fluorescence system, samples were derivatized as describe above. Derivatized samples were then analyzed on a liquid chromatographic system with fluorescence detection. The system consisted of two Shimadzu LC-10ADvp pumps, a 100 µL Shimadzu mixer, and a Rheodyne 9725i PEEK sample injector connected to a Phenomenex Synergi 4-µm Hydro-RP column (150 × 2.0 mm, Phenomenex, Torrance, CA) with a Phenomenex C18 guard cartridge. The binary gradient was controlled by a Shimadzu SCL-10vp system controller. Mobile phase A was 30 mM tetrabutylammonium hydroxide (TBA) in 25% methanol:75% water (v%:v%). Mobile phase B was 30 mM TBA in 100% methanol. The gradient was as follows: 0 - 2.0 min, 40% B; 2.0 - 3.5 min, 95% B; 3.5 – 4.0

min, 40% B; 4.0 – 6.0 min, 40% B. The Shimadzu 10AXL fluorescence detector was operated at an excitation wavelength of 490 nm and an emission wavelength of 520 nm.

4.2.3 TBARS Kit

Samples were analyzed for MDA concentration using a commercially available Thiobarbituric Acid Reactive Substances (TBARS) Kit (Cayman Chemical, Ann Arbor, MI). Because the original kit instructions required a 100 µL sample volume, but only 4 µL were availabe, the kit had to be modified and optimized in order to obtain good linearity and required limits of detection. The original kit assay required the following ratio of reagents: 100 µL sample/standard, 100 µL SDS, 4 mL of Color Reagent (50 mL of dilute acetic acid, 50 mL of dilute sodium hydroxide with 530 mg of thiobarbituric acid). The final volume of 4 mL lead to too much dilution of the 4 µL sample and therefore did not produce a signal. It was determined that three, 4 µL samples would have to be combined to make a 12 µL sample volume. The final reagent ratio was as follows: 12 µL sample/standard, 12 µL SDS, 200 µL Color Reagent. Samples were mixed in locking microtubes (Fisher Scientific, Pittsburg, PA) and boiled for one hour. After one hour, samples were placed in an ice bath for 10 minutes to stop the reaction. 200 µL of sample was placed in a 96-well black plate and analyzed using the SpectraMax Microplate Reader at Ex: 530 nm and Em: 550 nm.

4.2.4 TBARS Kit Validation via LC-Fl

In order to validate that the MDA assay kit would have linearity and limits of detection comparable to that of the more robust liquid chromatography-fluorescence system, samples were

derivatized as describe above, following the kit instructions. Derivatized samples were then analyzed on a liquid chromatographic system with fluorescence detection. The same system, mobile phase, and gradient described above were used to test the MDA kit. The Shimadzu 10AXL fluorescence detector was operated at an excitation wavelength of 530 nm and an emission wavelength of 550 nm.

4.2.5 Surgical Procedures

Animal experiments were carried out as described in Chapter 2. Briefly, surgical tools were sterilized using ROCCAL® prior to every experiment. Because these were not survival surgeries, autoclave sterilization was not necessary. Male Wistar Rats weighing 300-450 grams were used in this study. Rats were housed communally with free access to food and water until the time of the study. Rats were placed in an isoflurane chamber and pre-anesthetized via isoflurane inhalation for 5 minutes. The anesthetic cocktail of ketamine (80mg/kg)/ xylazine(10mg/kg) was administered I.P. and allowed to take effect. Once the rat was fully anesthetized via the cocktail, the hair on the skull was shaved as closely as possible. Booster doses of ketamine (40 mg/kg) were administered as needed to maintain adequate anesthesia. The animal's body temperature was maintained at approximately 37 °C using a PhysioSuite heating system.

4.2.6 Microdialysis Brain Probe Implantation

Once the rat was fully anesthetized, it was placed in the stereotaxic frame. The rat was securely in place and an incision approximately 3 cm in length was made in the midline of the skull using a 10 blade scalpel. Four tissue clamps were used to hold the skin to the side, and excess

tissue was removed using cotton tip applicators. Once the skull was removed of excess tissue and blood, the bregma coordinates were determined. The appropriate stereotaxic coordinates were calculated for the hippocampus (posterior 5.6 mm, lateral +4.8 mm, and ventral 5.0 mm). Two 1 mm holes were drilled arbitrarily around the desired probe location and anchor screws were inserted to serve as stability for the cannula. Next, a 3 mm hole was drilled at the calculated probe site. Once the hole had been drilled, the guide cannula was lowered to the appropriate depth and fixed to the skull with dental cement, covering the anchor screws. After the dental cement solidified, the dummy probe was removed from the cannula and replaced with a CMA 12 microdialysis probe with a 2 mm membrane length. The probe was perfused with either aCSF or 3-MPA for the duration of the experiment. The rat was maintained under anesthesia for the duration of the experiment using 40-50 mg/kg supplemental does of ketamine injected I.P. or I.M. At the termination of the experiment, the rat was euthanized using isoflurane overdose followed by decapitation. The brain was harvested for histological analysis.

4.2.7 Animal Experimental Design – Single Seizure

Chapters 2 and 3 discuss the development of an animal model for locally induced epilepsy with the induction of two seizure episodes. The animal experiments carried out in this study involved the induction of a single seizure. This allowed us to investigate the oxidative damage, specifically lipid peroxidation, associated with a locally induced seizure.

4.2.8 Control

Post operatively, animals were allowed to recover for one hour during which time aCSF was constantly perfused through the microdialysis probe at a flow rate of 1.0 μL/min with a CMA/100 microinjection pump. After a 60 minute recovery period, aCSF was perfused for one hour and collected in ten minute intervals to serves a basal level samples. After the basal collection, a solution of 10 mM 3-MPA in aCSF was administered through the probe at a rate of 1.0 μL/min for 30 minutes. After the induction of the single, 30 minute seizure, aCSF was perfused through the probe for a total of 90 minutes. These experiments serve as the controls for seizure induction. For all experiments, samples were collected in ten minute intervals. At the end of the experiment, the animal was euthanized via isoflurane overdose and decapitated for histological analysis.

4.2.9 Sham

To determine the raw amount of both GSH and MDA in the rat brain without any stimulation, sham experiments were performed. The exact same experimental design and protocol was performed as described above; however, no epileptic agent was administered to the animal. Instead, a constant perfusion of aCSF was administered for the duration of the experiment.

4.2.10 GSH Upregulation

To increase the amount of GSH in the brain, the animal was dosed with ɣ-glutamylcysteine ethyl ester 24 hours prior to the surgery and seizure induction. Animals were administered a 150

mg/kg dose of ɣ-glutamylcysteine ethyl ester. The solid compound was dissolved in sterile saline. The animal was anesthetized briefly using an isoflurane chamber for easier handling and dosing and the ɣ-glutamylcysteine ethyl ester was administered in a single bolus IP injection. The animal was marked and monitored until it was awake and freely moving. Animals were allowed to have food and water ad libitum until they were ready for the probe implantation.

4.2.11 GSH Downregulation

To decrease the amount of GSH in the animal, a second, separate set of animals were dosed with buthionine sulfoximine (BSO) 24 hours prior to the surgery and seizure induction. Animals were administered 160 mg/kg dose of BSO. The solid compound was dissolved in sterile saline. Again, the animal was anesthetized briefly using an isoflurane chamber for easier handling and dosing and the BSO was administered in a single bolus I.P. injection. The animal was marked and monitored until it was awake and freely moving. Animals were allowed to have food and water ad libitum until they were ready for the probe implantation.

4.3 Results and Discussion

4.3.1 Derivatization Kits versus LC-Fl Validation

Briefly, a GSH standard curve containing 8 concentrations was prepared ranging from 0.1563 µM to 10 µM in aCSF every time the assay was performed. Figure 4.4 shows a sample calibration curve obtained using the kit and microplate reader. A correlation coefficient of 0.9957 was obtained with limits of detection of 10 nM (S/N=3). Figure 4.5 shows a calibration curve that was

generated following the kit protocol, but analyzed on the LC-FL system described above. Figure 4.6 is a representative chromatogram for a 10 µM sample. Each concentration was run 4 times. A correlation coefficient of 0.9986 with limits of detection of 8.7 nM (S/N=3). While both the linearity and limits of detection appeard to be slightly improved using the LC-Fl system compared to the microplate reader, the LC-Fl analysis yielded less reproducible results, based on the variation of signal produced for each concentration, represented as the error bars. The GSH samples are not very stable and need to be analyzed as quickly as possible, which is difficult with a 5 min analysis time. This instability is what accounts for the large error bars on the LC-Fl calibration curve. By using the microplate reader, the samples were analyzed all at once, and therefore in a fraction of the time, reducing this deviation. These tests were enough to support the use of the microplate reader over the LC-Fl system for the analysis of GSH in the dialysate samples.

As stated earlier, for the TBARS kit detection of MDA, three, 4 µL samples had to be combined to make a 12 µL sample volume. While this reduced our temporal resolution, it did provide enough sample to obtain a correlation coefficient of 0.9987 over the concentration range of 0.0625 to 5 µM with limits of detection of 50 nM (S/N=3). An example calibration curve of this assay analyzed using the microplate reader is shown in Figure 4.7. Once again, the kit was validated using the LC-FL system described above. Figure 4.8 shows a calibration curve with N=4 runs of each concentration on this system. Figure 4.9 is a representative chromatogram for a 5 µM injection. Linearity was an R^2 = 0.9987 with limits of detection of 60 nM compared to the R^2 = 0.9986 with 50 nM limits of detection for the microplate analysis, showing little to no difference in the methods. Because the MDA-TBA adduct is much more stable than the GSH, reproducibility was not an issue. In this case, either the microplate or the LC-FL system could be used for sample

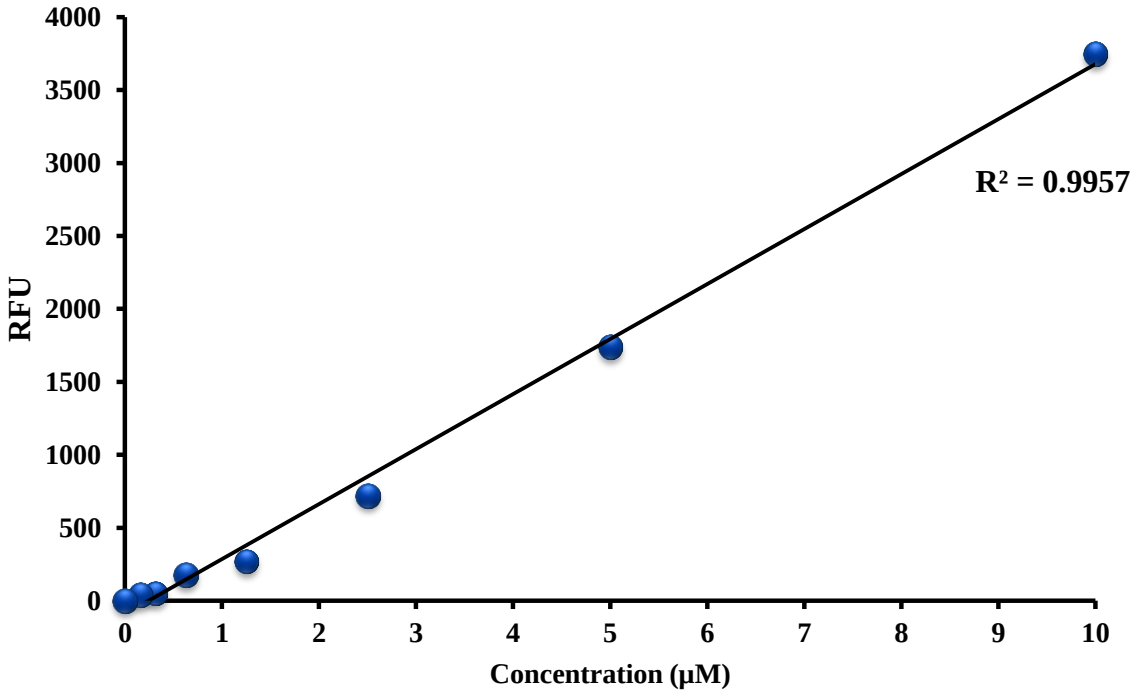

Figure 4.4: Relative Fluorescence Units versus Concentration calibration curve of GSH standards obtained from abcam© GSH/GSSG Ratio Detection Assay Kit analyzed on SpectraMax Microplate Reader (N=1).

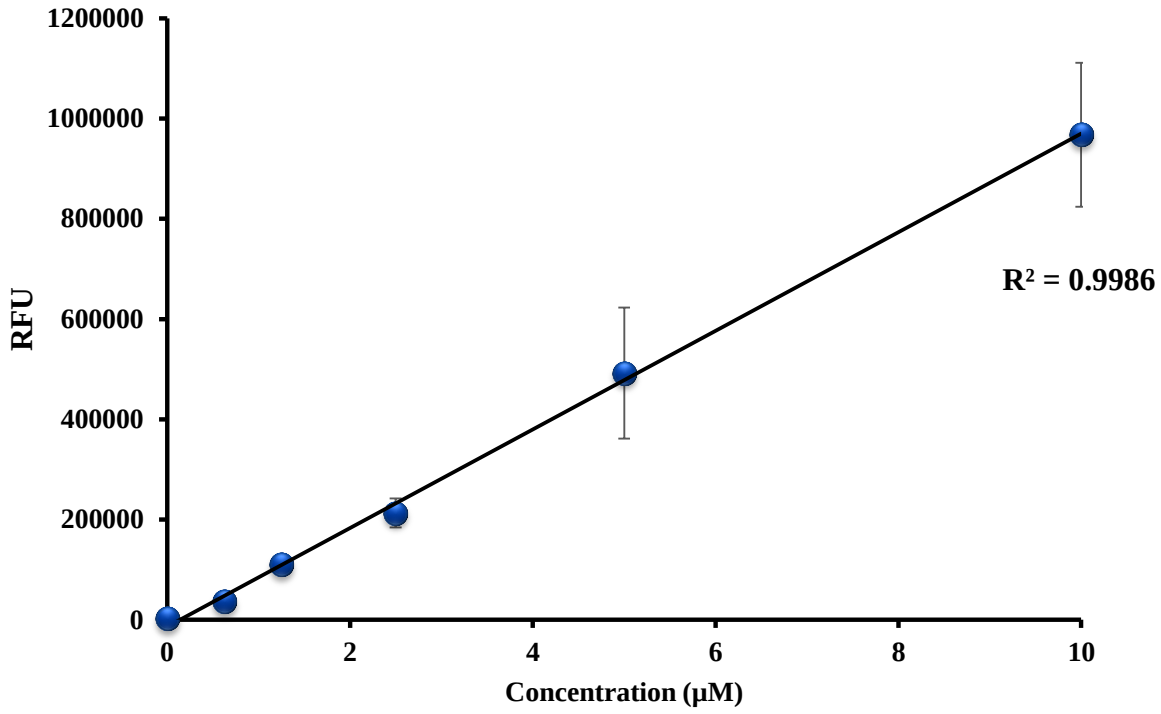

Figure 4.5: Relative Fluorescence Units versus Concentration calibration curve of GSH standards obtained from abcam© GSH/GSSG Ratio Detection Assay Kit analyzed on LC-Fl system (N=4).

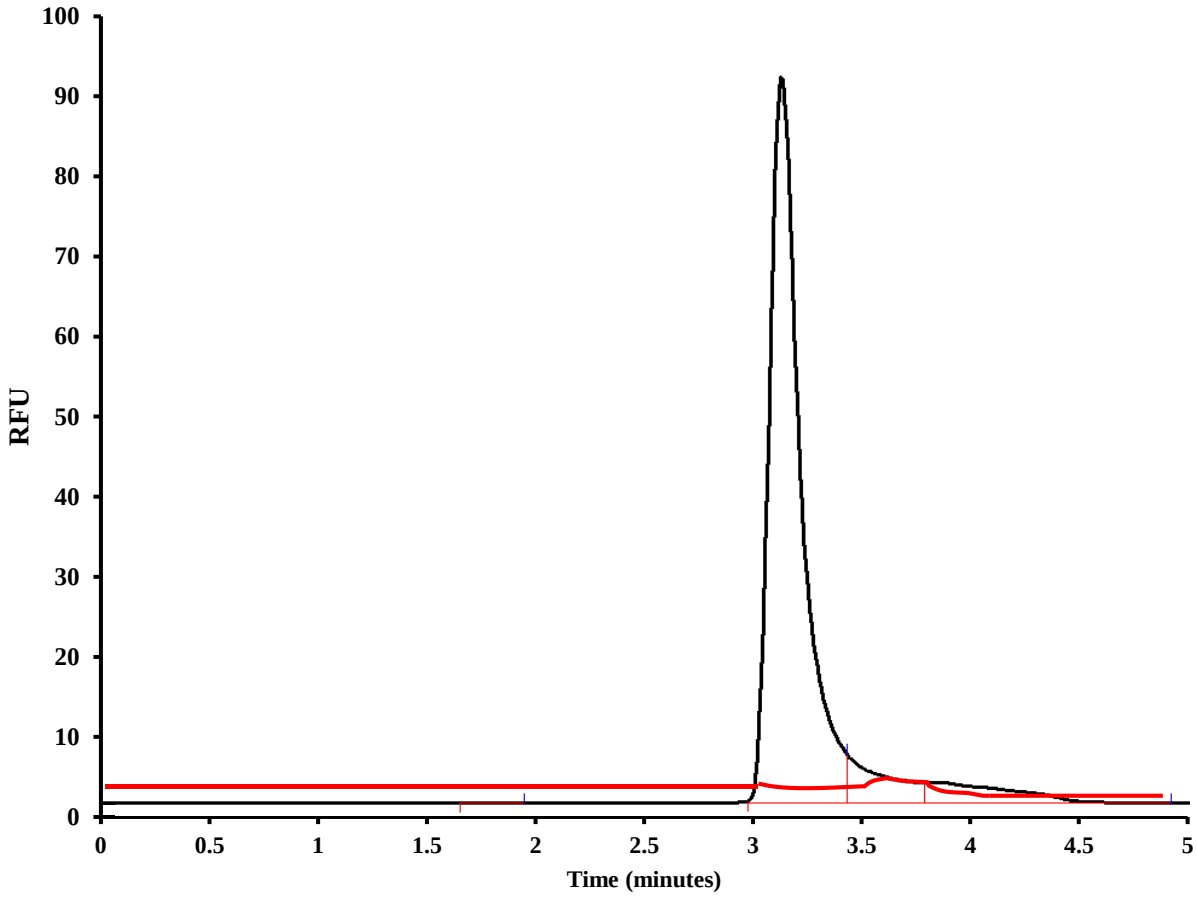

Figure 4.6: Representative LC-FL chromatogram of 0 µM (Red) and 10 µM (Black) GSH-Thiol Green adduct.

Tailing observed is most likely the cause of degradation products and excess Thiol Green Indicator.

Reverse phase column; MP. A: 30 mM TBA in 25% MeOH:75% H_2O (v%:v%), MP. B: 30 mM TBA in 100% MeOH; Ex.: 490 nm Em.: 520 nm.

analysis and results would be comparable. We chose to use the microplate reader because the analysis time is a fraction of that of the LC-FL system.

4.3.2 GSH Regulation

GSH was quantified before, during, and after the seizure for all experimental conditions. Table 4.1 shows the GSH concentration numbers for each of these experimental manipulations. The relative concentration for basal extracellular concentration of GSH for all conditions was about 0.64 µM. This is significantly less than the average expected basal concentration of 2 µM based on literature reports?[6, 14]. It is possible that we are only getting about a 30% recovery of GSH in these *in vivo* experiments due to the extraction efficiency of the MD probe, and therefore the relative recovery should be measured to confirm this. One and two-tailed, independent sample t-tests were done to determine if there were significant changes between each group. Table 4.2 shows the statistical analysis of the data. All conditions were statistically significant from each other with a confidence level of 90%. It was found in the experiments that the basal levels of GSH for all conditions were essentially the same. In the sham experiments, the concentration of GSH did not change significantly from basal. This was to be expected because these animals did not receive any epileptic agent or GSH regulating compound. However, there was a significant change in extracellular GSH concentration following a seizure induction. There was an overall increase in extracellular GSH concentration during the seizure for all animals that experienced a seizure.

The microdialysis samples from the BSO treated rats had lower concentration of GSH during the seizure compared to the control rats, approximately 39% less. Furthermore, the ɣ-glutamylcysteine ethyl ester treated rats had almost 50% more GSH release during the seizure

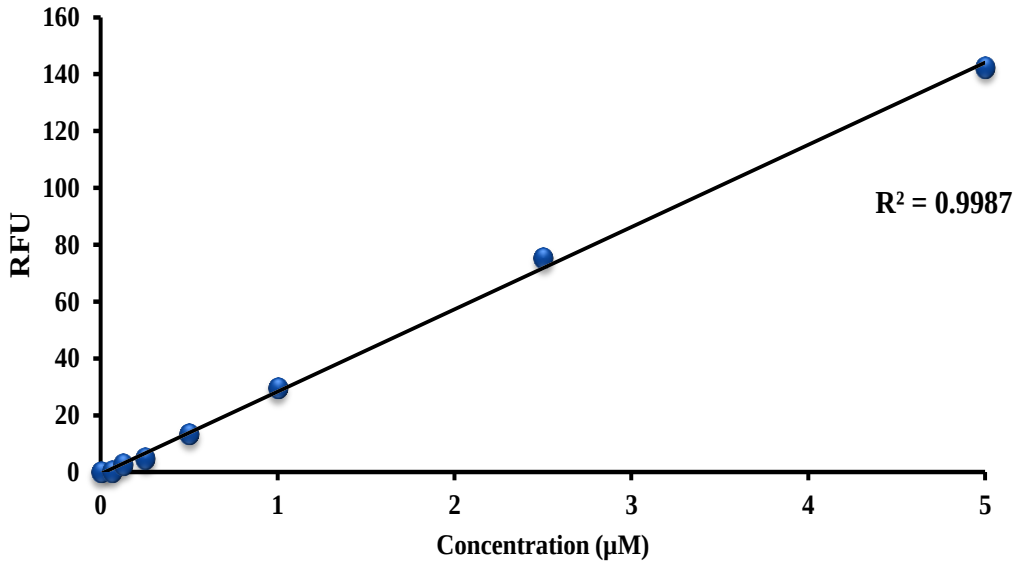

Figure 4.7: Calibration curve of MDA standards obtained by Thiobarbituric Acid Reactive Substances (TBARS) Kit analyzed on SpectraMax Microplate Reader (N=1).

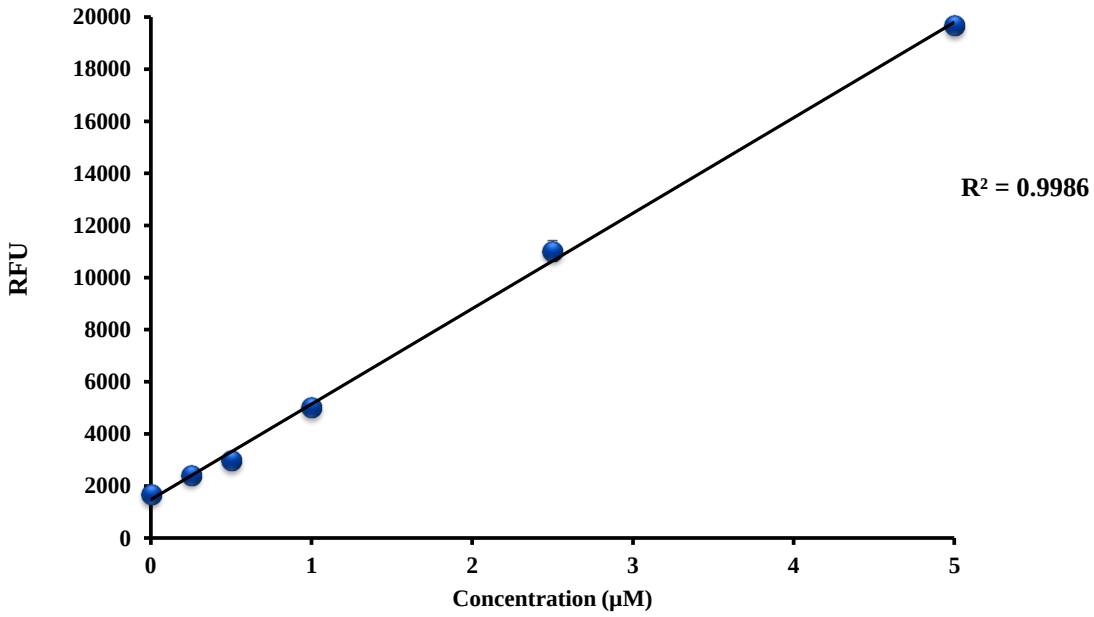

Figure 4.8: Calibration curve of MDA standards obtained by Thiobarbituric Acid Reactive Substances (TBARS) Kit analyzed on LC-Fl system (N=4).

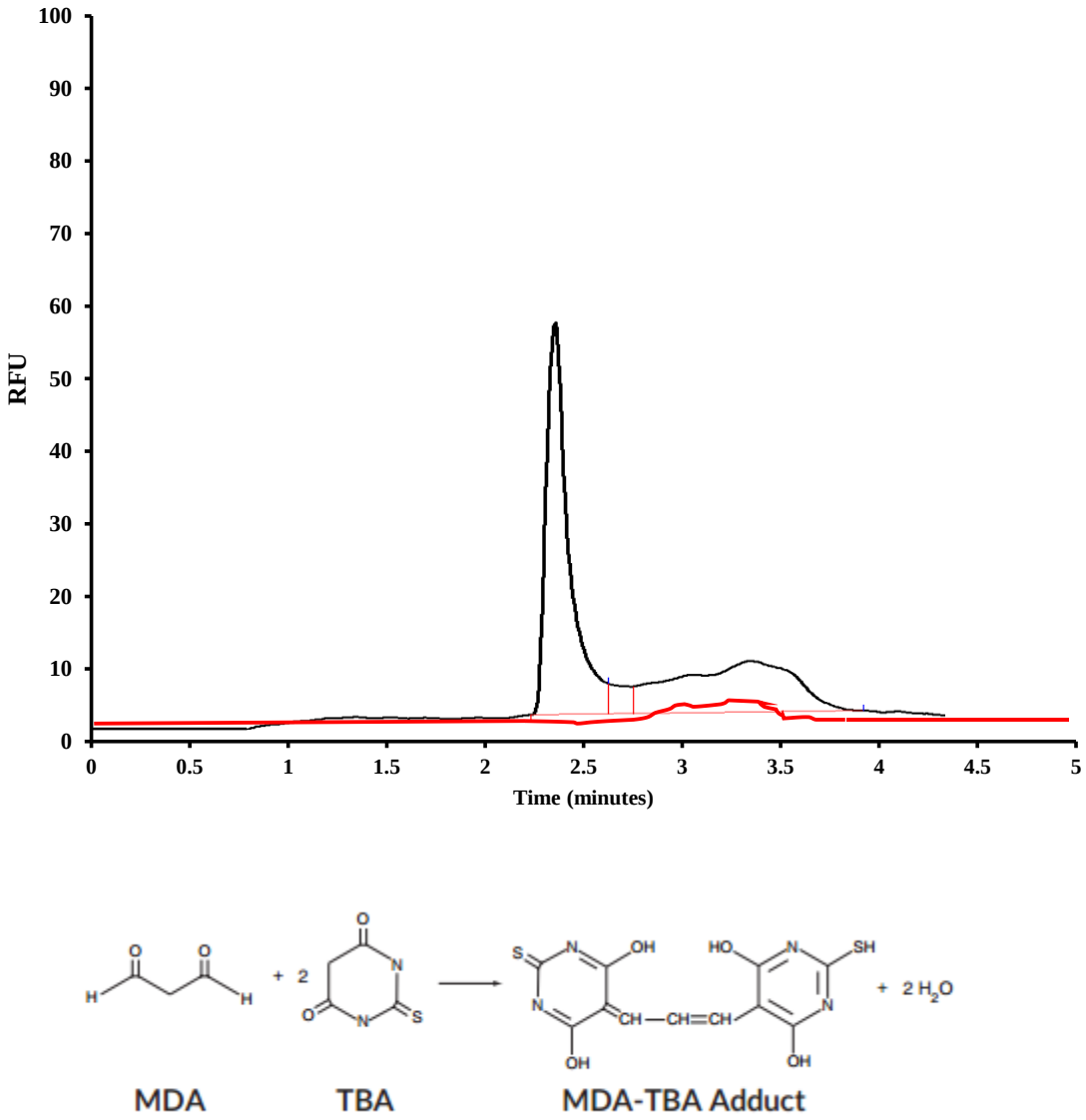

Figure 4.9: Representative LC-FL chromatograms of 0 µM (Red) and 5 µM MDA-TBA adduct (Black).

Tailing observed is most likely the cause of degradation products and excess TBA.

Reverse phase column; MP. A: 30 mM TBA in 25% MeOH:75% H_2O (v%:v%), MP. B: 30 mM TBA in 100% MeOH; Ex.: 530 nm Em.: 550 nm.

	Sham	Control	Down Reg	Up Reg
Basal	0.63 ± 0.01 µM	0.66 ± 0.02 µM	0.64 ± 0.01µM	0.52 ± 0.01 µM
Seizure	0.64 ± 0.01 µM	23 ± 8 µM	14 ± 4 µM	34 ± 8 µM
After	0.65 ± 0.01 µM	0.8 ± 0.3 µM	0.7 ± 0.1 µM	0.9 ± 0.4 µM
N =	3	4	6	5

Table 4.1: GSH concentrations before, during, and after the seizure for each experiment.

	p-value (one-tailed)	p-value (two-tailed)
Sham vs. Control	0.0008	0.002
Control vs. Down Reg	0.05	0.09
Control vs. Up Reg	0.05	0.10

Table 4.2: p-values from one and two-tailed, independent sample t-tests between GSH regulation experiments

compared to the control rats. This increase and decrease was as expected given the biochemical functions of BSO and ɣ-glutamylcysteine ethyl ester. It was unexpected, however, that the basal levels of GSH did not change with GSH regulating compounds. It was anticipated that the total GSH concentration would have changed, both extracellularly and intracellularly.

While GSH is not typically thought of as a neurotransmitter, studies have shown that astrocytes and glial cells will release GSH and cysteine when under stress, deomonstrating that GSH functions not as a neurotransmitter, but as a release modulator of the redox cycle[28, 29]. The GSH and cysteine are then available to be taken up by the neurons for synthesis of additional GSH to protect against oxidative damage[29, 30]. This was observed in this research as well, and could explain why there was an increase in extracellular GSH during the seizure and subsequent return to basal after the seizure. The astrocytes release GSH during the seizure, and then the neurons took up the GSH after the seizure.

Alternatively, as discussed in Chapter 3, the induction of the seizure also results in significant membrane damage and cell death. It is possible that the two GSH regulating compounds are affecting the intracellular GSH concentration only, and not the extracellular concentration. Therefore, when the seizure is induced, cells become damaged and spill their contents into the extracellular space. Intracellular concentrations of GSH are on the millimolar range, 1000 times higher than the ECF. This would account for such a high increase in extracellular GSH concentration during the seizure induction. It is most likely a combination of astrocyte release and cell damage which leads to this GSH increase.

In the future, GSSG should be monitored to see if the drop in GSH was accompanied with an increase in GSSG. A shift in the GSH to GSSG ratio would help confirm induced oxidative stress, this is discussed later in this chapter. Further experiments are necessary to make conclusions about

the large increase in GSH during the seizure induction. However, the goal of the GSH regulating compounds was achieved. BSO-dosed animals released less GSH compared to the respective controls and ɣ-glutamylcysteine ethyl ester dosed animals produced more GSH compared to the control experiments. The purpose of this study was to investigate the effects of GSH concentration on oxidative stress *in vivo* due to seizure induction.

4.3.3 MDA Production

Based on previous research by Dr. Carl Cooley, an increase in MDA production with the induction of a local seizure was anticipated[12]. Figures 4.10-4.12 are graphical representations of the changes in MDA concentration between the various experiments. Initial evaluation of the data suggested an increase in MDA concentrations, however, after statistical analysis, these changes indicate that they are not significant. One and two-tailed, independent sample t-tests were conducted comparing sham versus control, control versus GSH down regulated, and control versus GSH up regulated MDA values. The p-values for each of these analyses are shown in Table 4.3.

There was no significant difference in MDA production between any of the experiments, demonstrating that the results were too random to show any trend. This was surprising considering the results of Dr. Cooley. One possible explanation for this difference in results may have to do with the method of analysis. Dr. Cooley analyzed his samples using a capillary electrophoresis-fluorescence detection (CE-FL) system. The use of CE allowed for smaller injection volumes and resulted in less dilution. In his analysis, 5 µL of dialysate was derivatized and was hydrodynamically injected on the system. The use of the TBARS kit required 12 µL of sample which was then diluted with 200 µL of solvent to produce enough volume for microplate analysis.

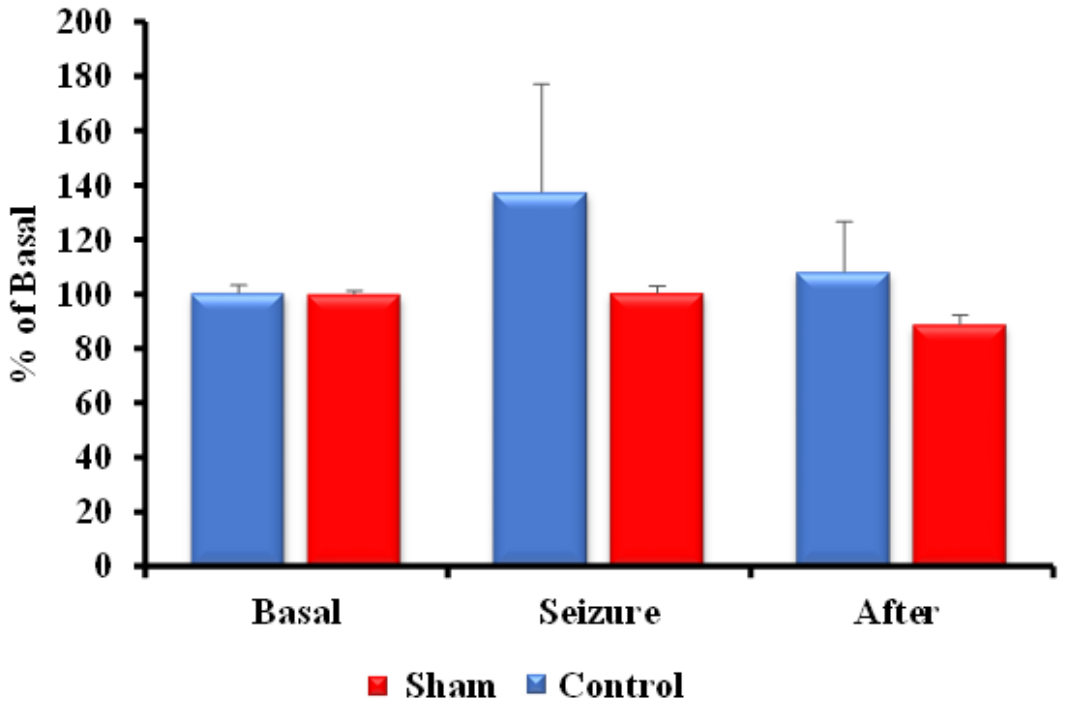

Figure 4.10: Comparison of sham versus control rats' MDA production before, during, and after the seizure induction.

(N=3 sham, N=4 control)

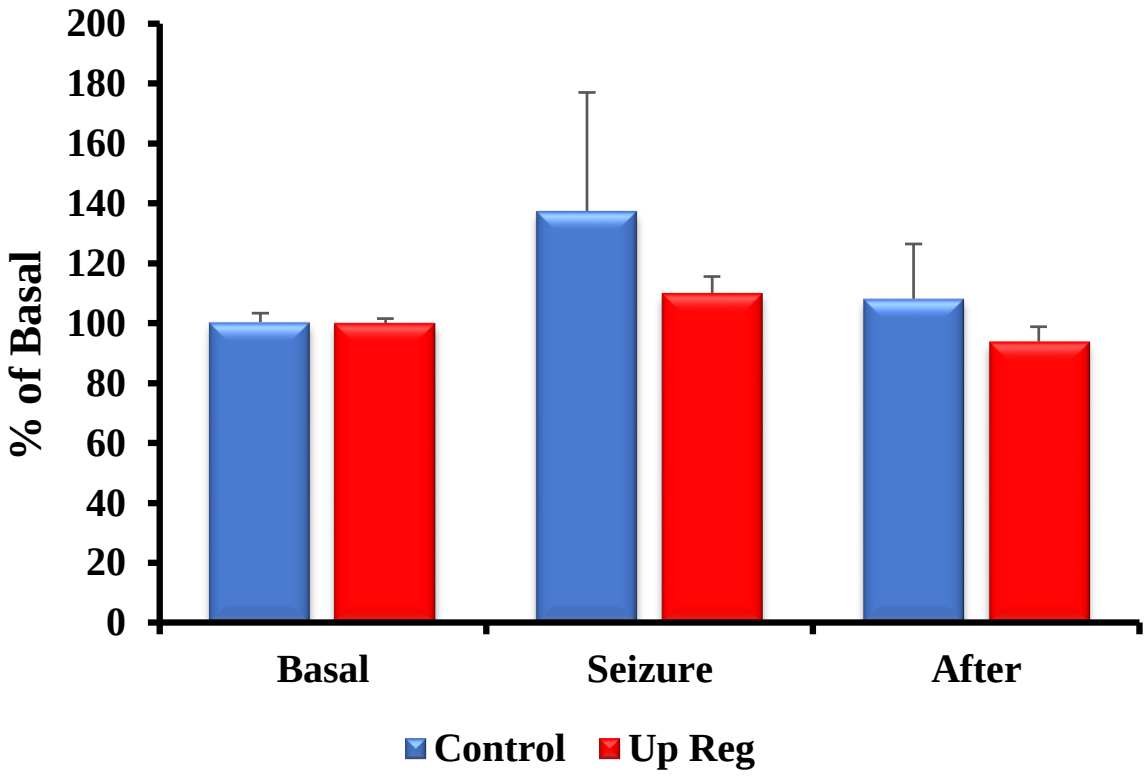

Figure 4.11: Comparison of control versus GSH-upregulated rats' MDA production before, during, and after seizure induction.

(N= 4 control, N=5 up reg)

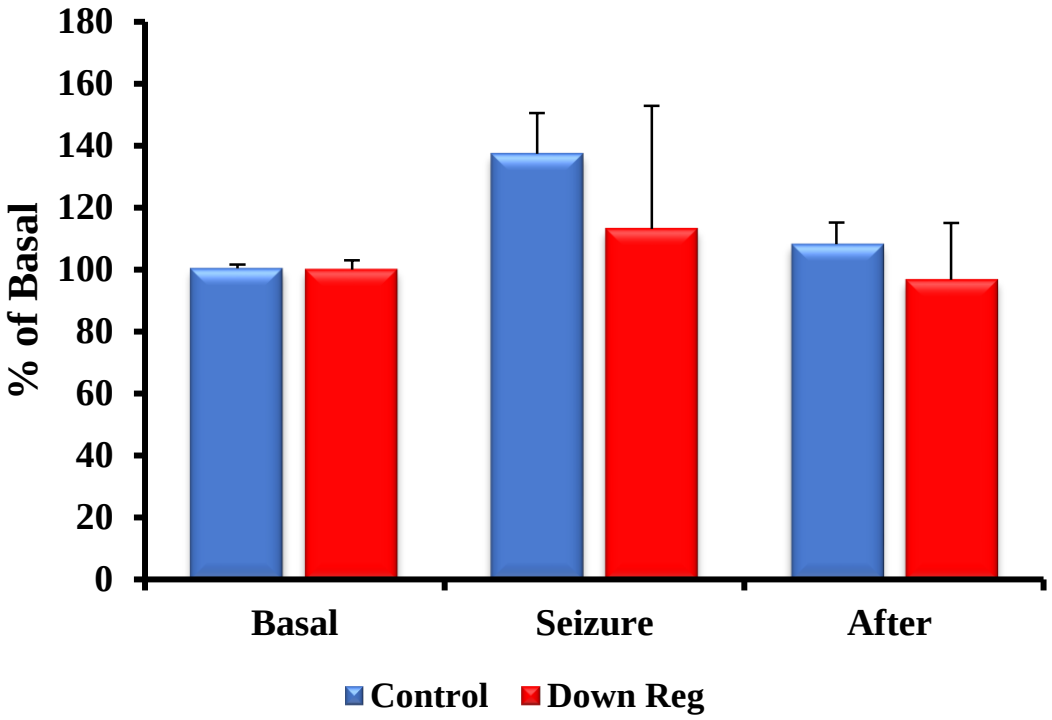

Figure 4.12: Comparison of control versus GSH-downregulated rats' change in MDA production before, during, and after seizure induction.

(N=4 control, N=6 down reg)

	p-value (one-tailed)	p-value (two-tailed)
Sham vs. Control	0.10	0.21
Control vs. Down Reg	0.17	0.34
Control vs. Up Reg	0.14	0.28

Table 4.3: p-values from one and two-tailed, independent sample t-tests for MDA production between GSH regulation experiments

It is possible that the sample preparation caused too much overall dilution, producing insignificant results. Furthermore, because three samples had to be combined, there was a significant loss in temporal resolution. It is possible that any significant changes in MDA are being missed due to the reduced time points.

4.4 Future Directions

4.4.1 Additional Malondialdehyde Studies

Since no significant difference between the GSH enhanced and depleted rats for MDA, additional animals must be done in hopes that higher N values will lead to statistically relevant results. Further modification and optimization of the TBARS assay should be made to reduce dilution and hopefully improve temporal resolution. Implementing the CE-FL method developed by Cooley may be another option so that these studies can be directly compared to those that he performed.

4.4.2 Role of Glutathione in Antioxidant Pathways

As discussed briefly earlier, ROS can be neutralized by two mechanisms: enzymatic and nonenzymatic. The three main enzymatic antioxidant pathways that involve GSH are glutathione peroxidase (GPx), glutathione reductase, and glutathione S-transferase (GST)[5]. GPx catalyzes the reduction of hydrogen peroxide in the presence of GSH to produce water and GSSG[15]. An increase in GSSG production could signify an increase in hydrogen peroxide, and therefore oxidative stress. Additionally, glutathione reductase catalyzes the reduction of GSSG using NADPH to produce two GSH molecules, which occurs when there is an imbalance in ROS in the body[16]. This process

occurs when there is an imbalance in ROS in the body. To improve on the research conducted in this chapter, it would be beneficial to also measure GSSG concentration. Oxidative damage can be quantified by measuring the ratio of GSH to GSSG. Measuring both GSH and GSSG would not only provide this ratio, but depending on the ratio shift could provide information on if GPx versus glutathione reductase was being affected in the experiments.

Finally, GST can conjugate GSH with electrophilic organic compounds. An activation of GST can reduce GSH levels, which can be detrimental to the body[31]. One specific study by Nagashima et al. suggests that GST activity was reduced after seizures to increase the amount of GSH available for ROS scavenging[32]. Furthermore, GST is also believed to help reduce lipid peroxidation by combining GSH with hydrophobic compounds to make them more water-soluble so they can be removed from the system[33]. Modifying GST activity may be more successful in modulating MDA production.

It would be beneficial to test different upregulating and downregulating compounds to see if they resulted in different effects. Specifically, diethyl maleate works to decrease GSH by forming an adduct with reduced GSH, which then gets metabolized by glutathione-S-transferase[34]. Diethyl maleate is faster-acting than BSO, but it is short-lived. This different mechanism should be explored to see if it produces different results.

4.5 Conclusions

The research discussed in this chapter was an investigation of the correlation between local seizures and oxidative damage. Chapter 3 demonstrated that significant cell damage was occurring during the seizure induction. It was anticipated that this damage was related to lipid peroxidation.

MDA was the biomarker selected to quantify the amount of lipid peroxidation because it is a very stable byproduct of these reactions. Unfortunately, there was no statistically significant change in MDA production between the various experiments. GSH was selected as a natural antioxidant that could be easily regulated *in vivo*. GSH was successfully upregulated and downregulated *in vivo*, however it still remains unclear which specific enzymatic pathways are being affected. Additional experiments must be done before further conclusions can be made. Specifically, measuring GSSG concentration, as well as glutathione peroxidase, reductase and GST activity would provide beneficial insight.

4.6 References

1. Bruce, A. J., and Baudry, M. (1995) Oxygen free radicals in rat limbic structures after kainate-induced seizures, *Free Radical Biology and Medicine 18*, 993-1002.
2. Emerit, J., Edeas, M., and Bricaire, F. (2004) Neurodegenerative diseases and oxidative stress, *Biomedicine & pharmacotherapy 58*, 39-46.
3. Lopez, J., González, M. E., Lorigados, L., Morales, L., Riveron, G., and Bauza, J. Y. (2007) Oxidative stress markers in surgically treated patients with refractory epilepsy, *Clinical biochemistry 40*, 292-298.
4. Love, S. (1999) Oxidative stress in brain ischemia, *Brain Pathology 9*, 119-131.
5. aacute, rdenas, R., iacute, guez, N., and iacute. (2014) Relevance of the Glutathione System in Temporal Lobe Epilepsy: Evidence in Human and Experimental Models, *Oxidative medicine and cellular longevity 2014*, 1-12.
6. Fiser, B., and la. Antioxidant Potential of Glutathione: A Theoretical Study, *The journal of physical chemistry. B 115*, 11269-11277.
7. Mandal, P. K. Brain Glutathione Levels – A Novel Biomarker for Mild Cognitive Impairment and Alzheimer's Disease, *Biological psychiatry (1969) 78*, 702-710.
8. Sonni, F. Antioxidant Action of Glutathione and the Ascorbic Acid/Glutathione Pair in a Model White Wine, *Journal of agricultural and food chemistry 59*, 3940-3949.
9. Bulut, M. Lipid peroxidation markers in adult attention deficit hyperactivity disorder: New findings for oxidative stress, *Psychiatry research 209*, 638.
10. Rathore, N., John, S., Kale, M., and Bhatnagar, D. (1998) Lipid peroxidation and antioxidant enzymes in isoproterenol induced oxidative stress in rat tissues, *Pharmacological Research 38*, 297-303.

11. Rola, R. a., Swiader, M., and Czuczwar, S. a. J. (2002) Electroconvulsions elevate the levels of lipid peroxidation products in mice, *Polish journal of pharmacology 54*, 521-530.

12. Cooley, J. C. (2013) *Determination of Lipid Peroxidation Associated with a Focal Seizure Model through In Vivo Microdialysis Sampling*.

13. Fathy, H. Glutathione as an Antioxidant Defense System in Schizophrenia and Bipolar 1 Disorder, *European psychiatry 30*, 544.

14. Rabinovic, A. D., and Hastings, T. G. (1998) Role of endogenous glutathione in the oxidation of dopamine, *Journal of neurochemistry 71*, 2071-2078.

15. Yu, F., and Fabiao, Y. Reversible near-infrared fluorescent probe introducing tellurium to mimetic glutathione peroxidase for monitoring the redox cycles between peroxynitrite and glutathione in vivo.(Report), *Journal of the American Chemical Society 135*, 7674-7680.

16. Harraz, M. M., Marden, J. J., Zhou, W., Zhang, Y., Williams, A., Schöneich, C., and Engelhardt, J. F. (2014) SOD1 mutations disrupt redox-sensitive Rac regulation of NADPH oxidase in a familial ALS model, American Society for Clinical Investigation.

17. Uttara, B., Singh, A. V., Zamboni, P., and Mahajan, R. T. (2009) Oxidative Stress and Neurodegenerative Diseases: A Review of Upstream and Downstream Antioxidant Therapeutic Options, *Current Neuropharmacology 7*, 65-74.

18. Basuroy, S., Bhattacharya, S., Tcheranova, D., Qu, Y., Regan, R. F., Leffler, C. W., and Parfenova, H. (2006) HO-2 provides endogenous protection against oxidative stress and apoptosis caused by TNF-α in cerebral vascular endothelial cells, *American Journal of Physiology-Cell Physiology 291*, C897-C908.

19. Halliwell, B., and Gutteridge, J. M. (2015) *Free radicals in biology and medicine*, Oxford University Press, USA.

20. Fraser, M., Bennet, L., Van Zijl, P. L., Mocatta, T. J., Williams, C. E., Gluckman, P. D., Winterbourn, C. C., and Gunn, A. J. (2008) Extracellular amino acids and lipid peroxidation products in periventricular white matter during and after cerebral ischemia in preterm fetal sheep, *Journal of neurochemistry 105*, 2214-2223.

21. Yang, C.-S., Tsai, P.-J., Wu, J.-P., Lin, N.-N., Chou, S.-T., and Kuo, J.-S. (1997) Evaluation of extracellular lipid peroxidation in brain cortex of anaesthetized rats by microdialysis perfusion and high-performance liquid chromatography with fluorimetric detection, *Journal of Chromatography B: Biomedical Sciences and Applications 693*, 257-263.

22. Tang, X. Structural and Antioxidant Modification of Wheat Peptides Modified by the Heat and Lipid Peroxidation Product Malondialdehyde, *Journal of food science 77*, H16-H22.

23. Tsikas, D. Assessment of lipid peroxidation by measuring malondialdehyde (MDA) and relatives in biological samples: Analytical and biological challenges, *Analytical biochemistry*.

24. Pileblad, E., and Magnusson, T. (1990) Effective depletion of glutathione in rat striatum and substantia nigra by L-buthionine sulfoximine in combination with 2-cyclohexene-1-one, *Life sciences 47*, 2333-2342.

25. Vanella, A., Di Giacomo, C., Sorrenti, V., Russo, A., Castorina, C., Campisi, A., Renis, M., and Perez-Polo, J. (1993) Free radical scavenger depletion in post-ischemic reperfusion brain damage, *Neurochemical research 18*, 1337-1340.

26. Scharf, G. (2003) Enhancement of glutathione and g-glutamylcysteine synthetase, the rate limiting enzyme of glutathione synthesis, by chemoprotective plant-derived food and

beverage components in the human hepatoma cell line HepG2, *Nutrition and cancer 45*, 74-83.

27. Drake, J., Kanski, J., Varadarajan, S., Tsoras, M., and Butterfield, D. A. (2002) Elevation of brain glutathione by γ-glutamylcysteine ethyl ester protects against peroxynitrite-induced oxidative stress, *Journal of neuroscience research 68*, 776-784.

28. Dringen, R., Pfeiffer, B., and Hamprecht, B. (1999) Synthesis of the antioxidant glutathione in neurons: supply by astrocytes of CysGly as precursor for neuronal glutathione, *The Journal of neuroscience 19*, 562-569.

29. Wang, X. F., and Cynader, M. S. (2000) Astrocytes provide cysteine to neurons by releasing glutathione, *Journal of neurochemistry 74*, 1434-1442.

30. Rana, S., and Dringen, R. (2007) Gap junction hemichannel-mediated release of glutathione from cultured rat astrocytes, *Neuroscience letters 415*, 45-48.

31. Moron, M. S., Depierre, J. W., and Mannervik, B. (1979) Levels of glutathione, glutathione reductase and glutathione S-transferase activities in rat lung and liver, *Biochimica et Biophysica Acta (BBA)-General Subjects 582*, 67-78.

32. Nagashima, R., Sano, S., Huong, N. Q., Shiba, T., and Ogita, K. (2010) Enhanced expression of glutathione S-transferase in the hippocampus following acute treatment with trimethyltin in vivo, *Journal of pharmacological sciences 113*, 267-270.

33. Singh, S. P., Coronella, J. A., Beneš, H., Cochrane, B. J., and Zimniak, P. (2001) Catalytic function of Drosophila melanogaster glutathione S-transferase DmGSTS1-1 (GST-2) in conjugation of lipid peroxidation end products, *European Journal of Biochemistry 268*, 2912-2923.

34. Deneke, S. M. Transient depletion of lung glutathione by diethylmaleate enhances oxygen toxicity, *Journal of applied physiology (1985) 58*, 571-574.

Chapter 5

Summary and Future Directions

5.1 Summary of the Research

The research discussed in this dissertation was a study of the correlation between locally induced seizures and oxidative damage. Chapter 2 discussed the development of an animal model for locally induced epilepsy. By definition, patients are diagnosed with epilepsy after experiencing two or more seizures. The goal of this work was to induce two local seizures within one animal experiment, thereby developing a model for locally induced epilepsy. Various intra-seizure time delays were explored. It was determined that 150 minutes were required for basal levels of neurotransmitters to be reestablished after the induction of the first seizure. The return to basal levels prior to the second seizure induction signifies two separate seizure events.

Unexpectedly, there was significant attenuation in glutamate release observed in the second seizure stimulation. Chapter 3 discussed a series of experiments that were performed to test various biochemical and neurochemical pathways which could be responsible for the observed glutamate diminution. It was determined that a combination of mitochondrial starvation and cell death lead to the glutamate depletion. Lactate supplementation of the perfusate helped encourage the KREB cycle production of glutamate, resulting in a significant increase in glutamate release in the second seizure episode. This verifies that the cells were being starved for key precursors to glutamate biosynthesis. Additionally, it was determined that 30-38% of the cells died prior to the induction of the second seizure episode. Because of this cell death, the neurons were unable to release additional glutamate. Further development and investigation of this model is necessary for it to be a working model for locally induced epilepsy. Lower concentrations of 3-MPA or different epileptic agents should be investigated to reduce the amount of damage being caused.

Chapter 4 discussed an investigation of epilepsy-induced oxidative damage and an attempt to mitigate lipid peroxidation by modulating the amount of the natural antioxidant GSH in the body. A series of experiments were carried out including, sham dosing, control, GSH upregulation, and GSH downregulation. Unfortunately, there was not a significant change in MDA production for any of the experiments; however, the overall goal of regulating GSH was achieved. It was concluded that the addition of up- and down-regulating compounds were able to modulate the amount of intracellular GSH, but not necessarily the amount of extracellular GSH. Increases in extracellular GSH were observed in all animals that experienced a seizure. Furthermore, GSH levels almost returned to basal after the seizure which could signify that the GSH was being released from astrocytes to combat the oxidative stress being cause by the seizure. In the future, GSSG should be monitored to see if the drop in GSH was accompanied with an increase in GSSG. Likewise, monitoring glutathione enzymatic pathways could provide additional insight on the involvement of GSH as an antioxidant.

5.2 Future Directions

5.2.1 MDA Measurement in Multiple Seizure Model

To further develop the project discussed in Chapter 4, MDA will be measured in the multiple seizure model. Significant cell damage is being observed in the two seizure model. It is anticipated that there would be compounding lipid peroxidation with additional seizures. Preliminary experiments have been done measuring MDA in the supplemented two seizure animal experiments. Figure 5.1 shows this preliminary data. There was an increase in the amount of MDA in the second seizure in both the glucose and lactate supplemented experiments. This is to be expected. Glucose and lactate caused an increase in glutamate release in the second seizure

induction. This increase in glutamate release could lead to increased excitotoxicity, causing more oxidative damage. Interestingly, with the DHK experiments, there was a slight decrease in the amount of MDA produced. As discussed in Chapter 3, there was no apparent difference in the amount of glutamate release in the control experiments compared to the DHK supplemented experiments. The N-values are not high enough to determine if these differences are statistically significant or not, and therefore additional animal experiments need to be done. Unfortunately, no multiple dose control experiments nor sham experiments were analyzed for MDA. It would be interesting to analyze both the control and sham experiments for MDA concentration to determine basal levels of MDA from the probe implantation itself as well as multiple seizure induction without supplements. However, this data does show potential of compounding oxidative damage with subsequent seizures.

5.2.2 Additional Lipid Peroxidation Pathways

To further confirm the relationship between oxidative damage and locally induced epilepsy, additional biomarkers should be investigated. Our lab has worked to develop analytical methods for several of these biomarkers including 8-OHdG, 8-oxoG, prostaglandins, Coenzyme Q_{10} (CoQ_{10}), and Phospholipase A_2, all of which can be easily monitored. This section discuses several experiments to modulate lipid peroxidation.

When DNA gets damaged by oxidation, the guanine bases lead to the production of 8-hydroxyguanine lesions that result in G-T conversions, further destroying the DNA. One way to help repair these lesions is through base excision repair[1-3]. This repair leads to the end products 8-OHdG and 8-oxoG. Both of these compounds are common biomarkers of oxidative stress

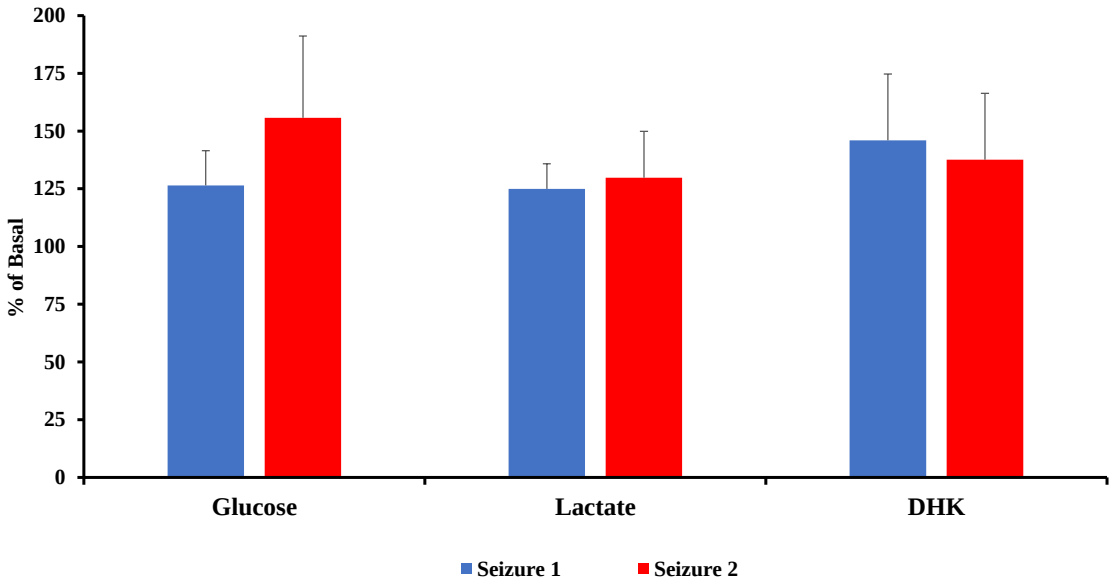

Figure 5.1: Preliminary results of MDA measured in multiple seizures.

(N=4 for each condition)

induced DNA damage. A capillary electrophoresis-electrochemical detection method has been developed in our lab that can be used to detect these compounds[4].

Another biomarker for the inflammatory response to oxidative stress are prostaglandins (PGs). They can be used as a biomarker for the enzymatic breakdown of arachidonic acid (ARA). The most common PGs formed during an inflammatory response are PGE_2, PGD_2, and PGF_2[5-7]. We are interested in modulating cyclooxygenase (COX) pathways to affect the production of ROS as well as the breakdown of ARA. COX-1 and COX-2 are enzymes that are involved in the formation of oxygen free radicals[8]. They are also involved in the conversion of ARA into prostaglandins. The COX pathways naturally become accelerated during seizure induction, which can be seen by an increase in ROS, leading to lipid peroxidation and therefore prostaglandin production. In hopes to reduce this damage, a COX inhibitor such as indomethacin could be administered to the animals prior to the induction of the seizures. Indomethacin would block the activation of the COX pathway, hopefully reducing the amount of lipid peroxidation and DNA damage. Literature has shown that dosing indomethacin to seizure-susceptible rodents has decreased both the DNA damage associated with the seizure as well as the frequency of seizures[9]. By giving the rat indomethacin prior to the induction of the seizures, we anticipate to see a decrease in lipid peroxidation biomarkers such as prostaglandins and MDA.

As discussed in Chapter 3, it is apparent that using 3-MPA to induce seizures leads to mitochondrial starvation. To further investigate this hypothesis, coenzyme Q_{10} (CoQ_{10}) can be modulated to hopefully decrease the amount of mitochondrial dysfunction. Studies have shown that CoQ_{10} can work as a preventative drug for neurodegenerative diseases and mitochondrial myopathies[10-12]. CoQ_{10} functions to move electrons between the redox components of the electron transport chain within the mitochondrial membrane, increasing the generation of ATP. During

oxidative stress, there is a breakdown of electron transport across the mitochondrial membrane, leading to an increase in free radicals and ROS. By dosing animals with CoQ_{10} for an extended period of time prior to seizure induction, the relationship between CoQ_{10} and seizure induced oxidative damage could be explored.

Finally, to further investigate seizure induced lipid peroxidation, phospholipase A_2 (PLA_2) could be modulated. PLA_2 is the enzyme responsible for the release of ARA from cell membranes. The influx of Ca^{2+} ions during a seizure activate the calcium-dependent PLA_2 or $cPLA_2$[13, 14]. This activation leads to an increase in ARA and therefore lipid peroxidation. Palmitoyl trifluoromethyl ketone ($PACOCF_3$) is a non-specific inhibitor of both calcium dependent and independent PLA_2. Giving $PACOCF_3$ to the rats prior to the induction of the seizure will decrease the amount of lipid peroxidation by preventing ARA release from cell membranes. It is evident that oxidative stress affects a multitude of complex pathways, all of which can play a key role in understanding locally induced epilepsy.

5.2.3 Other Models for Epilepsy

5.2.3.1 Awake Studies

All of the animal models discussed in this dissertation were anesthetized. While this allows for a more controlled system, the anesthetic effects can significantly alter neurochemical responses. Ketamine specifically has been shown to lead to spikes and dips in dopamine and serotonin[15, 16]. By allowing the animal to wake up after the microdialysis probe implantation, the animal will have sufficient time to recover from the surgery, reducing any inflammation and excitation caused by the surgery. This would allow the experiment to extend from hours to days

and possibly even weeks. This allows for the potential to add additional seizures to the animal model. Significant glutamate diminution was observed in the second seizure episode. Another way to further investigate the glutamate attenuation would be to add additional seizures to the model; third and fourth seizure responses could then be compared. Allowing the animal to be awake for the duration of the experiment would also permit increased time between seizure inductions. Currently, the model requires 150 minutes of recovery after the first seizure before basal levels are established; however, it is evident that this is still not enough time for the entire biochemical system to be restored based on the results in Chapter 3. In an awake study, intraseizure time could be increased to days rather than hours.

5.2.3.2 Kindling Model

Finally, as discussed briefly in Chapter 1, kindling models for epilepsy are most representative of clinical human patients. In these models, a subconvulsant dose of an epileptic agent is given to an animal everyday over time until the animal becomes sensitized to the epileptic agent and begins experiencing seizures. The seizures are unpredictable, similar to seizures in human patients. Rocha *et al.* has previously developed a kindling model for epilepsy using pentylenetetrazol (PTZ), which could be adapted for comparison to our 3-MPA model. Awake animal experiments could also be implemented in this study[17, 18]. A microdialysis probe would be implanted into the hippocampus of the rat. The animal would then be able to wake up and recover from surgery. The animal would be administered PTZ every day until the animal experiences consecutive seizures, signifying that the kindling has taken effect[19, 20].

Similar to the anesthetized, induced model, samples would be collected before, during, and after the compound administration. It is hypothesized that subsequent doses of PTZ will lead to

an increase in seizure activity and the production of ROS and RNS, thereby resulting in oxidative damage.

5.3 Final Conclusions

All of the data presented here demonstrates the complexity of the biochemical processes that occur as a result of seizure induced oxidative stress. While significant progress in understanding the correlation between local seizures and oxidative damage, specifically lipid peroxidation, has been made with this research, there will always be more questions to be answered and more pathways to be investigated.

5.4 References

1. Lan, J., Henshall, D. C., Simon, R. P., and Chen, J. (2000) Formation of the Base Modification 8-Hydroxyl-2′-Deoxyguanosine and DNA Fragmentation Following Seizures Induced by Systemic Kainic Acid in the Rat, *Journal of neurochemistry 74*, 302-309.
2. Richter, C. (1997) Free-radical-mediated DNA oxidation, *Free radical toxicology eds. by Wallace KB*, 89-113.
3. Fraga, C. G., Shigenaga, M. K., Park, J.-W., Degan, P., and Ames, B. N. (1990) Oxidative damage to DNA during aging: 8-hydroxy-2'-deoxyguanosine in rat organ DNA and urine, *Proceedings of the National Academy of Sciences 87*, 4533-4537.
4. Dorris, M. (2013) Development of Dual-Electrode Amperometric Detectors for Liquid Chromatography and Capillary Electrophoresis, (Lunte, C., Johnson, M., Lunte, S., Rivera, M., and Scott, E., Eds.), ProQuest Dissertations Publishing.
5. Wiswedel, I., Hirsch, D., Nourooz-Zadeh, J., Flechsig, A., Lück-Lambrecht, A., and Augustin, W. (2009) Analysis of monohydroxyeicosatetraenoic acids and F2-isoprostanes as markers of lipid peroxidation in rat brain mitochondria, *Free radical research*.
6. Montuschi, P., Barnes, P. J., and Roberts, L. J. (2004) Isoprostanes: markers and mediators of oxidative stress, *The FASEB Journal 18*, 1791-1800.
7. Yue, H., Jansen, S. A., Strauss, K. I., Borenstein, M. R., Barbe, M. F., Rossi, L. J., and Murphy, E. (2007) A liquid chromatography/mass spectrometric method for simultaneous analysis of arachidonic acid and its endogenous eicosanoid metabolites prostaglandins, dihydroxyeicosatrienoic acids, hydroxyeicosatetraenoic acids, and epoxyeicosatrienoic acids in rat brain tissue, *Journal of pharmaceutical and biomedical analysis 43*, 1122-1134.

8. Pepicelli, O., Fedele, E., Berardi, M., Raiteri, M., Levi, G., Greco, A., Ajmone-Cat, M. A., and Minghetti, L. (2005) Cyclo-oxygenase-1 and-2 differently contribute to prostaglandin E2 synthesis and lipid peroxidation after in vivo activation of N-methyl-D-aspartate receptors in rat hippocampus, *Journal of neurochemistry 93*, 1561-1567.

9. Miyamoto, O., Tamae, K., Kasai, H., Hirakawa, H., Hayashida, Y., Konishi, R., and Itano, T. (2003) Suppression of hyperemia and DNA oxidation by indomethacin in cerebral ischemia, *European journal of pharmacology 459*, 179-186.

10. Littarru, G. P., and Tiano, L. (2005) Clinical aspects of coenzyme Q10: an update, *Current Opinion in Clinical Nutrition & Metabolic Care 8*, 641-646.

11. Chew, G., and Watts, G. (2004) Coenzyme Q10 and diabetic endotheliopathy: oxidative stress and the 'recoupling hypothesis', *Qjm 97*, 537-548.

12. Dhanasekaran, M., and Ren, J. (2005) The emerging role of coenzyme Q-10 in aging, neurodegeneration, cardiovascular disease, cancer and diabetes mellitus, *Current Neurovascular Research 2*, 447-459.

13. Lehman, J. J., Brown, K. A., Ramanadham, S., Turk, J., and Gross, R. W. (1993) Arachidonic acid release from aortic smooth muscle cells induced by [Arg8] vasopressin is largely mediated by calcium-independent phospholipase A2, *Journal of Biological Chemistry 268*, 20713-20716.

14. Yue, H.-Y., Fujita, T., and Kumamoto, E. (2005) Phospholipase A 2 activation by melittin enhances spontaneous glutamatergic excitatory transmission in rat substantia gelatinosa neurons, *Neuroscience 135*, 485-495.

15. Ordek, G., and Ordek, G. Differential effects of ketamine/xylazine anesthesia on the cerebral and cerebellar cortical activities in the rat, *Journal of neurophysiology 109*, 1435-1443.

16. Oose, Y. Imbalanced suppression of excitatory and inhibitory synaptic transmission onto mouse striatal projection neurons during induction of anesthesia with sevoflurane in vitro Suppression of striatal IPSC with sevoflurane, *The European journal of neuroscience 35*, 1396-1405.

17. Rocha, L., Briones, M., Ackermann, R., Anton, B., Maidment, N., Evans, C., and Engel, J. (1996) Pentylenetetrazol-induced kindling: early involvement of excitatory and inhibitory systems, *Epilepsy research 26*, 105-113.

18. da Silva, L. F., and Da Silva, L. F. A Neuropharmacological Analysis of PTZ-Induced Kindling in Mice, *General pharmacology 31*, 47-50.

19. McNamara, J. O., Byrne, M. C., Dasheiff, R. M., and Fitz, J. G. (1980) The kindling model of epilepsy: a review, *Progress in neurobiology 15*, 139-159.

20. Bolkvadze, T. A., and Bolkvadze, T. Kindling-induced hippocampal cell death in rats, *Neuroscience and behavioral physiology 38*, 359-36

Appendix 1

Investigation of Human Plasma Protein Binding by Microdialysis Sampling

Background and Significance

Measurement of plasma protein binding (PPB) of drugs is critical to understanding their pharmacokinetics and efficacy. According to the free drug hypothesis, only the fraction of the drug that remains unbound to serum proteins is responsible for its therapeutic activity[1]. One method that can be employed to measure the free drug fraction is microdialysis sampling. This technique can be applied both *in vitro* and *in vivo*, making it an attractive technique in preclinical drug discovery[2]. In this study, plasma protein binding of five commercially available, albumin binding compounds with known PPB values was measured using microdialysis sampling. Perfusate modifications were investigated to achieve optimal compound recovery while reducing nonspecific binding to the membrane. It was determined that plasma ultrafiltrate served as the best perfusate option, as it did not negatively impact the extraction efficiency of the probe or compound PPB. In addition, plasma ultrafiltrate mimics in vivo physiological matrices, allowing for easy transition to *in vivo* microdialysis studies.

Plasma Protein Binding

When a drug is introduced to a biological system, a portion of the drug becomes unavailable to elicit a pharmacological effect due to binding to proteins such as human serum albumin or globulins (e.g. alpha-1-acid glycoprotein). Only the free drug fraction is accessible to drug transporters and drug metabolizing enzymes, as well as the intended drug target[3-5]. The extent of

PPB influences the distribution of the drug in the body and is therefore routinely measured during optimization of potential candidates during drug discovery. The ability to accurately measure the unbound fraction (f_u) of a drug is critical to understanding both the pharmacokinetics and pharmacodynamics of the drug[6]. Multiple techniques are available for measuring f_u of drugs in vitro including equilibrium dialysis (ED) and ultrafiltration (UF) and have been reviewed extensively elsewhere[7-10]. Currently, classical equilibrium dialysis is considered the gold standard for definitive measurement of plasma protein binding[11]. Rapid equilibrium dialysis (RED) has improved PPB throughput of binding studies, making it a highly utilized screening technique[12]. While the RED device allows for parallel processing of multiple samples at the same time, the assay still requires long incubation times for equilibrium to be established, making the technique time consuming[12]. UF is a quicker technique, reducing equilibrium time from hours to minutes. However, this method is highly susceptible to nonspecific binding of the compound to the device and typically has a very low throughput, making the assay time consuming resulting in loss of sample[13]. More recently, microdialysis (MD) has emerged as an alternative to ED and UF for measuring PPB in vitro[2, 14-18].

Human Serum Albumin

Human serum albumin (HSA) is the most abundant protein in human blood, making up nearly 50% of all serum proteins[19]. It is produced in the liver and its primary function is to maintain the oncotic pressure in the body which is needed for the distribution of bodily fluids between the blood vessels and tissue[6]. It can also function to transport hormones, fatty acids, and other small compounds, such as drugs, through the body. Small compounds are able to bind to HSA, allowing

them to be transported to the liver. This binding also affects the drug's half-life and metabolism. All of the drugs investigated in this study were HSA binding compounds.

Free Fraction

It is widely accepted that it is the free fraction of drug that is pharmacologically active. This is the fraction that interacts with receptors, is metabolized, and ultimately excreted. This concept is known as the free drug hypothesis. Most drug targets are in the tissues themselves and not in the vasculature. This makes measuring the free fraction very difficult in the pre-clinical and clinical setting. By measuring the free fraction in the vasculature, i.e. blood plasma, pharmaceutical researchers can get an idea of the amount of free drug in the body, assuming the amount of drug in the plasma is in equilibrium with the amount at the active site[1]. Accurately measuring the amount of free drug in the body is essential for drug development and determining the optimal dosage. Because only the free fraction is available to generate a pharmaceutical effect, the amount of protein binding is directly proportional to dosage[4]. Several techniques are available to measure the PPB values, all with advantages and disadvantages and are described in detail below.

Common Methods of Measurement

Ultrafiltration

Ultrafiltration is an *in vivo* microsampling technique in which sampling occurs across a semipermeable membrane. For ultrafiltration sampling, a vacuum is applied to the probe and

sampling occurs via bulk transport of ECF into the probe instead of diffusion driven with microdialysis sampling. Since bulk ECF is collected, the analyte concentration in the sample is the same as that in the tissue and calibration is not required. The most common sampling sites for ultrafiltration are subcutaneous tissue and biological fluids, such as blood[10, 13]. Denser tissues, such as in the brain, are unsuitable for ultrafiltration sampling, limiting its versatility. Furthermore, due to the high vacuum required the plasma protein binding values can be altered by potential changes in protein concentration due to the abrasive pressure of the sampling.

Equilibrium Dialysis

Similar to classical dialysis, equilibrium dialysis (ED) involves the passing of molecules across a semipermeable membrane. ED is a specific application of dialysis that involves the binding of small molecules to proteins. Small molecules such as drugs, are allowed to passively diffuse across a membrane from one chamber to another across a semipermeable membrane with a low molecular weight cut-off[1, 11]. This is allowed to happen for a length of time (typically 18 hours) until equilibrium is established. The set-up is relatively simple and easy to implement, making it an attractive option. However, the length of time for equilibrium to be established is quite lengthy, reducing data output.

Rapid Equilibrium Dialysis

Finally, rapid equilibrium dialysis (RED) can also be used to measure concentrations in the extracellular fluid *in vitro*; however, the device cannot be implanted directly into an animal, therefore, it is not applicable to *in vivo* studies. With major applications for ADME and

pharmacokinetic studies, rapid equilibrium dialysis is an improvement on traditional equilibrium dialysis. The RED apparatus consists of Teflon based plates containing disposable dialysis cells, shown in Figure 1.1[12]. They are comprised of single-use disposable two-sided chambers that can be filled with sample and sample matrix. Over time, the free drug is allowed to passively diffuse across the membrane and is then collected in one of the two chambers. The inserts can be placed in a 96-well plate which makes it easy for high through-put analysis. While this is an excellent way to perform plasma protein binding studies, there are still limitations to this technique. The quickest time achievable for the study is 100 minutes. Because there is no laminar flow involved, it takes a long time for complete diffusion to occur and for equilibrium to be established. For this reason, implementing microdialysis to perform PPB studies can be a faster, just as reliable method for studying drug binding both *in vitro* and *in vivo.*

Microdialysis in PPB Studies

In MD sampling, a probe containing a semi-permeable membrane with a low molecular weight cut-off (e.g. 20 kDa) is placed into the sampling space such as the brain, liver, or vein. Matrix-compatible solution, termed perfusate, is slowly pumped through the probe allowing small analytes to cross the membrane by passive diffusion that is driven by a concentration gradient, allowing for both recovery of free compound in the sample and delivery of compounds to the surrounding matrix[20-22]. Small molecules diffuse across the membrane depending on the direction of the concentration gradient and are collected as dialysate. The low molecular weight cutoff of the membrane prevents large macromolecules, such as proteins and blood cells, from crossing into the dialysate sample. Because protein bound drug is unable to enter the probe, only the free

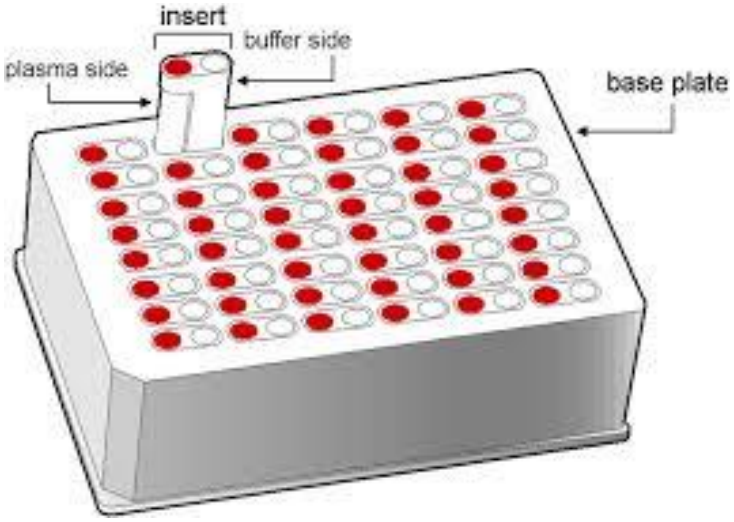

Figure 1.1: Rapid equilibrium device[11]

fraction of the drug is collected, making this technique ideal for PPB studies using direct sampling[15, 22].

Previous studies have demonstrated the utility of microdialysis to measure plasma protein binding *in vitro*[15, 21]. In these studies, low and moderately bound drugs, (i.e., fu = 90-50%) were investigated using long membrane lengths, (up to 30 mm) to increase analyte recovery. While these studies demonstrated the basic application of MD to in vitro PPB studies, difficult to monitor compounds including those that are extensively protein bound (>95%) or subject to significant non-specific binding to PPB device components, were not taken into consideration. While the long membrane length improved overall analyte recovery, it is not practical for use in *in vivo* applications due to the loss of spatial resolution. Therefore, the goal in the present studies was to use optimized microdialysis sampling techniques to accurately measure the protein binding of difficult compounds including warfarin and rosiglitazone *in vivo*.

The current study has improved on previous work by expanding the range of protein bound compounds to include extensively bound compounds. Additionally, the probe membrane length has been significantly reduced to 10 mm, making it more applicable to in vivo studies. Five commercially available albumin binding drugs (Table 1.1) with reported UF or ED PPB values including extensively protein bound drugs and those subject to significant nonspecific binding, were successfully monitored with the addition of perfusate modifiers, further demonstrating the versatility and applicability of microdialysis to measure the unbound fraction of drugs.

Compound	% Bound Literature[5, 23-25]	Literature Method of Measurement
Levofloxacin	25-38%	RED[12]
Carbamazepine	63.7-82.5%	UF[26]
Warfarin	96-99%	UF[13]/RED[11, 12]
Clozapine	84-95%	RED[12]
Rosiglitazone	99.8%	UF[23]

Table 1.1: Literature values for protein binding of study compounds

Probe Considerations

Several factors play a role in selecting the appropriate MD probe for the study. Sampling location is the initial parameter. For plasma studies, a flexible probe is most ideal because it can not only be used *in vitro* but can then be easily implanted in the vasculature for *in vivo* studies. Other factors such as membrane length, membrane type, and molecular weight cut-off are important considerations to make[27]. All parameters greatly affect analyte delivery and recovery. Longer membrane lengths, for example, provide more surface area of analytes to defuse across; however, spatial resolution is greatly compromised. There are a variety of membrane materials available including polycarbonate (PC), polyarylethersulphone (PAES), cuprophan, and cellulose acetate. Membrane material selection is directly related to the hydrophobicity and hydrophilicity of your analyte. Hydrophobic analytes will prefer a hydrophobic membrane and vice versa.

Materials and Methods

Chemicals

All compounds were purchased from Sigma Aldrich (St. Louis, MO). Ringer's Solution was purchased from VWR (Philadelphia, PA). Pooled, mixed gender, heparinized human plasma and plasma ultrafiltrate were purchased from BioreclamationIVT (New York, NY). The plasma ultrafiltrate was pooled, mixed gender, heparinized human plasma filtered using ultra-filtration with a 10 kDa filter to free the sample of proteins and larger macromolecules.

Microdialysis Probe

CMA 20 Elite Microdialysis Probes were purchased from Harvard Apparatus (Holliston, MA, USA). Probes consisted of a 10 mm polyarylethersulphone (PAES) membrane with a 20 kDa molecular weight cutoff. Probes were flexible and had 200 mm of tubing on either side of the membrane. The probes and tubing were filled with perfusion fluid and checked for proper flow prior to sample collection.

In Vitro Microdialysis

Extraction Efficiency

In order to accurately quantify the amount of free drug in the matrix of interest, the extraction efficiency for a given probe was determined. Extraction efficiency studies were carried out in vitro in 4 mL amber glass vials at 37°C and stirred constantly at 350 rpm with micro stir bars (Figure 1.2). 3 mL of Ringer's solution (99.28% water, 0.68% sodium chloride, 0.02% sodium bicarbonate, 0.01% potassium chloride, 0.01% calcium chloride dehydrate) was spiked with 1 µM of compound. The probe was placed in the vial, ensuring that the entire membrane was submerged in the solution. Analyte-free Ringer's solution was pumped through the probe at a flow rate of 1 µL/minute using a syringe pump. Samples were collected in 20 minute intervals.

Probe Validation

To verify probe integrity for the duration of the experiment, nadolol samples were collected before and after the experiment to serve as controls. Nadalol was chosen as the control because it

has similar chemical properties as the compounds of interest, but was not highly susceptible to non-specific binding. The probe integrity was validated if nadalol extraction efficiencies from before and after the experiment matched within a 20% threshold. The extraction efficiency of the probe was determined for each compound by collecting triplicate dialysate samples along with 20 µL aliquots from the sample vial to determine the actual spiked concentration. The analyte concentration in the collected dialysate was then determined analytically using liquid chromatography-tandem mass spectrometry (LC-MS) and probe recovery was calculated using equation 1 were $C_{dialysate}$ is the concentration of compound measured in the dialysate and C_{sample} is the concentration of compound spiked into the vial. Extraction efficiency measurements were carried out for each of the five test compounds.

$$\text{Extraction Efficiency} = \frac{C_{dialysate}}{C_{sample}} \text{ x } 100$$

Equation 1

Plasma Protein Binding of Commercial Compounds

Once the extraction efficiency of each compound had been determined, protein binding studies were carried out in the same manner as the extraction efficacy, replacing the Ringer's solution in the vial with 3 mL of pooled, mixed gender, heparinized human plasma and spiking it with 1 µM of test compound. Once again, three, 20 minute samples were collected. This was repeated three times for a total of nine collections. A blank plasma dialysate sample was collected between each triplicate set. Samples were diluted to 2 or 3 fold depending on the analyte and analyzed via LC-MS. After the samples had been quantified, PPB was calculated using equation

2, where $C_{dialysate}$ is the experimentally determined free drug concentration, percent probe recovery is the calculated extraction efficiency, and CRT is the concentration of analyte spiked into the reaction vial.

$$\% \text{ Free Fraction} = \frac{C_{dialysate}}{\% \text{ Probe Recovery}} \text{x} \frac{100}{(C_{RT})} \text{x } 100$$

Equation 2

Liquid Chromatography – Mass Spectrometry

Method Optimization

A generic LC-MS method was modified and optimized for sample analysis[28, 29]. Dialysate samples were collected directly into a 96 well plate and diluted by adding 50:50 (v/v) acetonitrile/Ringer's solution to the samples to be within the linear range of the calibration curve. A sample calibration curve for clozapine is shown in Figure 1.3. Standards were made in their respective perfusate used in each of the protein binding studies. Concentrations tested ranged from 0.5 nM to 1000 nM and demonstrated linearity with R2= 0.9998 and a lower limit of quantitation of 0.1 nM, with a S/N=10. 1000 ng/mL tolbutamide was added to all samples and standards to serve as an internal standard. The plate was vortexed, centrifuged, and placed on the auto sampler for injection. All compounds were detected in positive ionization mode. Each drug was individually infused to determined optimal parameters. Samples were analyzed using a SIL-HTc autosampler/system controller with two LC-20AD Shimazdu pumps and an Applied Biosystems

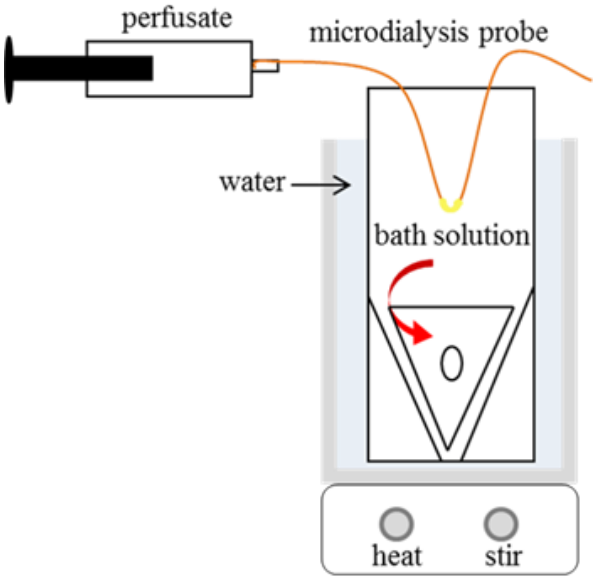

Figure 1.2: in vitro microdialysis set-up

AB MDS Sciex 4000 Q Trap mass spectrometer operated in MRM mode. The analysis time was 5 minutes with a linear gradient of solvent A: water with 0.1% formic acid and solvent B: acetonitrile with 0.1% formic acid at a flow rate of 0.500 mL/min.

Quality Control

In order to validate the concentrations of the standard and therefore the standard curve, quality control samples were also run in parallel with the standard and samples. Quality control samples were run in triplicate with a low, mid, and high concentration within the calibration curve. Quality control samples needed to be within 25% of the curve standards to be considered passing, thereby validating the standards to be used for quantitation.

Perfusate Modifications

Protein binding experiments with perfusate modifiers were carried out as described above. In the modified experiments, the Ringer's solution in the perfusion needle was replaced with either 5% human serum albumin (HSA) in Ringer's, or with plasma ultrafiltrate. Similarly, standards were made up in the respective modified solutions for LC-MS analysis.

Results and Discussion

Extraction efficiencies and protein binding were experimentally determined for 5 commercially available albumin binding compounds ranging in protein binding from 12% bound to 99.8% bound using microdialysis sampling and compared with values determined using

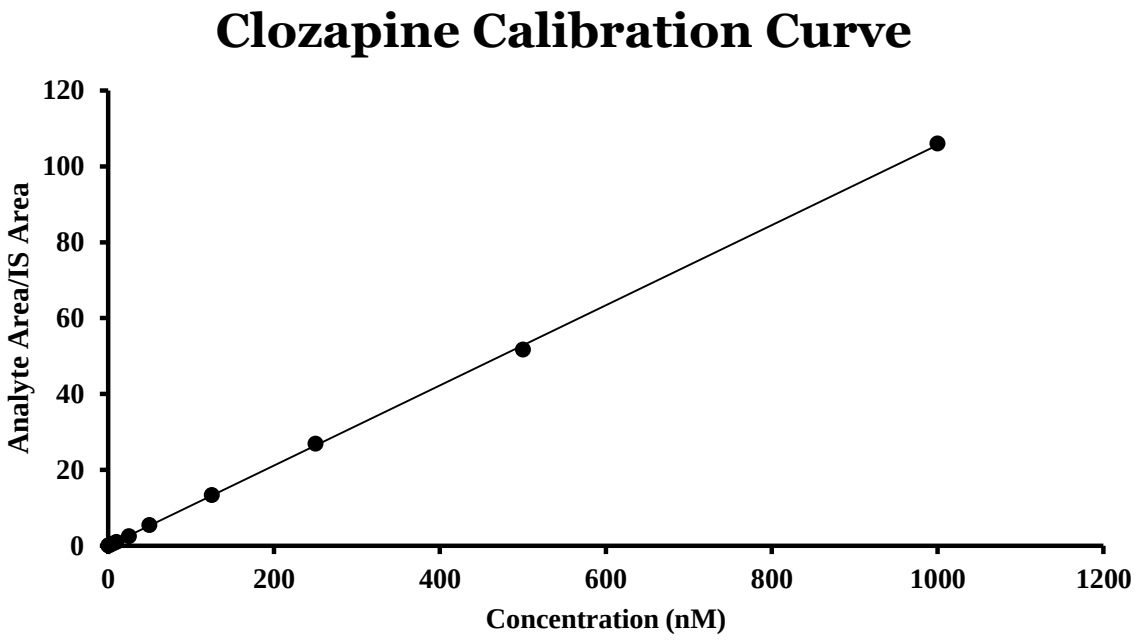

Figure 1.3: Representative calibration curve of clozapine in Ringer's solution.

Analyzed via MS/MS using parent ion m/z = 327 and daughter ion m/z = 270

currently available methods (Table 1.2). A variety of compounds were investigated to increase extraction efficiency and obviate non-specific adsorption.

Human Serum Albumin

In an attempt to increase the extraction efficiency of the probe for the measurement of extensively protein bound drugs, 5% HSA was added to the Ringer's solution perfusate to increase the drug's affinity for the perfusate, and to decrease nonspecific binding to the microdialysis components. Recoveries of over 100% were obtained for highly and extensively bound drugs. One hypothesis for these high recoveries is the free drug is binding to the HSA and then being released upon the denaturing of the protein in the dialysate prior to analysis. Recoveries for low and moderately bound drugs were significantly lower in HSA modified perfusate in comparison to unmodified Ringer's. This is most likely due to the compound affinity and binding properties to HSA versus other plasma proteins, since no HSA was added to the sample vial. While the extraction efficiencies were significantly affected by the addition of HSA to the perfusate, it should be noted that the protein binding numbers were not affected do to the mathematical calculation. PPB values determined using HSA modified perfusate matched reported ED/UF literature values reasonably well.

Plasma Ultrafiltrate

To remove the need to denature the proteins associated with the HSA modification, plasma ultrafiltrate was additionally tested as a perfusion fluid. Ultrafiltrate was selected in an attempt to closely mimic the sampling medium, plasma, but remain protein free (> 10Kda) for easier sample

cleanup and analysis. Table 1.2 shows that the ultrafiltrate did not significantly affect the extraction efficiency of the probe and also allowed for extensively bound drugs to be measured. Because the plasma ultrafiltrate is protein-free, there were no sites available for drug to bind to the perfusate, thereby removing the issue of extraction efficiencies over 100%. Protein binding numbers measured using ultrafiltrate as the perfusion fluid match literature values for compounds from all levels of protein binding, further validating it as an ideal perfusate option. Additionally, plasma ultrafiltrate directly mimics the physiological matrix, making for an easy transition to in vivo experiments. Future exploration of this project would include investigation of different perfusate modifications or additivities to further increase compound recovery. Once the in vitro PPB parameters have been fully optimized, they can be directly applied to in vivo pharmacokinetic and pharmacodynamic studies.

Conclusions and Future Directions

From this limited compound set, it can be concluded that plasma ultrafiltrate may be used as a universal perfusion fluid for the accurate measuring of low to extensively protein bound compounds using microdialysis. Additionally, because plasma ultrafiltrate is a direct match of physiological conditions, the transition to *in vivo* studies could easily be carried out without further methodological modifications. MD allows for real time monitoring of PPB measurements, making it an ideal technique for preclinical drug discovery.

TABLE 1.2: Extraction Efficiencies and PPB data for Microdialysis Studies

Compound	Levofloxacin	Carbamazepine	Warfarin	Clozapine	Rosiglitazone
PPB Ultrafiltrate	36.13±2.16%	70.44±1.58%	98.63±0.32%	90.27±4.85%	97.54±1.97%
Extraction Efficiency (Ultrafiltrate)	79.15%	89.92%	91.60%	46.82%	68.47%
PPB HSA Modified	28.44±2.12%	70.97±1.43%	97.04±0.30%	90.98±1.37%	97.30±1.00%
Extraction Efficiency (HSA Modified)	50.36%	57.66%	175%	116%	165%
PPB Ringers	25.17±3.07%	69.53±1.52%	98.03±0.19%	82.10±7.54%	97.34±2.02%
Extraction Efficiency (Ringers)	79.40%	95.47%	73.76%	41.13%	73.34%

N=3, data expressed as Mean ± Standard deviation

References

1. Di, L., Umland, J. P., Trapa, P. E., and Maurer, T. S. (2012) Impact of recovery on fraction unbound using equilibrium dialysis, *Journal of Pharmaceutical Sciences 101*, 1327-1335.
2. (2011) *Applications of Microdialysis in Pharmaceutical Science*, Wiley, Hoboken, US.
3. Bohnert, T., and Gan, L.-S. (2013) Plasma protein binding: From discovery to development, *Journal of Pharmaceutical Sciences 102*, 2953-2994.
4. Dasgupta, A. (2007) Usefulness of monitoring free (unbound) concentrations of therapeutic drugs in patient management, *Clinica Chimica Acta 377*, 1-13.
5. Jensen, B., Chin, P., and Begg, E. (2011) Quantification of total and free concentrations of R- and S-warfarin in human plasma by ultrafiltration and LC-MS/MS, *Anal Bioanal Chem 401*, 2187-2193.
6. Schmidt, S., Gonzalez, D., and Derendorf, H. (2010) Significance of Protein Binding in Pharmacokinetics and Pharmacodynamics, *Journal of Pharmaceutical Sciences 99*, 1107-1122.
7. Brocks, D. R. (2006) Drug disposition in three dimensions: an update on stereoselectivity in pharmacokinetics, *Biopharmaceutics & Drug Disposition 27*, 387-406.
8. Ruiz-Garcia, A., Bermejo, M., Moss, A., and Casabo, V. G. (2008) Pharmacokinetics in Drug Discovery, *Journal of Pharmaceutical Sciences 97*, 654-690.
9. Wang, H., Zrada, M., Anderson, K., Katwaru, R., Harradine, P., Choi, B., Tong, V., Pajkovic, N., Mazenko, R., Cox, K., and Cohen, L. H. (2014) Understanding and Reducing the Experimental Variability of In Vitro Plasma Protein Binding Measurements, *Journal of Pharmaceutical Sciences 103*, 3302-3309.

10. Lam, H., Davies, M., and E. Lunte, C. (1996) Vacuum ultrafiltration sampling for determination of plasma protein binding of drugs, *Journal of pharmaceutical and biomedical analysis 14*, 1753-1757.

11. van Liempd, S., Morrison, D., Sysmans, L., Nelis, P., and Mortishire-Smith, R. (2011) Development and Validation of a Higher-Throughput Equilibrium Dialysis Assay for Plasma Protein Binding, *Journal of the Association for Laboratory Automation 16*, 56-67.

12. Waters, N. J., Jones, R., Williams, G., and Sohal, B. (2008) Validation of a rapid equilibrium dialysis approach for the measurement of plasma protein binding, *Journal of Pharmaceutical Sciences 97*, 4586-4595.

13. Wang, C., and Williams, N. S. (2013) A mass balance approach for calculation of recovery and binding enables the use of ultrafiltration as a rapid method for measurement of plasma protein binding for even highly lipophilic compounds, *Journal of pharmaceutical and biomedical analysis 75*, 112-117.

14. Brunner, M. Microdialysis: an in vivo approach for measuring drug delivery in oncology, *European journal of clinical pharmacology 58*, 227-234.

15. Hansen, D. K., Davies, M. I., Lunte, S. M., and Lunte, C. E. (1999) Pharmacokinetic and Metabolism Studies Using Microdialysis Sampling, *Journal of Pharmaceutical Sciences 88*, 14-27.

16. J. (2011) Clinical microdialysis in neuro-oncology： principles and applications - Clinical microdialysis in neuro-oncology： principles and applications, *Ai zheng 30*, 173-181.

17. Mathy, F.-x., Preat, V., and Verbeeck, R. K. (2001) Validation of subcutaneous microdialysis sampling for pharmacokinetic studies of flurbiprofen in the rat, *Journal of Pharmaceutical Sciences 90*, 1897-1906.

18. Verbeeck, R. K. (2000) Blood microdialysis in pharmacokinetic and drug metabolism studies, *Advanced Drug Delivery Reviews 45*, 217-228.

19. Zhivkova, Z., and Doytchinova, I. (2012) Quantitative structure—plasma protein binding relationships of acidic drugs, *Journal of Pharmaceutical Sciences 101*, 4627-4641.

20. Joukhadar, C. (2005) Microdialysis - Current applications in clinical pharmacokinetic studies and its potential role in the future, *Clinical pharmacokinetics 44*, 895-913.

21. Mukker, J. K., Singh, R. P., and Derendorf, H. (2014) Determination of Atypical Nonlinear Plasma–Protein-Binding Behavior of Tigecycline Using an In Vitro Microdialysis Technique, *Journal of Pharmaceutical Sciences 103*, 1013-1019.

22. uuml, and ller, M. Microdialysis in clinical drug delivery studies, *Advanced drug delivery reviews 45*, 255-269.

23. Cox, P. J., Ryan, D. A., Hollis, F. J., Harris, A.-M., Miller, A. K., Vousden, M., and Cowley, H. (2000) Absorption, Disposition, and Metabolism of Rosiglitazone, a Potent Thiazolidinedione Insulin Sensitizer, in Humans, *Drug Metabolism and Disposition 28*, 772-780.

24. Riccardi, K., Cawley, S., Yates, P. D., Chang, C., Funk, C., Niosi, M., Lin, J., and Di, L. (2015) Plasma Protein Binding of Challenging Compounds, *Journal of Pharmaceutical Sciences 104*, 2627-2636.

25. Zhang, F., Xue, J., Shao, J., and Jia, L. (2012) Compilation of 222 drugs' plasma protein binding data and guidance for study designs, *Drug Discovery Today 17*, 475-485.

26. Fortuna, A., Alves, G., Soares-da-Silva, P., and Falcão, A. (2013) Pharmacokinetics, brain distribution and plasma protein binding of carbamazepine and nine derivatives: New set of data for predictive in silico ADME models, *Epilepsy research 107*, 37-50.

27. Plock, N. Microdialysis—theoretical background and recent implementation in applied life-sciences, *European journal of pharmaceutical sciences 25*, 1-24.

28. Sun, L. An in vivo microdialysis coupled with liquid chromatography/tandem mass spectrometry study of cortisol metabolism in monkey adipose tissue, *Analytical biochemistry 381*, 214-223.

29. Wang, C. Microdialysis combined with liquid chromatography–tandem mass spectrometry for the determination of levo-tetrahydropalmatine in the rat striatum, *Journal of pharmaceutical and biomedical analysis 64-65*, 1-7.